12

NON-INTRUSIVE NOISE MEASURING ON A TELEVISION PICTURE USING SPECTRUM ANALYSIS

by CORNELIUS JANSE VAN RENSBURG

Submitted to the University of Cape Town in partial fulfillment of the requirements for the degree of Master of Science in Engineering. September 1990.

12

NON-INTRUSIVE NOISE MEASURING ON A TELEVISION PICTURE USING SPECTRUM ANALYSIS

by CORNELIUS JANSE VAN RENSBURG

Submitted to the University of Cape Town in partial fulfillment of the requirements for the degree of Master of Science in Engineering. September 1990.

ACKNOWLEDGEMENTS

First of all I would like to thank Professor de Jager, my supervisor. His encouragement and support was very helpful.

Secondly I thank A.Dachs for his many routines that I could use in my software. Also a word of thanks to T.Rees for the use of his optimized two dimensional fourier transform routine. Without these routines my research would not have been such a pleasure as it was. Furthermore, I would like to thank P.Symmonds for his routines in the developement of the Area Of Interest method.

The assistance of the South African Broadcasting Corporation, and in particular A.L. Curle, who sponsored this project and made their facilities available is also gratefully acknowledged.

I would also like to thank T.Leubane for her continual support during this thesis.

Finally I express thanks to the Foundation for Research and Development for the financial support.

SYNOPSIS

The objective of this thesis is to develop a new measuring technique to measure noise on a television picture non-intrusively.

Existing methods measure noise intrusively by injecting test signals into the system or using techniques which make use of lines outside the picture area. From a system point of view one may assume no prior knowledge about the picture characteristics. The only knowledge assumed is that the noise is uniformly spread over the picture. Contrary to this, we propose that we do know the characteristics of a typical television picture through system and viewer constraints.

Through spectrum analysis it will be proved that a television picture can indeed be characterized. For it to be acceptable to the general viewing public, it has to have a spectrum that is rapidly decreasing with increasing frequency. In fact, at the highest frequencies the picture spectrum should be virtually non-existent. On the other hand, the noise spectrum which has a flat spectrum over the whole frequency range, is most detectable at the high-frequencies. Thus, the high-frequency power of a picture spectrum can be used to estimate the noise power in the picture. Because the noise spectrum is not perfectly flat, a least squares error estimation is made by averaging the high-frequency spectrum points into one noise power estimate. This implies an assumed white noise spectrum.

A method to make this noise estimation more robust against high-frequency harmonics, due to structure in the picture, is to tessellate the image into sub-images. This is done in order to obtain a statistical estimation of noise from the picture, because the picture spectrum estimation is a statistical estimation. All the noise estimations of all the sub-images are used to build a histogram to determine a noise estimate for the whole picture.

The noise measuring technique, the Two Dimensional Noise Measuring Technique (2DSMT) was developed in Turbo Pascal (version 5) to run on an IBM PC. A minimum run-time of 50 seconds was obtained when run on a 25MHz 80386 machine with a numeric co-processor.

A problem encountered was when composite video was digitized in the framegrabber. Due to the frequency division multiplexing of the PAL color system, the high-frequency power is not primarily due to noise, but due to color information. Therefore the 2DSMT only works on monochrome input, which may be a decoded red, green or blue signal.

The 2DSMT compared favorably with the existing analogue noise measuring techniques where a constant luminance signal is used as input. Furthermore, it compared well with a noise measuring technique developed during the testing operation which measured constant luminance areas on cartoon pictures.

NOMENCLATURE

These symbols are listed in the order in which the appear in this dissertation.

Symbol		Page
I(t)	In phase component of noise vector	2.4
Q(t)	Quadrature component of noise vector	2.4
N(t)	Noise vector	2.4
A_c	Vector representing FM-carrier	2.4
f_c	Carrier frequency of FM-modulation	2.4
P	Resultant vector of N(t) and A_c	2.4
$\Theta(t)$	Phase of FM-modulated signal	2.4
CNR	Carrier to noise ratio	3.1
SNR	Signal to noise ratio	3.1
AM	Amplitude modulation	3.3
PM	Phase modulation	3.3
γ	Proportionallity between light output of a tube to voltage input	4.3
Ec	Light impinging on camera sensors	4.3
Lu	Illumination of CRT	4.3
Vc	Voltage input for CRT	4.3
Y	Luminance component of composite video signal	4.6
R	Red component of decoded composite video signal	4.6
G	Green component of decoded composite video signal	4.6
B	Blue component of decoded composite video signal	4.6
V	Color difference component of composite video signal (Red component)	4.7
U	Color difference component of composite video signal (Blue component)	4.6
Kb	Weighting factor of U	4.7
Ku	Weighting factor of V	4.7
COMP	Composite video signal	4.7

Symbol		Page
S	Saturation	4.8
α	Hue	4.8
x(i,n)	Array of pixels	4.9
I(w)	Periodogram estimation of one row in x(i,n)	4.9
$B_{xx}(w)$	Bartlett spectrum estimation of I(w)	4.9
f(t)	Input signal	4.10
g(t)	Output image	4.10
G(w)	Spectrum of g(t)	4.10
F(w)	Spectrum of f(t)	4.10
n(t)	Noise degrading input image	4.11
N(w)	Spectrum of noise	4.11
S(f)	Picture spectrum estimation	4.11
B	Bandwidth of image	4.12
L(x)	Pulse in an image	4.15
$\phi(\tau)$	Autocorrelation of L(x)	4.15
$\Phi(w)$	Spectrum of $\phi(\tau)$	4.15
H	Height of television screen	4.17
P_L	Power in monochrome image	5.1
B_L	Bandwidth of monochrome image	5.1
σ^2	Variance estimation	5.6
N	Number of sample points	5.6
ϕ_{xx}	Two dimensional autocorrelation function	5.7
E[]	Expected value	5.7
$Px_nx_m()$	Probability function	5.7
X(m)	Power Spectrum	5.10
m_x	Average value of x(n)	5.18
MS	Mean square value of x(n)	5.18
$P_{xx}(n)$	Power density function of x(n)	5.20
RMS	Root mean square value	5.21
h(i)	Histogram estimation of noise power	5.25
Ch(i)	Cumulative distribution of h(i)	5.25
D(i)	Differential of Ch(i)	5.25

Symbol		Page
P_f	Signal power	6.2
P_n	Noise power	6.3
p(t)	Second order polynomial fitting	6.3
P_{uw}	Unweighted noise power measurement	6.4
Pw	Weighted noise power estimation	6.4
x_1,x_2	Random numbers	6.7
g_1,g_2	Gaussian random numbers	6.7
d	Quantization step	6.15
v_{in}	Analogue input	6.15
b	Number of bits in A/D	6.17

TABLE OF CONTENTS

Appendix F : Description of the software developed in this thesis. **F.1**

CHAPTER 1

INTRODUCTION

Television picture quality is of major concern to all in the broadcasting industry because it is the final product after many processing stages, delivered to the viewing public, and for that matter the world. The public forms its opinion of the broadcasting corporation in question, from this picture quality. The factors affecting picture quality are many, and although we do not yet know all of them, some, like camera focus, color bias or television noise are very important.

1.1 TELEVISION NOISE

One of these factors affecting picture quality, namely television noise, has been described by Schreiber et al (1988) as probably the most important factor affecting picture quality. It has also been proven by Oliphant et al (1987) that the viewing public are now more sensitive to noise than twenty years ago. This trend will probably continue and it is expected that noise will become a factor of ever increasing importance in picture quality with the advent of the new high definition television.

Since television broadcasting technology has advanced so much recently, picture quality is now less a function of the equipment and the channel than the care with which these are operated. Nevertheless, picture noise, whether due to camera limitations, multi-generation recording in video editing, film grain or low level of the received signal, remains a problem.

1.2 NOISE MEASUREMENT

It has therefore become necessary to measure the noise on the picture, be it for real-time operation to measure the broadcast quality, or to specify noise limits on advertisements from clients, or films being bought from film producers abroad. This noise measuring facility becomes even more important where film to video, or NTSC to PAL transfers have to be made, because these processes degrade the picture quality and no measuring technique exists to measure this degradation.

Until now, noise measurement has mostly been done in an intrusive manner. That is, transmission is interrupted and the system is stimulated with a constant luminance

signal, so that the noise can be measured from the fluctuations on this constant signal. There are also non-intrusive methods, such as measuring the noise on the clear lines in the vertical blanking interval or in the line blanking interval. Not only do these techniques not measure the picture noise directly, but the vertical blanking intervals are often regenerated in the playback and transmission process so that they bear only a tenuous relation to the picture noise. Furthermore, the widely used stimulus response techniques of measuring noise with a constant luminance signal rest on the questionable assumption that channel noise is representative of the picture noise. In fact with the channel technology of today this is rarely the case.

Apart from a television camera performance measurement on a uniformly illuminated white field, the broadcasting industry does not even attempt to measure picture noise directly.

1.3 A NEW METHOD

It was therefore decided to develop a noise measuring technique that could measure the noise on the picture directly, the way the eye sees it. The rationale is that if the eye can detect and grade noise, (to a certain extent) why should it not be possible to teach a machine to do something similar ?

Furthermore this proposed method have application wider than just the broadcasting industry. Rees (1990) proves the robustness of his machine vision system by degrading his input images with known amounts of noise. This method would measure the total amount of noise on the picture which would be more accurate than the existing method which measures only the added noise, thereby ignoring the inherent noise in the original image. Dachs (1990) has stated in a similar application that the Hough transform rejects small amounts of noise, but the process is severely degraded in the presence of large amounts of noise. It is clear that a noise measuring technique can leave its mark even in these applications.

1.4 THE SPECTRAL APPROACH

In this thesis it will be proven both theoretically and practically that the picture power density spectrum (PDS) differs significantly from the PDS of the noise.

Although the different pixels in a moving sequence of pictures can vary rapidly and independently, the shape of the two-dimensional Power density spectrum (2D PDS) does not change much with time. The shape of the spectrum is more a function of picture attributes and television system constraints than of picture content. Schreiber

(1986) asserts that picture attributes that are important to human observers are (a) that the picture movement in the picture must be slow enough to be noticeable, (b) scenes may not change so rapidly as to be disturbing, and (c) there should not be too much detail and clutter in the image. An example of the latter is the high spatial frequency information in an area of the SABC circle test pattern that skimmers with Moire' effects and is fatiguing and unpleasant to look at for any length of time. System constraints include amplitude/frequency response limitations (5,5 MHz in the South African television standard) and other signal amplitude limits. In short the whole picture is bandlimited in the horizontal, vertical and time domain.

Contrary to this, the PDS of white noise is known to be flat over the whole frequency range. Therefore, it is possible to differentiate between the two components in the spectrum and measure the white noise on the picture.

1.5 THE OBJECTIVES OF THIS THESIS

This thesis had five objectives in mind:

(1) To Investigate the possibility of detecting or measuring the noise on a television picture non-intrusively.

(2) If (1) was possible then to develop a technique to measure the noise non-intrusively.

(3) To calibrate the measuring technique in (2) with existing methods.

(4) To optimize the measuring technique in (2).

1.6 THE STRUCTURE OF THIS THESIS

Chapter 2 is an investigation of the different noise types commonly found in the broadcasting industry. Here we strive to answer which noise type is the most disturbing to the viewers, or the most widespread one. This is followed in the next chapter by the existing methods of noise measurement. Also incorporated in chapter 3 are some methods of noise reduction as this is closely linked with noise measurement. Chapter 4 describes video images in general and some of their characteristics. It describes most of the theory of the thesis.

Chapter 5 describes a new method of noise measurement, the two dimensional spectral noise measuring technique (2DSMT). This is followed in chapter 6 by results of tests of the new method. The basic problem in chapter 6 is that since the 2DSMT is the only

available method to measure the noise on the picture directly, some other measuring techniques had to be developed to also measure the noise on the picture directly, which could then be used to test the 2DSMT. The limitations to the 2DSMT are also described in this chapter.

Finally Conclusions are drawn in chapter 7.

CHAPTER 2

A TAXONOMY OF TELEVISION NOISE

2.1 INTRODUCTION

Noise is the generic name given to all forms of unwanted disturbances which the video signal can acquire, to the detriment of the picture. Although many noise types exist, this study is only concerned with the random noise types and not with the systematic types like mains hum and periodic noise. Much has been written about random noise, but it is important to introduce this subject within the context of building a non-intrusive noise measuring machine.

In order that the reader may be orientated in the field of television noise, the taxonomy of noise sources and processes is given in Fig.2.1 on the next page.

This chapter will start by explaining the origin of the main noise types generated in the processes of Fig.2.1.

Furthermore, the investigation on the visibility of noise in PAL television, by Oliphant et al (1988) will be discussed, since this is relevant in any measurement of a particular type of noise.

2.2 DIFFERENT NOISE TYPES

2.2.1 Film grain noise

This type of noise is of particular importance in the specialized case where a film to video transfer is made. A detailed description is given by Powell and Kennel (1987). Since this noise originates in the scanning of the film, it is a specialised kind of noise not covered here.

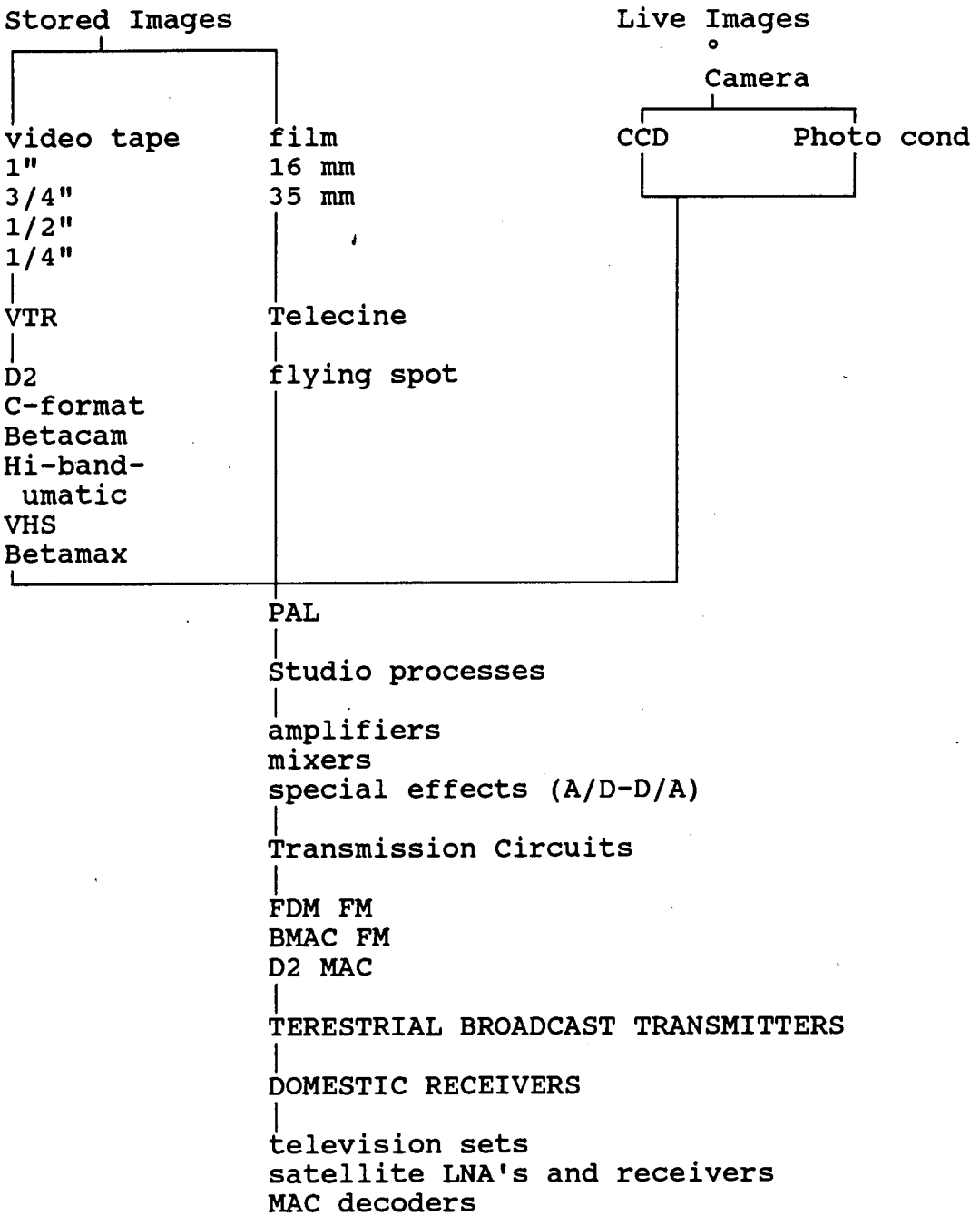

Figure 2.1 Taxonomy of television noise sources and processes.

2.2.2 Continuous random white noise

This is the most important noise type (according to Weaver 1977) since it is universally encountered. Random noise has many origins, the most important ones in the broadcasting industry being the statistical nature of every operation carried out upon a signal by active devices such as a transistor.

Alternatively noisy pictures are generated in the studio according to Efrein (1971):
(1) When there is bad lighting, the pictures would appear noisy because the camera is being "pushed" to produce pictures below it's optimum settings.
(2) The studio set and props can be noisy. Some noisy pictures are mere perceptual illusions, for example: Pictures look noisy if there are no highlights in the picture.
(3) Noise is more evident in the middle gray range than in the darker or lighter areas of the picture.

Random white noise consists of an ensemble of narrow pulses whose amplitudes vary in principle, from zero to infinity, although in practice the amplitude range must be limited. One cannot predict the amplitude of a random signal at any instant in time, but only the probability that any given amplitude will not be exceeded.
The other consequence of the view of random noise as a statistical ensemble of pulse waveforms is the continuous nature of its spectrum which, however, takes a number of forms according to the source of the noise. One basic form is white noise in which the spectral amplitudes are constant with frequency; the noise generated by many amplifiers and by an image orthicon tube is substantially flat. The common name "white" noise, is derived from the fact that since light as ordinarily generated is a type of very high-frequency noise, and true white light has a flat spectrum over the band of visible frequencies.

2.2.3 Triangular noise

The third important basic form is triangular noise, whose spectral amplitudes are directly proportional to frequency and the spectral power is proportional to frequency squared. Its principal source is in FM modulation and demodulation, but camera tubes of the photoconductive type also generate substantially triangular noise. The name is derived from the shape of the spectrum when drawn as amplitude against frequency. In practice most types of noise lie between triangular and white noise, due to the effect of pre-emphasis circuits and other types of correction. However one particular variety is also encountered, known as hypertriangular, where the spectral amplitudes increase more rapidly than with triangular noise, particular towards the upper end of the video band.

2.2.4 FM-clicks (Impulsive noise)

Another important form of noise is known as FM-clicks, from the click sound it makes in FM radio receivers. It is actually just a special case of triangular noise which is generated during the FM demodulation process, in the low signal to noise ratio case. The actual generation was described by Gallois A.P, and Böck A.M, (1987) as follows:

"An unmodulated carrier with bandlimited stationary Gaussian noise at the input of an FM-discriminator can be described in terms of the in-phase, I(t), and quadrature, Q(t), components of the noise, N(t), added to the carrier, A_c. Consequently, the composite signal can be thought of as rotating with an angular frequency of 2π times the carrier frequency, f_c, around the origin, O. Fig.2.2 shows the phase relationship between the carrier, Ac, and the noise, N(t).

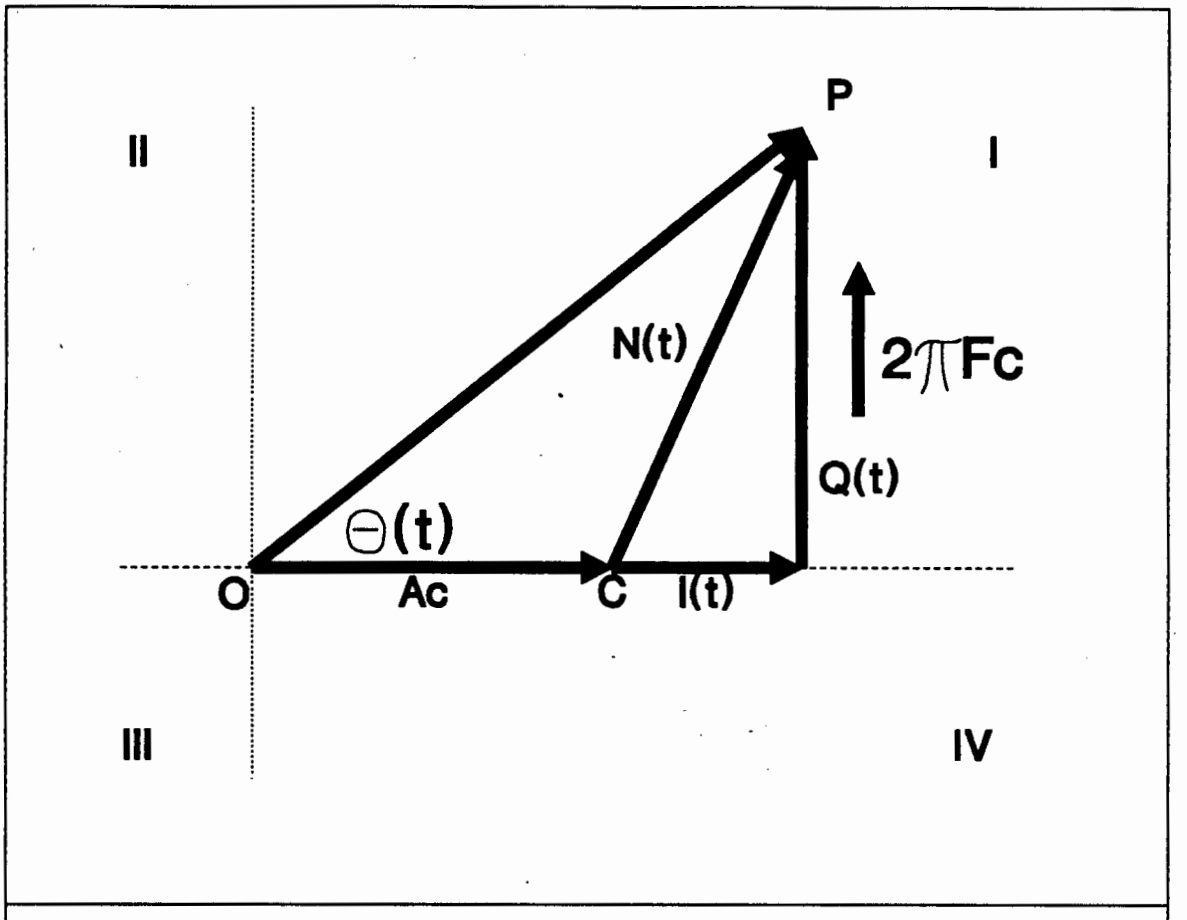

Figure 2.2 Phase relationship between carrier A_c and noise N(t).

The output of the FM-discriminator will follow the derivative of the phase:

$$\frac{d\Theta(t)}{dt} = \frac{d}{dt} \tan^{-1} \frac{Q(t)}{A_c + I(t)}$$

Since, for high carrier-to-noise ratio, P will stay in the vicinity of C, this calculation is often approximated as:

$$\frac{d\Theta(t)}{dt} \approx \frac{1}{A_c} \frac{dQ(t)}{dt}$$

thus resulting in the well known triangular noise spectrum. As the carrier-to-noise ratio decreases, probability that P encircles the origin becomes significant. In this region known as the onset of the FM-threshold, P will encircle O very close to O, thus causing an impulse like signal at the output of the descriminator, which is commonly referred to as a click."

2.2.4.1 The effect of the De-emphasis filter on the FM-click

Since the spectrum of a typical picture decreases exponentially with frequency and that of white noise is constant with frequency, the noise is significant in the high frequencies. A typical method of decreasing this high-frequency noise, is to lowpass filter (de-emphasize) the demodulated signal. The transmitted signal now has to be pre-corrected (pre-emphasized), to be equivalent to the de-emphasized signal. The de-emphasis filter is usually just the inverse function of the pre-emphasis filter. This method improves the signal to noise ratio for a certain field strength.

Before de-emphasis an FM-click is very narrow, but after de-emphasis, it is stretched out in time according to the impulse response of the de-emphasis filter. This makes it look like a comet with a bright head and a rapidly decreasing tail (Rhodes 1985). This is also known as a comet tail. Such an FM-click was simulated by Gallois et al (1987) and is shown in Fig.2.3

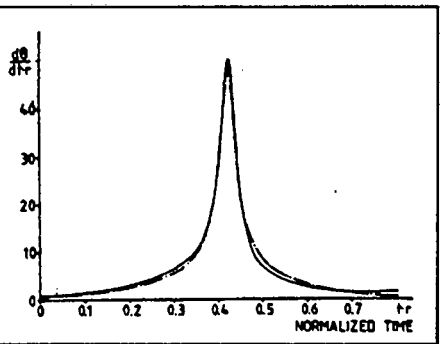

Figure 2.3 Simulated FM-click

2.2.4.2 FM-clicks in a satellite receiver

It has been observed by Curle and Conradie (1989), that the FM-clicks appear at the sharp transition areas in the picture, of a satellite reception.

Palmer (1986) explains that this phenomenon is due to the characteristics of the traveling wave tube amplifier (TWTA) in the satellite transponder. The channel filters prior to the satellite TWTA convert the constant-envelope FM signal into a signal with a fluctuating envelope. These fluctuations depend on the content of the video signal. For example, large envelope fluctuations will result from video waveforms that have abrupt transitions (the color bar patterns are particularly vulnerable to this phenomenon). These envelope fluctuations are converted to phase fluctuations by the AM/PM characteristic of the TWTA output filter.

As the thermal noise level at the input to the demodulator increases, impulse noise becomes more likely and the receiver enters the threshold region. This is partly because of the envelope fluctuations.

2.2.5 VSB noise

Vestigial sideband (VSB) noise arises from VSB demodulation, and the spectrum is shown in Fig. 2.4. This form of noise has a flat spectrum above 1.25 Mhz, but is 3dB lower at lower frequencies. Since the high-frequency noise is less visible than the low-frequency noise, it is assumed that VSB noise is less disturbing than white noise. One other disadvantage of VSB modulation is that mistuning at the receiver causes a boost or attenuation of low frequency components which can blur the sharp edges according to Lowry (1984).

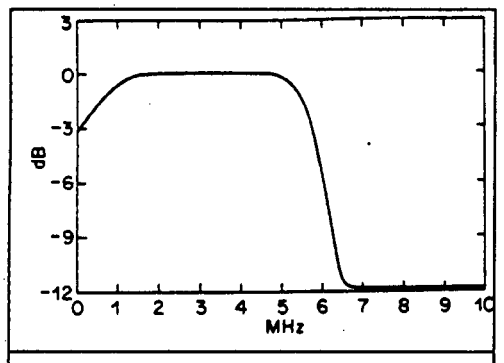

Figure 2.4 Frequency spectrum of VSB noise as measured by Oliphant et al (1988).

2.3 THE IMPAIRMENT CAUSED BY THE DIFFERENT NOISE TYPES

The subjective impairment caused by a given RMS noise voltage depends on its spectral distribution. Triangular noise for example, is subjectively less troublesome than flat noise, because it has a visual structure with a much finer grain due to the greater proportion of high-frequency components.

The visibility of different noise types on television has been studied since the early days of television, because this is a very important in determining the overall picture quality. For this reason the BBC did research on the "Visibility of noise in system I PAL color television" Oliphant et al (1988). They compared the subjective impairment as perceived by viewers for three types of noise added in discrete quantities. Their experimental setup is shown in Fig.2.5.

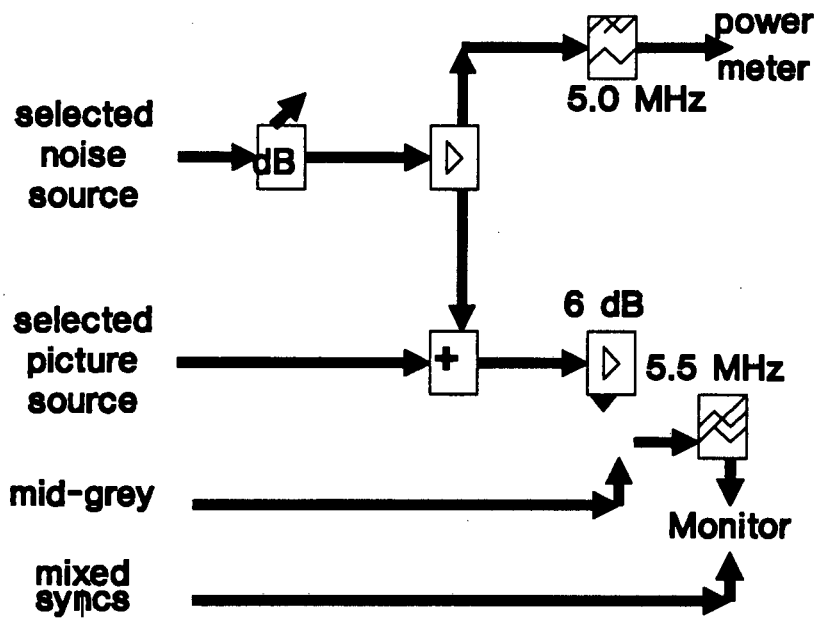

Figure 2.5 The simplified block diagram of the test equipment used by Oliphant et al (1988).

It is seen from Fig.2.5 that they could measure the noise added to the picture, and compare that with the subjective impairment of the picture, on the monitor, as rated by the viewers. The three types of noise which were used are: white noise, VSB and de-emphasized triangular noise. No reasons were given for this particular choice, so it is assumed that these noise types cause the most impairment, i.e. of the random noise types.
There main conclusions were:

(1) A given level of white noise causes the same impairment as a level of VSB noise 1.3 dB greater or a level of de-emphasized triangular noise 5 dB greater.

(2) Movement in pictures do not mask the effects of noise.

(3) A given level of white noise produced the same degree of perceived impairment as a level 2½ dB higher, 20 years ago.

(4) Chrominance noise is more visible in areas of highly saturated color.

(5) De-emphasized triangular noise has a higher high-frequency content, and therefore gives more chrominance noise - which is more visible in the highly saturated areas of the picture.

(6) Comparisons of noise visibility based on the application of weighting functions should be treated with some reserve. To quote from Oliphant et al (1988, p.11): "Noise weighting functions are intended to give a rough-and-ready estimate of noise visibility for convenience in operational measurements, they should not be treated as precision instruments." This is understandable when considering that the weighting network's response is only in the horizontal direction on the television screen, while the eye's response is horizontal, vertical and temporal.

(7) With modern PAL equipment, chrominance noise is less important than had been believed.

2.4 DISCUSSION

For a noise measurement to be meaningful, the measurement should be proportional to picture impairment. It is of no use to measure a noise that does not significantly impair the picture. According to this chapter, white noise causes the most impairment to the picture, thus justifying the development of a white noise estimator that specifically measures an accurate estimate of white noise as defined in signal processing terms, without using weighting functions. A further justification is that when many different types of noise add, through the law of large numbers the resultant noise becomes white. However, we cannot say that white noise is the most important noise type in the broadcasting industry.

Since movement in the picture does not affect the visibility of the noise, it is not necessary to bring this into calculation. Since chrominance noise is of lesser importance, a good estimate of noise can be made on the luminance part of the signal only.

Noise measuring algorithms will become more important in future because the viewing public will become more critical of picture quality, as has been proved by Oliphant et al (1988).

CHAPTER 3

EXISTING METHODS OF NOISE MEASURING/REDUCING TECHNIQUES

3.1 INTRODUCTION

Existing methods of noise measurement in the broadcasting industry are continually being revised and updated. However they all suffer from the same inability to measure the noise on the picture non-intrusively since none of them can distinguish between normal pictures and noise. These methods all need special signals, generated in the laboratory, as input. Even in measuring the performance of video recorders or cameras some known input is required like a known 100% saturation red bar or by pointing the camera at a uniformly lit white surface. We are going to introduce some methods that can measure noise on normal pictures, this we will call blind noise estimators as they will not have any a priory knowledge of the picture while they will estimate the noise on the picture.

Although the Broadcasting industry do not at present have any equipment to distinguish between normal pictures and the noise that degrades these pictures, it has built noise reducing apparatus such as those by the BBC and the BTS. These are in some sense similar to the noise measuring machines, because once the noise has been reduced, the difference between the processed and unprocessed picture is an estimation of the noise in the original picture. Whereas this method is limited to the amount of noise reduction possible, it is an interesting approach to the problem.

Similarly, median filtering is used extensively in removing FM-clicks. A real-time FM-click reduction algorithm has been proposed by Perlman et al (1987) and will be discussed.

Another approach is that of trying to determine the relationship between the carrier to noise ratio (CNR), and the picture signal to noise ratio (SNR). This is non-intrusive measuring of noise, but unfortunately this method only measures the noise created in the channel, and cannot detect noise originating in the early stages of video processing like the video recorder or the camera.

Lastly, but more relevant to this study, Meer et al (1990) and Besl and Jain (1988), have published work on blind noise estimation. This is similar to this study in that they also estimate the noise on top of a randomly changing picture background. Nonetheless there is a difference in our modeling of the signal characteristics, and therefore our approach to the problem.

3.2 EXISTING NOISE MEASURING TECHNIQUES USING TEST-INPUTS

Here follows a list of noise measuring techniques found during an on-line literature search. The search was done using the **DIALOG** service, from the Information services for physics, electronics and computing (INSPEC) database. The keywords supplied was: Television, noise and satellite reception. Other material was obtained from the South African Broadcasting Corporation.

1 A standard method of noise measurement in the South African Broadcasting Corporation, is with the use of one of the machines built by Rohde & Schwarz (1983), called the UPSF1 and UPSF2. These machines accept a constant luminance midgrey bar as input, where they fit a second order polynomial to the data and calculate the noise variance as the root mean square value of the difference between the input signal and the polynomial.

2 Weaver (1977) proposed a method of measuring the noise by visual inspection of the peak to peak value of a noisy midgrey bar on a waveform monitor. He admitted that it is not very accurate as the reading is quite subjective. A better method is to match this noisy bar with a signal from a calibrated noise generator. The noise reading is then taken from the noise generator.

3 A paper by Lokshin et al (1983) seemed relevant, judging from the title and abstract, but could not be retrieved. They proposed a new method of measuring the signal to background noise of a TV channel when the energy of the FM signal is dispersed.

4 Nakagawa (1977) measures chrominance noise (amplitude and phase errors in the decoding of the color information) as follows: The test signal (a 100% constant red signal) is detected by an amplitude and phase detector, after being filtered by a bandpass filter. The blanking

portion can be eliminated by a gate circuit and an output of pure noise can be measured by a power meter. In 1979 Nakagawa proposed his chrominance noise measuring machine working on the above mentioned principle.

5 Johnson (1987) used spectrum analysis to measure video tape noise. By storing single frequencies on casette, he could measure the distortions in the spectrum.

One main shortcoming of these methods are that they all measure the noise only horizontally on the television screen, whereas the eye sees the noise in the horizontal, vertical and the temporal directions. Nevertheless international comittees have accepted recommendations on the following noise measuring techniques:

1 The IEC(1981) accepted a recommendation to measure the chrominance noise separately in terms of the AM-noise and the PM-noise. The AM-noise is the root mean square (RMS) voltage of the amplitude modulated component of the noise in the chrominance band width, and the PM-noise is the RMS voltage of the phase modulated component of the noise in the chrominance band width. The input is an all red signal with 100% color saturation.

2 The CCIR(1986) recommended the following noise measuring procedure. To quote: "In general, measurements should be made with r.m.s.-reading instruments. Depending on the type of instrument to be used, the circuit will carry either no signal or a specified repetitive signal. ... For power measurement, the measuring instrument should have an effective time constant or integrating time of approximately 1 second."
They also specified that impulsive noise, and low-frequency noise should be measured by means of an oscilloscope.
However, we are proposing a new method where the circuit will carry normal picture signal but for power measurement an integrating time of 1 second can still be retained.

3.3 NOISE REDUCTION

Noise reduction is similar to noise measurement, because the difference between the reduced and original signals is an estimation of the noise present in the original signal.

There are, according to Richter (1989), basically two types of noise reducers, linear and nonlinear. The nonlinear techniques change the linear relationship between the input and output signals. Fundamentally the non-linear technique interprets the small signal variations as noise. This is very easy to implement, but not so effective, because the small signal variations are distorted.

The linear method on the other hand can be again subdivided into the adaptive and the non-adaptive techniques. The adaptive ones control the spatial and temporal frequency response of the signal according to the movement in the signal. In the non-adaptive ones, on the other hand, the type and extent of the signal changes are constant. The advantages and disadvantages of these techniques are listed in table 3.1.

Table 3.1 The advantages and disadvantages of the different noise reducing techniques.

Signal Processing	Advantages	Disadvantages
Non linear	Easy implementation.	Distortion in fine detail.
	No bandwidth reduction for large signal.	Limited amount of noise reduction.
Linear Non Adaptive	Easy implementation.	Bandwidth reduction Limited noise reduction.
Linear Adaptive	No bandwidth reduction. Noise reduction in wide range.	Complex signal processing.

The application of some of these techniques will now be discussed.

3.3.1 White noise reduction

The BTS has produced noise reducers that use adaptive linear signal processing (Richter 1989). Basically they are recursive filters as shown in Fig.3.1.

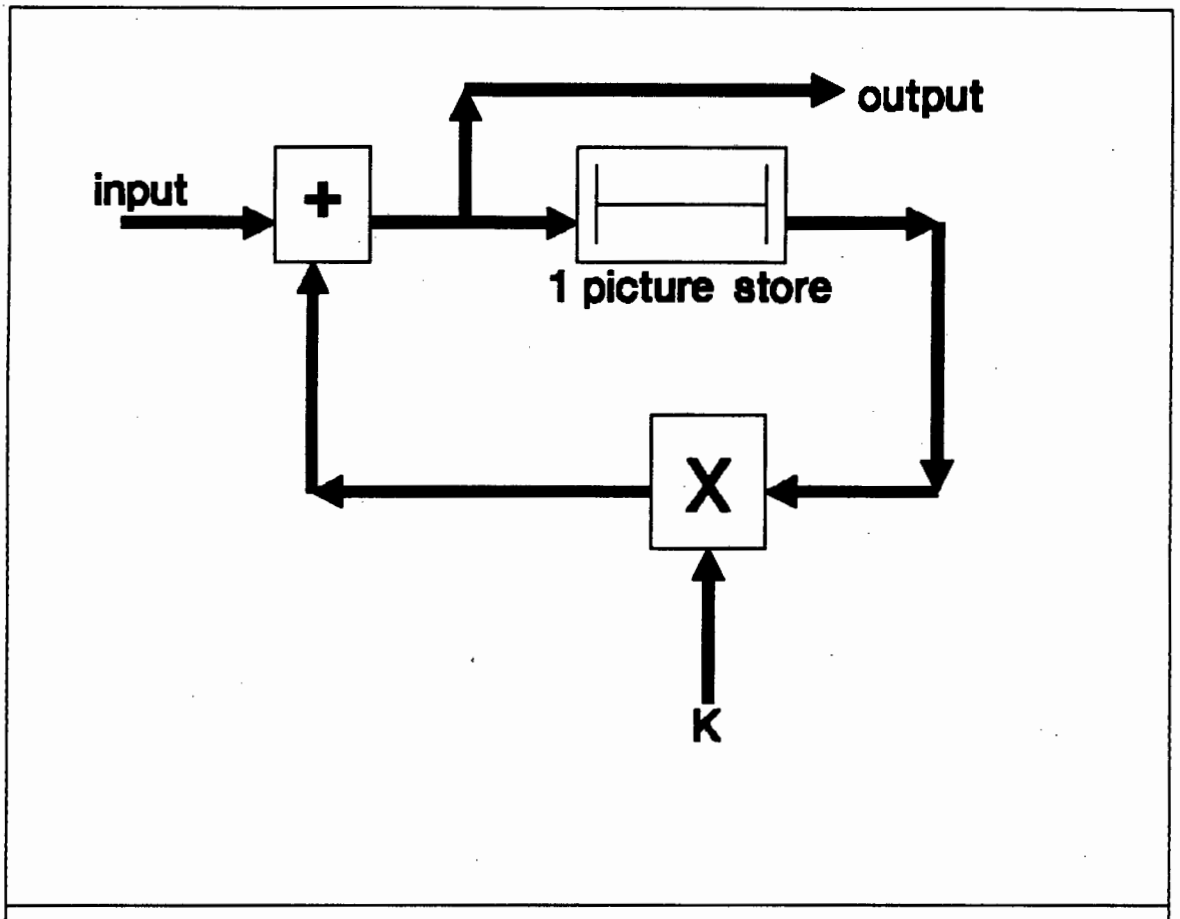

Figure 3.1 A basic recursive filter as a noise reducer.

A recursive filter assumes that the picture stays constant for a particular time. By increasing the weighting factor K, in the feedback loop, noise is reduced more, but the picture is blurred more because of motion. A more sophisticated method would be to measure the movement and with that control the K factor, as the BTS noise reducers do.

A similar approach was taken by Drewery et al (1984) of the BBC. They described a video and film grain noise reducer which was based on a first order recursive temporal filter. In this noise reducer they inhibited the filtering of moving detail because of the reasons mentioned previously. Therefore they incorporated in this machine a motion detector to control the filtering. Large intra-frame differences were due to movement and small differences were due to noise. Much research was done on motion detection and especially on spatially correlated methods of motion detection, as a simple binary decision of motion/no-motion proved insufficient.

For the purposes of this study this proves that implementing a simple recursive filter for a noise measuring technique would have to be accompanied by a complicated motion detection machine.

Even in a non-broadcasting context, namely that of X-ray imaging systems, Tsuda and Kimura (1986) accepts that adaptive noise reduction (recursive filtering) gives a good improvement of SNR. However, they propose a new method called the peak hold method, which implements a logarithmic conversion and subtraction algorithm.

3.3.2 FM-clicks reduction

Perlman et al (1987) developed a two dimensional 3x3 median filter to remove real time impulse noise in an adaptive manner. This filter can improve the FM-threshold performance with about 3dB Carrier to noise ratio (CNR). Their 1x3 vertical median filter proved to be very effective as long as the CNR exceeded 3 dB.

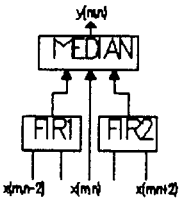

Figure 3.2 A unidirectional FMH filter (vertical direction).

Salo et al (1988) combined the good properties of linear and median filters to create a finite impulse response hybrid (FMH) filter as shown in Fig. 3.2

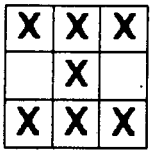

Figure 3.3 A seven point median filter mask (2 dimensional) for noise suppression as used by Salo et al (1988).

The main advantage of this combination of filters, is that the speed of the linear filter is combined with the median filter's ability to preserve edges because a five point median filter still operates at the speed of a conventional three point median filter.

Furthermore they developed a two dimensional seven point median filter mask which proved to perform best (according to subjective tests) to suppress noise as well as to reduce motion blur. This seven point filter mask is shown in Fig.3.3.

3.4 RADIO FREQUENCY CARRIER POWER ESTIMATION

Radio frequency (RF) Carrier power estimators is another technique for measuring the noise on the picture. By relating the RF carrier power to the video signal power, an estimation of the SNR can be obtained from the Carrier to noise ratio (CNR). The assumption here is that the dominant noise originates in the channel, because this is the only noise that this method measures.

3.4.1 Radio frequency demodulation

When an FM-modulated signal is demodulated to baseband, the carrier mixes down to zero frequency. This zero frequency signal is then taken as an estimation of the carrier power and the field strength of the RF signal. It is also used as a feedback to the RF amplifier in any television receiver as shown in Fig.3.4.

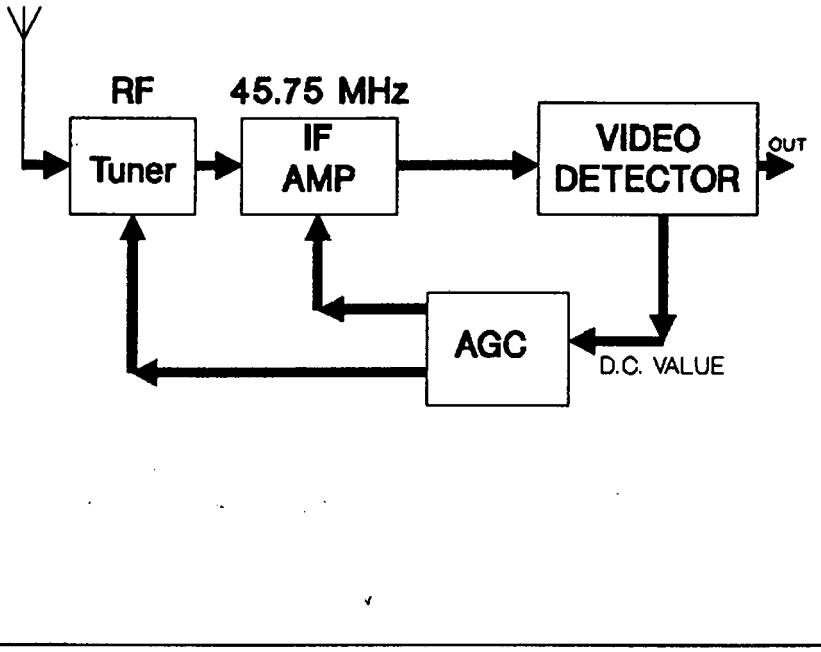

Figure 3.4 The Automatic gain control feedback loop in the receiver.

The purpose of this configuration is explained by Wilcox (1987) where he sates that the tuner has to amplify the desired frequency and convert it to an intermediate frequency (IF). The RF signal in the antenna can vary between 10 micro volts and 0.5 Volts RMS, depending on the strength of the received signal, and since the output baseband video must be constant at 1 V_{p-p}, the television has a very effective automatic gain control (AGC) system which detects increases in the output D.C.carrier and compensates by decreasing the gain in the IF amplifier and the tuner. This output of the AGC is then inversely proportional to the carrier power.

3.4.2 SNR estimation

Middleton (1983) derived the relationship between the signal to noise ratio and the carrier-to-noise spectral density ratio in a form of a conversion factor so that a spectrum analyzer reading could give a signal to noise ratio.

Similarly, Robinson (1987) derived a relationship between the vision CNR and the picture signal-to-noise-ratio. He proved theoretically and practically that the SNR is 8dB less than the CNR.

Isono and Ohmaru (1988) determined the carrier power of a satellite broadcast signal accurately by employing a standard-gain horn antenna attaining a high carrier-to-noise ratio by the cancellation of modulation components at the receiver.

3.5 BLIND NOISE ESTIMATION

Blind noise estimation techniques are very rare, because they are so difficult to implement. Nonetheless, this is the most effective solution to noise estimation, because it measures the noise that the eye sees, without any assumptions of where the most noise originates or which noise is the most visible.

Besl and Jain (1988) calculated the noise on a 3x3 block in the picture by fitting a surface to the block. They then assumed that all deviations from the surface was due to noise. Their a priory knowledge of the picture is that any sub-image of a natural scene could be fitted to a known surface, and that the slope anywhere in the picture can not be more than 8 levels/pixel, due to the correlation of the pixels. Another approach was to take the mean square difference of a median filtered image and the original as an estimation of the noise.

Meer et al (1990) criticized this method by Besl and Jain (1988) as not being robust enough especially in the low signal to noise ratio case. Alternatively Meer et al (1990) proposed to tessellate the image into small blocks of size mxm, where $m = 2^k$ and k is 1,2,3,..8. They calculated the mean and variance of every block and retained the four lowest variance values for every tessellation. This they used to estimate the noise with an accuracy of more than 80% for 98% of the time.

3.6 CONCLUSIONS

Since the existing measuring techniques rely on test inputs, they are of no use to this study. The field strength measuring techniques are of little use either, because they do not measure the noise on the picture itself, but merely assume that most of the noise originates in the channel.

The noise reduction methods on the other hand, offer an interesting approach, but due to the complicated motion detectors that have to accompany them, they seem to be computationally expensive.

Lastly the blind noise estimators are the ideal solution to our problem, because they measure the noise on the picture itself. The criticism by Meer et al (1990) of Besl and Jain's method, is valid, but Meer's method is not very robust because so called "flat" blocks are very rare in pictures of natural scenes, and their method is very computationally expensive.

We are proposing a new blind noise estimation method with many advantages compared to these methods.

CHAPTER 4

CHARACTERISTICS OF VIDEO IMAGES AND THEIR SPECTRA

4.1 INTRODUCTION

A television picture is unique in the sense that the limitations of the transmission system, together with the limitations of the viewer, restricts the picture content in such a sense that it has a very particular quality different to other visual media.

For example the difference between a television picture and a film is that in film the different pictures are flashed successively to simulate motion, whereas the television picture consists of lines as the electron gun scans across the screen. Together with the different aspect ratio is it possible to increase the size of the film projection much more than the television picture. Also, movement can only take place between pictures in film, whereas it can happen between lines in television. This makes television more susceptible to motion blur.

This example only highlights two differences which distinguishes television pictures from those of film. There are countless more examples but this serves just to illustrate the point.

The limitations of the viewer, mentioned previously are, that there should not be to much detail on the screen, nor should the movement be to fast, nor may the scenery change to rapidly. Considering these factors, this chapter will try to characterize television pictures; from where we will try to characterize the spectra of television pictures. Spectral analyses will then be investigated in greater detail.

The basic operation of color television will be explained and the effects of the PAL color system on the composite image will be investigated, but Patchett (1970) describes television operation and the PAL color system in greater detail.

Many people have researched the video baseband spectrum since 1965 (Rowe). In the context of a digitised image, this is similar to determining the spectrum of each line in the picture. Therefore this route will be taken initially. It will be called the one Dimensional spectral case (1DS).

The constraints on the television picture mentioned previously, was investigated by Schreiber (1986). This proved to have interesting implications on the two dimensional spectrum (2DS). This route was then followed.

4.2 TRANSMISSION

In television, a two dimensional picture has to be transmitted and reconstructed somewhere else. Since it is not possible to transmit a two dimensional signal instantaneously, some method is used to transmit all the information serially.

A short description of the operation of a simplified monochrome television system will now follow. This model, as shown in Fig.4.1, will be extended to a color system in a later section.

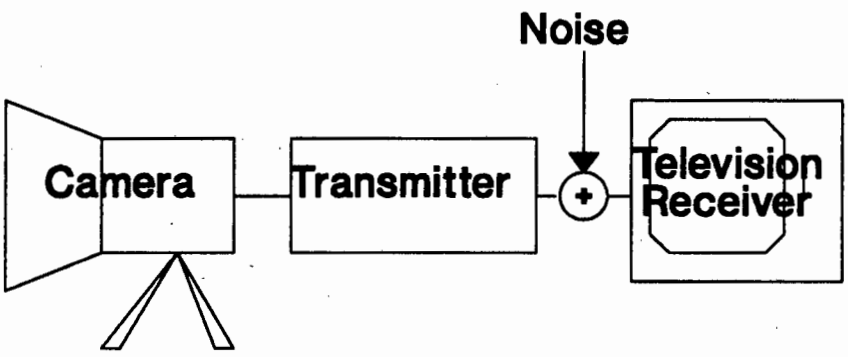

Figure 4.1 A simplified monochrome television transmission system.

4.2.1 Image formation

The simplified system shown in Fig.4.1, consists of a camera, transmitter, noisy transmission media and a monochrome television receiver. The picture is reconstructed in the receiver, when the electron beam in the cathode ray tube (CRT), of the receiver, stimulates the phosphor on the screen which causes the phosphors to glow for some time. The electron beam scans across the screen horizontally 512 times to cover the whole picture. The picture is therefore reconstructed out of 512 lines of picture information, although there are a total of 625 lines, the others being used for

transmission purposes. However, the electron beam does not scan all the lines in the first scanning. It first scans all the even lines and then returns to scan all the odd lines. This is known as the even and odd field respectively and together they form one frame, or one picture. This formation of the fields are shown in Fig.4.2.

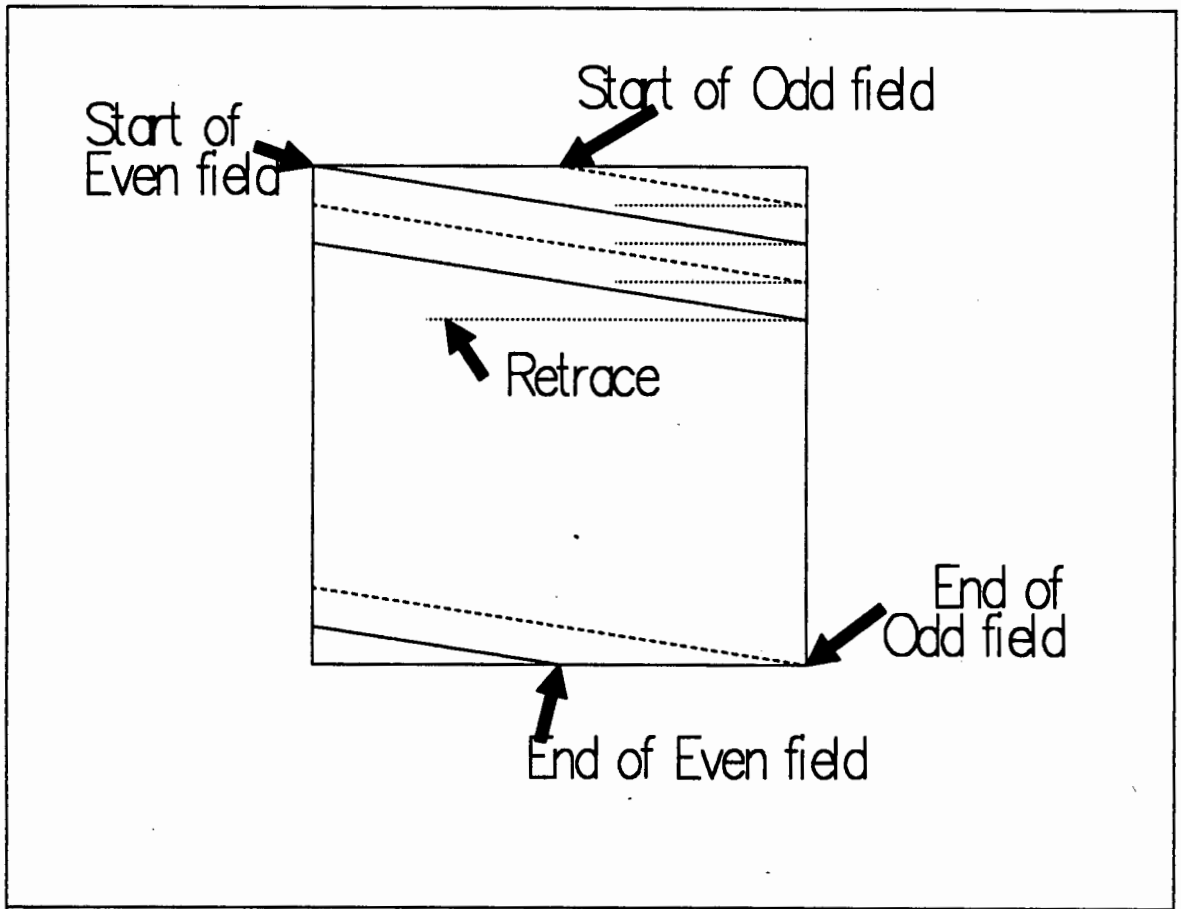

Figure 4.2 The television picture is formed when the electron beam first scans across the screen to cover the even lines (even field), and then returns to cover all the odd lines (odd field).

This explains the formation of the television picture. Another important factor is to ensure that the output light of the receiver television is linearly proportional to the light falling into the camera. This is called gamma (γ) correction and will be explained now.

4.2.2 Gamma (γ) correction

When the system in Fig.4.1 is considered, the light falling into the camera (Ec) should be linearly proportional to the light emitted by the receiver, Lu. This is expressed mathematically as

$$Ec \propto Lu .$$

However, the light that the CRT, in the receiver, emits (Lu) is proportional to the input voltage (Vc) as follows :

$$Lu \quad \propto \quad (Vc)^{\gamma} .$$

Since the voltage out of the camera is ideally equal to the voltage into the receiver CRT, it is necessary to predistort the output of the camera (Vc) to

$$Vc \quad \propto \quad (Ec)^{1/\gamma} ,$$

so that the receiver CRT can redistort the signal to

$$Lu \quad \propto \quad (Vc)^{\gamma} .$$

If Vc is now replaced with $Ec^{1/\gamma}$ we have

$$Lu \quad \propto \quad (Ec^{1/\gamma})^{\gamma}$$

and that creates the desired situation,

$$Lu \quad \propto \quad Ec$$

which means that we have a linear system. The SABC specifies that γ should be 2.8 ± 0.3

4.3 THE PAL COLOR SYSTEM AND COLOR THEORY.

The basis of any color television system, is summarized by Grassman's law (Rossouw 1976):" The impression created in the eye, when Red(R), Green(G) and Blue(B) light impinge on the same spot, is similar to when one light source, with the same intensity as each of the Red, Green and Blue beams, impinge with the eye."
All color pictures are therefore transformed in the camera into Red, Green and Blue signals, and the Red, Green and Blue signals are then used to reconstruct the color pictures in the receiver. The Red, Green and Blue are chosen from the so called color triangle, or C.I.E. triangle, as explained next.

Figure 4.3 The C.I.E. color triangle

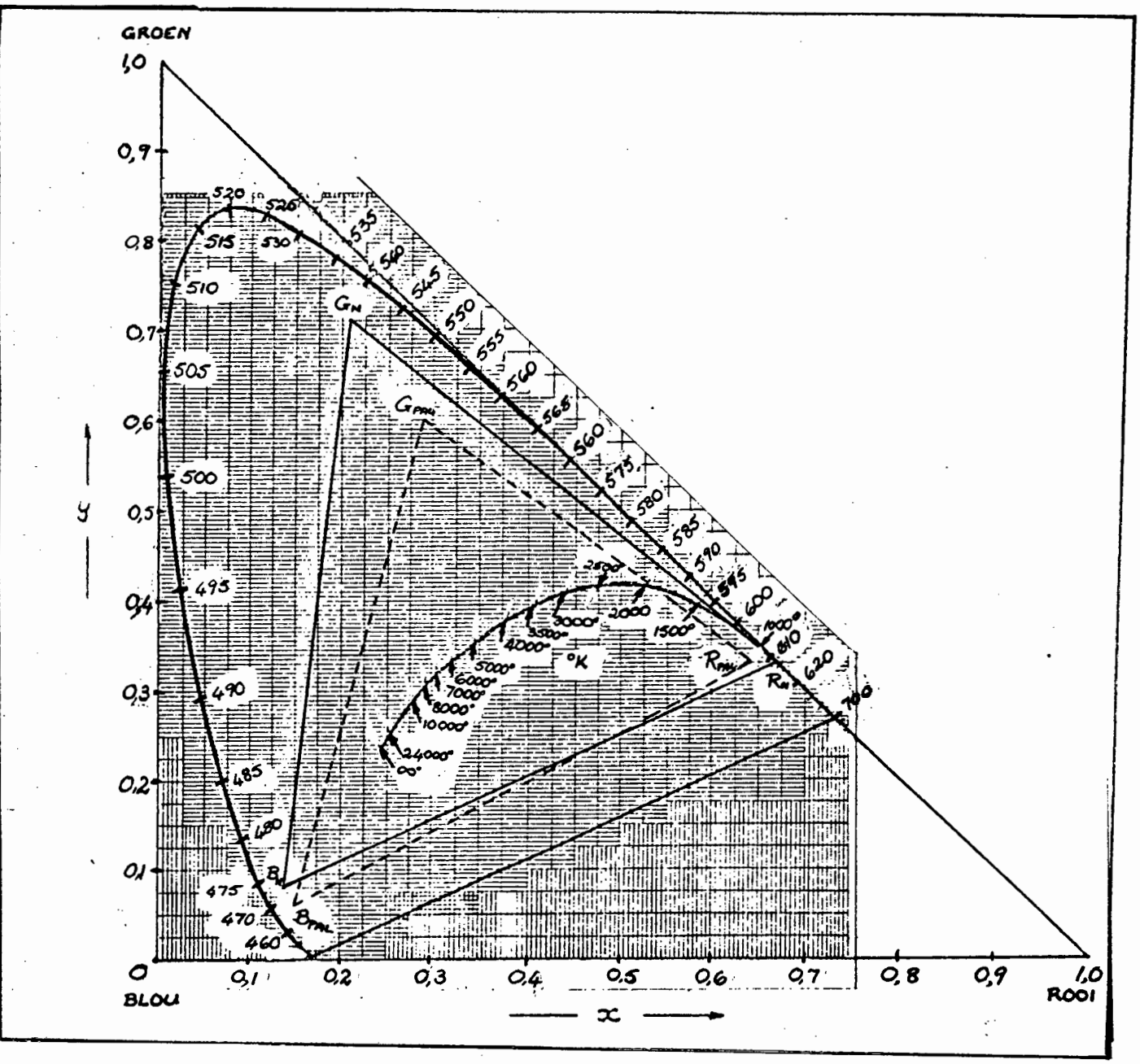

4.3.1 The C.I.E. Triangle

The Commission Internationale de'l' Eclairage (C.I.E) proposed a triangle, as shown in Fig.4.3, with corners so that the full visible spectrum lies inside a horseshoe shaped area inside the triangle.

If the 3 primary colors (Red, Green and Blue) are chosen as the corners of a triangle inside the big triangle, for a particular system, all colors inside the small triangle will be available to that system.

In Fig.4.3 Rn,Gn,Bn are the corners chosen for the NTSC system, and Rpal,Bpal,Gpal are the corners chosen for the PAL system. From Fig.4.3 it can be seen that NTSC has more colors available than PAL, because the area of the NTSC triangle is bigger than that of the PAL triangle. However, due to the better clarity in the phosphors on the screen of the PAL system, the PAL system is still acceptable with less colors.

4.3.2 Formation of the PAL composite video signal

The color signal must be compatible with the monochrome signal. Since the monochrome signal only has a luminance component, the composite color video signal has to consist of a luminance signal and some color information. The luminance (Y) is constructed from the Red, Green and Blue signals in the following way:

$$Y = rR + gG + bB$$

Where the constants r,g and b, are determined from the sensitivity curve of the eye shown in Fig.4.4 (Mothersole L.M, 1967). The eye is about twice as sensitive to green as to red, and about three times as sensitive of red as to blue. This means that there should be twice as much green as red information in the picture, so as to be pleasing to the viewer.

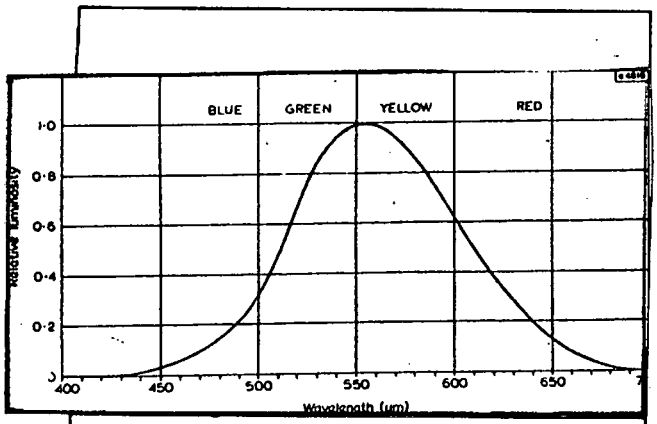

Figure 4.4 The sensitivity curve: The visibility curve for a normal eye. This curve indicates the relative brightness of equal energies of spectrum colors as a function of wavelength.

Thus:

$$Y=0,3R+0,6G+0,1B$$

or more accurately:

$$Y=0,299R+0,587G+0,114B$$

Since Y forms the main component in the composite signal, it is only necessary to use either two of R,G or B. The third will be reconstructed at the receiver. It was decided to use the difference signals, R-Y and B-Y, as the color signals. This choice of color signals simplified the receiver so that green could be reconstructed without an amplifier. These difference signals are weighted so that the composite video signal can have a peak to peak value of 1V maximum.

Therefore

$$V=Kb*(B-Y) \text{ and}$$
$$U=Kr*(R-Y)$$

Where U and V are the chrominance information and the values of Kb and Kr are:

$$Kb=0,493$$
$$Kr=0.877$$

The U and V signals are amplitude modulated onto a color carrier frequency, f_c = 4,43361875MHz ± 1Hz. The U is modulated with sin(wt) and V with sin($wt \pm 90°$). The phase of the V signal thus leads the color carrier in one line and lags it in the next, thus from there the name :Phase alternating Line (PAL).

The composite video signal (COMP(w)), is then formed from these components as follows:

$$COMP(w) = Y + U + V$$

where U+V can be rewritten as:

$$U+V=\sqrt{(V^2+U^2)}\ \sin(wt+\alpha)$$

where $\alpha=\arctan(U/V)$

If another term S (saturation), is set equal to $|U+V|$, COMP(w) can be rewritten as:

$$COMP(w) = Y + S\ \sin(wt + \alpha)$$

All the information is thus contained in Y,S and α, or luminance, saturation and hue.

4.3.3 A comparison of the noise powers in the 3 colors

Now that it is known how the composite video signal is formed, an estimation can be made how a certain impairment of white noise to the composite signal, will effect the different color signals.

It is seen from the weighting factors, Kb and Kr, that the blue signal is attenuated by 1/0.493 (1/0.493=2.028), and the red signal is attenuated by 1/0.877 (1/0.877=1.140). Since the green signal has to be reconstructed at the receiver as follows,

$$G = 1,67Y - 0,5R - 0,17B$$

the total attenuation is calculated :

$$\begin{aligned} G_{ATT} &= 1,67 - 0,5*1,14 - 0,17*2,02 \\ &= 1,67 - 0,57 - 0,343 \\ &= 0,757 \end{aligned}$$

This means that in the composite video image, the blue signal component is the smallest, and will thus be the most affected by a certain impairment of noise.The Red and Green signal components are respectively bigger and they will be affected progressively less by an impairment of noise.

4.4 SPECTRAL ANALYSES

For any television picture, irrespective of color, spectral analyses is a method of analyzing the signal characteristics.

4.4.1 One Dimensional spectral analyses

Since the picture consists of many lines, a spectrum estimation is made of a picture by taking the spectrum of each line, and using this to estimate a spectrum for the picture. The different lines differ in terms of picture content, but not in terms of picture quality and characteristics. In order to obtain one spectrum estimation per picture, it is important to reduce the variance of the different line spectrum estimates. A standard approach to reducing the variance of estimates is to average over a number of independent estimates. The application of this approach to spectrum estimation is often attributed to Bartlett. In this approach the picture $x(i,n)$, $0 \le n \le N-1$, $0 \le i \le N-1$, is divided into K line segments of M samples each so that $N=KM$; i.e., we form the segments

$$x^i(n) = x(i,n), \qquad 0 \le n \le M-1, \quad 1 \le i \le K$$

and compute the K periodograms

$$I^i(w) = \frac{1}{M} \sum_{n=0}^{M-1} | x^i(n) e^{-jwn} |^2, \qquad 1 \le i \le K$$

If the autocorrelation function $\phi_{xx}(m)$, is small for $m > M$, then it is reasonable to assume the periodograms $I^i(w)$ are independent of each other. The spectrum estimate is defined as

$$B_{xx}(w) = \frac{1}{K} \sum_{i=1}^{K} I^i(w)$$

(Oppenheim and Schafer, 1975, p548).

A logarithmic scale is used for display purposes, due to the wide dynamic range of the spectrum. These averages therefore represent a typical video spectrum, and are shown in Appendix A. The shape of these spectra has been described as long ago as in 1965 by Rowe, and later confirmed by Böck (1989). Since the experiments done by Böck was on the composite video baseband signal, this model had to be verified for the special case where the input is digitized and only the picture information used. A probability plot was made of 10 different pictures spectra. This was repeated for the red, green, blue and composite images. These are shown in appendix B. The results are similar to those obtained by Böck et.al. (1989). Fig.4.5 shows a typical video spectrum with the estimated curve superimposed. The estimation seems to be quite accurate in this case.

In section 4.2.1 we saw how the television picture is made up of an odd and an even field, to form one frame. When this picture is digitized, it becomes an array of 512x512 numbers in the computer memory. The rows in the array corresponds to the lines in the picture as explained previously. However, when one looks at the columns of this array, this does not correspond to anything that has been described previously. When the spectra are taken of these columns, purely spatial information are in the spectra. However, due to the fact that every picture is made of two fields, of every two neighboring numbers in the column, one will belong to the odd field, and the other will belong to the even field. This means that these two neighboring pixel were created 64x256 micro seconds apart. During this time some movement could have taken place at the input scene, which would mean that the two numbers are less correlated than expected. This is called motion blur and will manifest itself in the spectrum as very high frequency power. This is clearly seen in the column spectra plotted in appendix C.

It is now important to note the effect of variations in brightness, noise, and contrast on the spectrum.

4.4.1.1 Contrast.

When the contrast of an image is changed it corresponds to multiplication of the intensity of each pixel by a constant. For an input image f(t) and an output image g(t),

Let $g(t) = a\ f(t)$ where a is the constant multiplier and let :

$$g(t) \quad \text{Fourier Transforms} => G(w)$$

$$f(t) \quad \text{Fourier Transforms} => F(w)$$

Then on a logarithmic scale

$$\log \{G(w)\} = \log \{F(w)\} + \log (a)$$

This means that the shape of the spectrum does not change when a is changed, only the absolute values are shifted when we adjust the contrast in an image.

4.4.1.2 Brightness (Day/Night scenes)

Again, for an input image f(t) and an output image g(t), when the light level increases it corresponds to a uniform intensity of the irradiation increasing by a constant amount. (This is only true for a constant reflectance in the image formation stage.) Then

$$g(t) = a + f(t) \qquad \text{where a is a constant}$$

In the transform

$$G(w) = F(w) \text{ for } w > 0$$

but $$G(0) <> F(0)$$

Therefore only the level of the origin of the spectrum changes (the dc value).

4.4.1.3 Noise

Again, for an input image f(t) and an output image g(t), when the input image is degraded by the addition of white (Gaussian) noise, we can write

$$g(t) = f(t) + n(t)$$

$$G(w) = F(w) + N(w)$$

$$\log \{G(w)\} = \log \{F(w) + N(w)\}$$

$$\log \{<G(w)>\} = \log\{<F(w)> + N\}$$

where $< >$ indicate an average over the picture and N is a constant independent of w. The "average" of the image power spectral density has been modelled as (Carpenter et al 1989):

$$S(f) = \frac{P' B}{B^2 + f^2} = \frac{P'}{B(1 + (f^2/B^2))} \qquad (4.1)$$

with B the "picture bandwidth" of the luminance signal which is about 50 kHz,

P' is the power of the luminance signal and

$$P = BP'$$

f varies from 0 to 5 MHz.

Because $B^2 << f^2$ over most of the spectrum, we can write

$$S(f) \approx \frac{P'}{B\,(f^2/B^2)}$$

$$= \frac{B\,P'}{f^2} \qquad = \frac{P}{f^2} \tag{4.2}$$

Hence $\log \{<G(w)>\} = \log \{BP/f^2 + N\}$

Now from the characteristics of logarithmic plots we would expect that the constant noise added should show up most in regions where the level of the other term is smallest. This is indeed the case as can be seen if we look at the extremes in frequency i.e. f=1 Hz and $f=5.10^6$ Hz:

$$\log \{BP/f^2 + N\} \mid_{f=1} = \log \{BP + N\} \approx \log \{BP\}$$

$$\log \{BP/f^2 + N\} \mid_{f=5e6} = \log \{BP/25\ 10^{12} + N\} \approx \log\{N\}$$

The result is therefore a much more visible increase in the power spectral density due to white noise at the higher frequencies, where the image power spectral density is much lower and the noise to signal ratio is therefore much larger.

4.4.1.4 An example of determining the expected noise and signal levels

In equation 4.1, we obtained an expression for a power spectral density plot for a typical television picture. At 50kHz we find the -3dB point of the picture spectrum. If this bandwidth is used in our model we can obtain an expected signal power level ratio

at any frequency. For instance, we can calculate the expected signal power level at f = 5 MHz compared to 20 kHz. (This is 1/256 of 5Mhz, the highest frequency resolution on our plot.)

We had

$$S(f) = \frac{P}{B^2 + f^2}$$

We can calculate the drop in power level as we go from 20kHz to 5MHz in dB:

$$10 \log (S(f_{20kHz})/S(f_{5MHz}))$$

$$= 10 \log \frac{[(50.10^3)^2 + (20.10^3)^2]}{[(50.10^3)^2 + (5.10^6)^2]}$$

$$= 10\log\{(2900.10^6)/(25.10^{12})\}$$

$$= -39.4 \text{ dB}$$

A plot of the average spectrum of an actual broadcast television picture is shown in figure 4.5. The smooth curve is a plot of equation 4.1, fitted to the data. It can be seen that there is the expected drop of about 40 dB between the first point (not zero frequency) and about 5 Mhz.

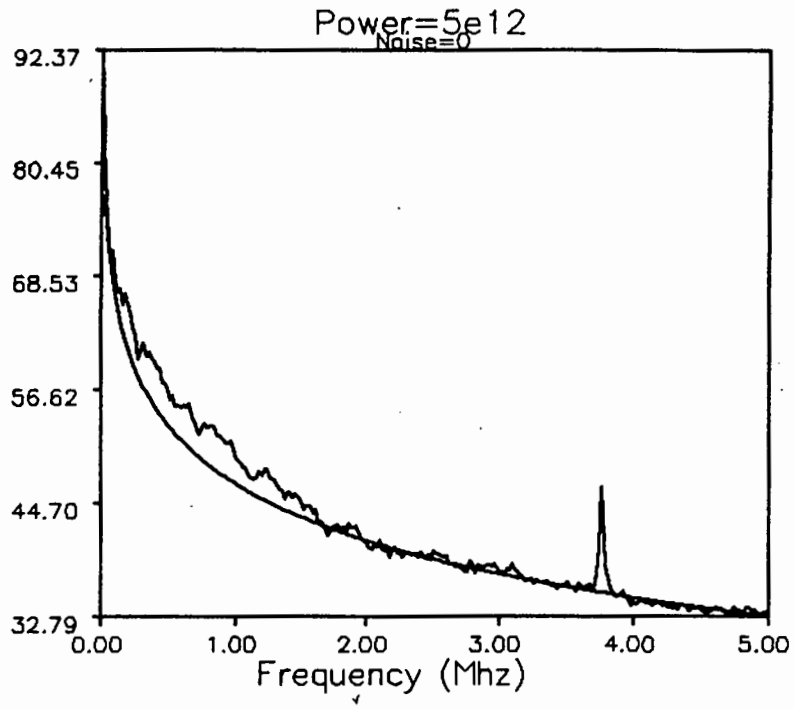

Figure 4.5 The average spectrum of an actual broadcast television picture showing the decrease in power spectral density with frequency. The smooth curve represents the expression given in equation 4.1 for a model of the spectrum.

It was, however, not possible to determine a least squares error (LSE) approximation of equation (4.2) to real data. This is because the spectrum only approximates equation (4.2) on a logarithmic display, on a power display the two deviate significantly in the low frequencies. In this case this will upset the whole approximation as the errors in the low frequencies are quite severe.

Another approach is to take the picture as a whole, to determine the constraints put by the viewer and find the characteristics of the 2DS of the picture.

4.4.2 Two Dimensional analyses

Most of the work in this section is taken from Schreiber (1986, pp.42-46). Some insight into the shape of the spectrum can be gained by considering the distribution of types and size of objects usually depicted. From this information the autocorrelation function can be calculated, and from the latter the general shape of the spectrum can be inferred. (Ritterman, 1952).

Sensible images must depict objects that are mostly larger than the smallest resolvable spot, or else the image would look like sand on a beach. For the present purpose, let us suppose that the (one-dimensional) image $L(x)$ consists of a number of uniform patches of random width and intensity. The autocorrelation function $\phi(\tau)$ is defined as

$$\phi(\tau) = \frac{1}{2a} \int_{-a}^{a} L(x)L(x-\tau)dx.$$

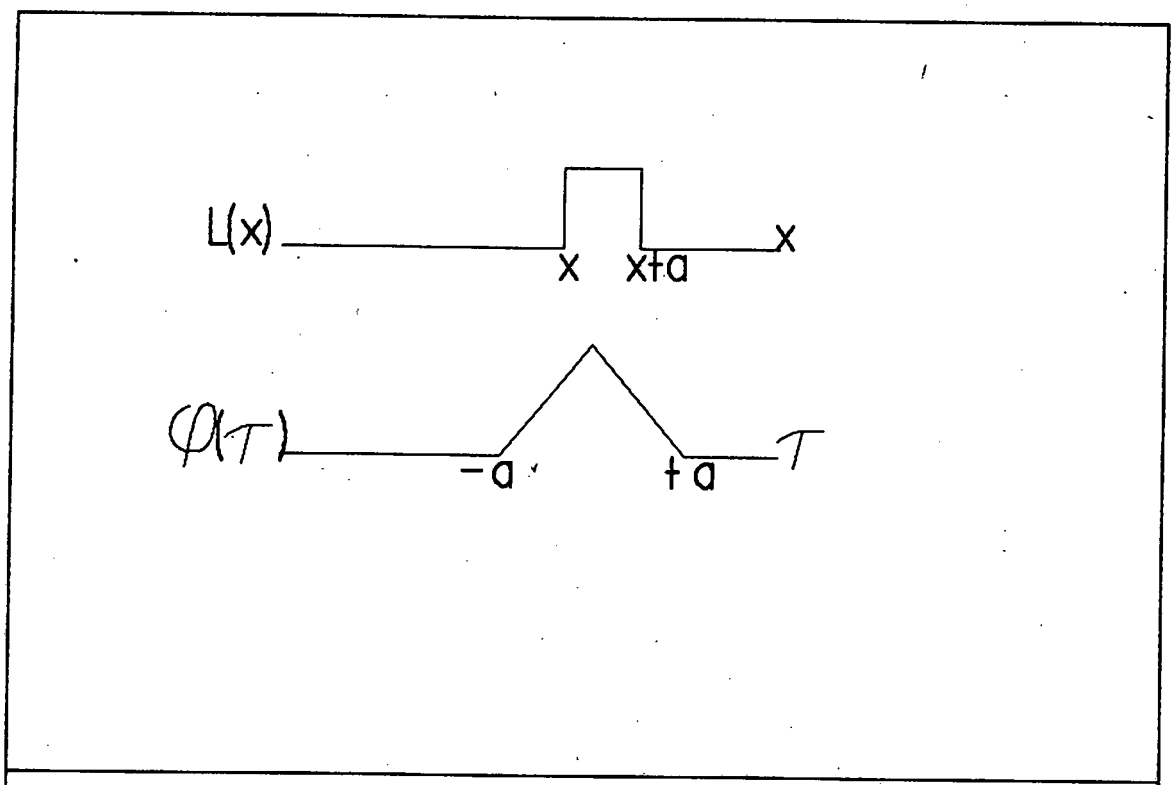

Figure 4.6 A pulse and its correlation function.

For the pulse in Fig.4.6 $\phi(\tau)$ is a triangle of base 2a. The sum of a large number of triangles with various heights and widths can be assumed without serious error as

$$\phi(\tau) = k \exp(-k_1 \mid \tau \mid).$$

Where k and k_1 are constants depending on the input, $L(x)$.

Actual measurements confirms the generally exponential behavior of the autocorrelation function. (Kretzmer, 1952)

We define the power spectrum of function $L(x)$ as :

$$\Phi(w) = A(w)A(w)^*,$$

where $A(w)$ is the Fourier transform of $L(x)$. The Wiener-Khinchine theorem shows that

$$\Phi(w) = \int_{-\infty}^{\infty} \phi(\tau) \exp(-jw\tau)d\tau,$$

i.e., the autocorrelation function and the power spectrum are a Fourier transform pair. For the symmetrical exponential above,

$$\Phi(w) = \frac{2k_1}{(k_1^2+w^2)} .$$

Thus we see that amplitude of the power spectrum begins to decrease at $w=k_1$ and, at high spatial frequencies, falls as $1/w^2$. Since k_1 depends on the typical object size, the break point is higher for images with copious fine detail.

In a two dimensional image, a similar exponential autocorrelation function can also be expected, not because of the size of the objects, but because the image can change only slowly in time if motion is well depicted. Thus, in the time direction also, the spectral intensity decreases rapidly with frequency.

The two dimensional spectra of the red, green, blue and composite images are plotted in Appendix D. These spectra are each the average of 10 spectra. This is similar to the approach taken by Ulichney (1988), to average many spectra to obtain a periodogram.

4.5 HOW THE EYE PERCEIVES NOISE

In the previous sections much has been said about the spectral characteristics of images. Another approach will now be followed trying to detect how the eye sees noise.

The eye notices noise best on a flat surface with no movement and no sharp edges. There must therefore not be any high frequency components in the picture, in any one of the three domains, for the noise to be most noticeable. This is because the eye acts as a differentiator at low frequencies, where it can differentiate the background away. It also detects the faster movement (eg.noise) better than the slow movement (picture information) because high frequencies are accentuated in the differentiation process. This makes one think that it is the high frequency components of the noise that makes it the most visible. Contrary to this the higher the frequency of the noise, the smaller the size of the impairment, and the less the eye can see it as proven by the sensitivity curve of noise in Fig.4.7 (Lowry 1984).

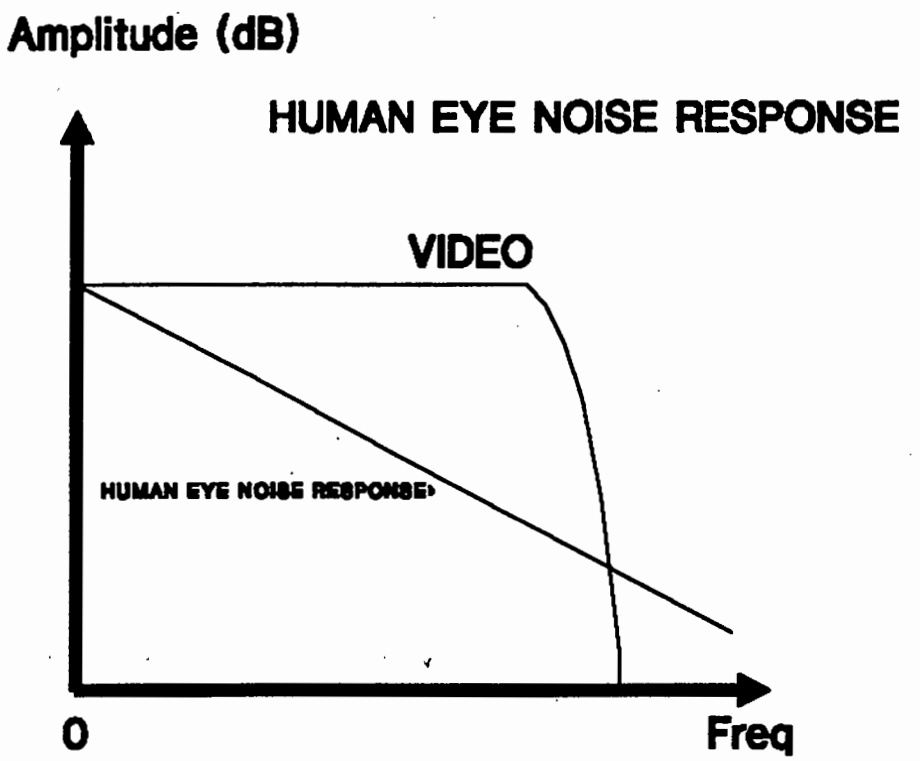

Figure 4.7 The human eye perceives a noise characteristic which is essentially triangular, decreasing with frequency.

This controversy can be cleared up by looking at some of the characteristics of the eye. In Fig.4.8 (Caelli T., 1981.) the spatial contrast sensitivity function shows that the eye differentiates below a certain frequency and it integrates above another.

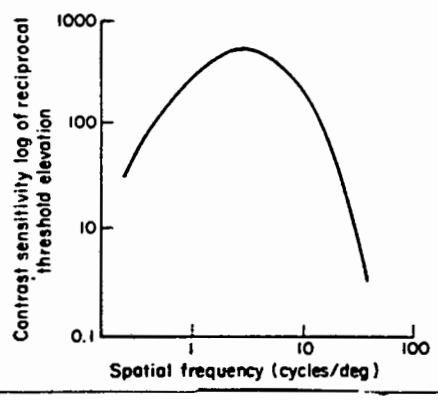

Figure 4.8 Typical contrast sensitivity function for the human visual system; sine-wave grating stimulus.

It is now important to discover in which range this problem lies. In watching television, it is necessary to be $6H$ away from the television, where H is the height of the television. This means that the eye has a range over an angle of

$$\Theta = \tan^{-1}(1/6)$$

$$= 9.46°.$$

Since we want to know how the eye's response is at f cycles/deg,

$$f = 1/9.64°$$

$$= 0.1 \text{ cycles/deg.}$$

This is the lowest limit on the graph. In normal conditions the eye has a visual acuity of one minute of arc according to Moses et. al. (1975) (minimum angular distance between two objects without merging). This corresponds to an f of 60 cycles/deg which is the highest limit of the graph. Therefore television uses a wide range of visible frequencies.

Now we see that there is no contradiction any more, because the eye cannot see the highest frequency noise, due to integration , and neither the very lowest frequency noise due to differentiation. Therefore, there is an optimum frequency for the eye to see the noise.

However, it is better to look at a three dimensional display of the eye sensitivity response as in Fig.4.9. This display adds the temporal frequency response to Fig.4.8.

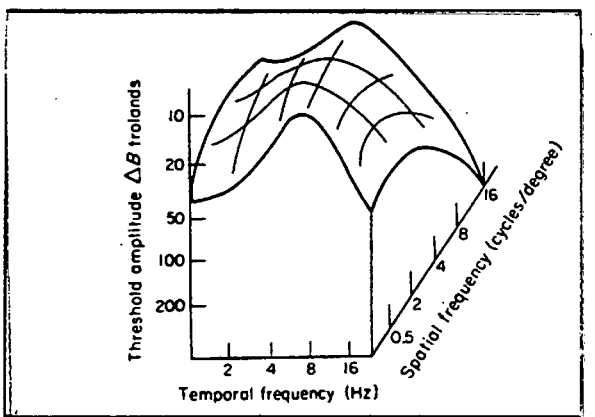

Figure 4.9 Spatio-temporal contrast sensitivity function examined by Kelly (1978).

An example will prove the need of the third dimension: If the whole picture became lighter or darker (i.e. low spatial frequency noise), the disturbance to the viewer will actually depend on the temporal rate of change than the spatial rate of change, thus the need for the third dimension.

This information can now be used to measure the quality of the television picture by eye simulation (Pomerleau A; Sylvain D; 1982). Unfortunately this eye simulation could not be investigated further. While it is a very interesting approach, a more robust method seemes to be spectral analyses.

4.6 CONCLUSIONS

From this chapter some conclusions can be drawn regarding the characterictics of television pictures and their spectra:

1 Image formation

1.1 Due to the interlacing in picture formation, motion blur manifest itself as high frequency power in the spectrum.

1.2 Due to the constants Kb and Kr, the blue image is the most noisy, and then the red and green images are progressively better.

1.3 Due to the color carrier at 4.3 MHz in the composite image, the high-frequency power in the composite spectrum is not primarily due to noise. A monochrome image or one of the red, green, or blue images must be used in future for noise estimation in spectrum analyses.

2 Spectrum analyses

2.1 One dimensional spectrum analyses gives good results in noise estimation, but it does not account for the fact that the eye sees noise in three dimensions.

2.2 Because three dimensional analyses is very complex, due to the large ammount of data (512^3), two dimensional analyses is a good compromise between true 3D noise visibility estimation and computation time.

3 Shape of the spectrum

3.1 A change in contrast does not change the shape of the spectrum, only the spectral offset.

3.2 A change in brightness does not change the shape of the spectrum, only the zero frequency value.

3.3 Addition of noise to a picture is like adding a constant to the spectrum. This constant is most significant in the high frequencies.

3.4 The shape of the two dimensional spectrum is 1/frequency^2 in the high-frequencies, in both dimensions.

CHAPTER 5

THE 2 DIMENSIONAL SPECTRAL METHOD OF NOISE MEASUREMENT

5.1 INTRODUCTION

We have seen in the previous chapter that although the different pixels in a moving sequence of pictures can vary rapidly and independently, the shape of the two-dimensional Power density spectrum (2D PDS) does not change much with time. The shape of the spectrum is more a function of picture attributes and television system constraints than of picture content. Schreiber (1986) asserts that picture attributes that are important to human observers are that the picture movement in the picture must be slow enough to be noticeable, scenes may not change so rapidly as to be disturbing, and there should not be too much detail and clutter in the image. An example of the latter is the high spatial frequency information in an area of the SABC circle test pattern that skimmers with Moire' effects and is fatiguing and unpleasant to look at for any length of time. System constraints include amplitude/frequency response limitations (5,5 MHz in the South African television standard) and other signal amplitude limits. In short the whole picture is bandlimited in the horizontal, vertical and time domain. In fact the shape of the spectrum is well known and has been described by (Böck, A. M. ,Gallois, A. P. and Carpenter, D.C,September 1989), as:

$$S_L(f) = P_L B_L/(B_L^2+f^2) \qquad (5.1)$$

Where $S_L(f)$ is the PDS of the luminance signal

P_L is the luminance power

B_L is the luminance bandwidth

Schreiber's two dimensional spectrum prediction in chapter 4, can also be extended to :

$$S(f_x,f_y) = S_L(f_x)\, S_L(f_y)$$

According to these formulae, very low picture power is expected in the high frequencies. This is indeed the case as can be seen from fig. 5.1.

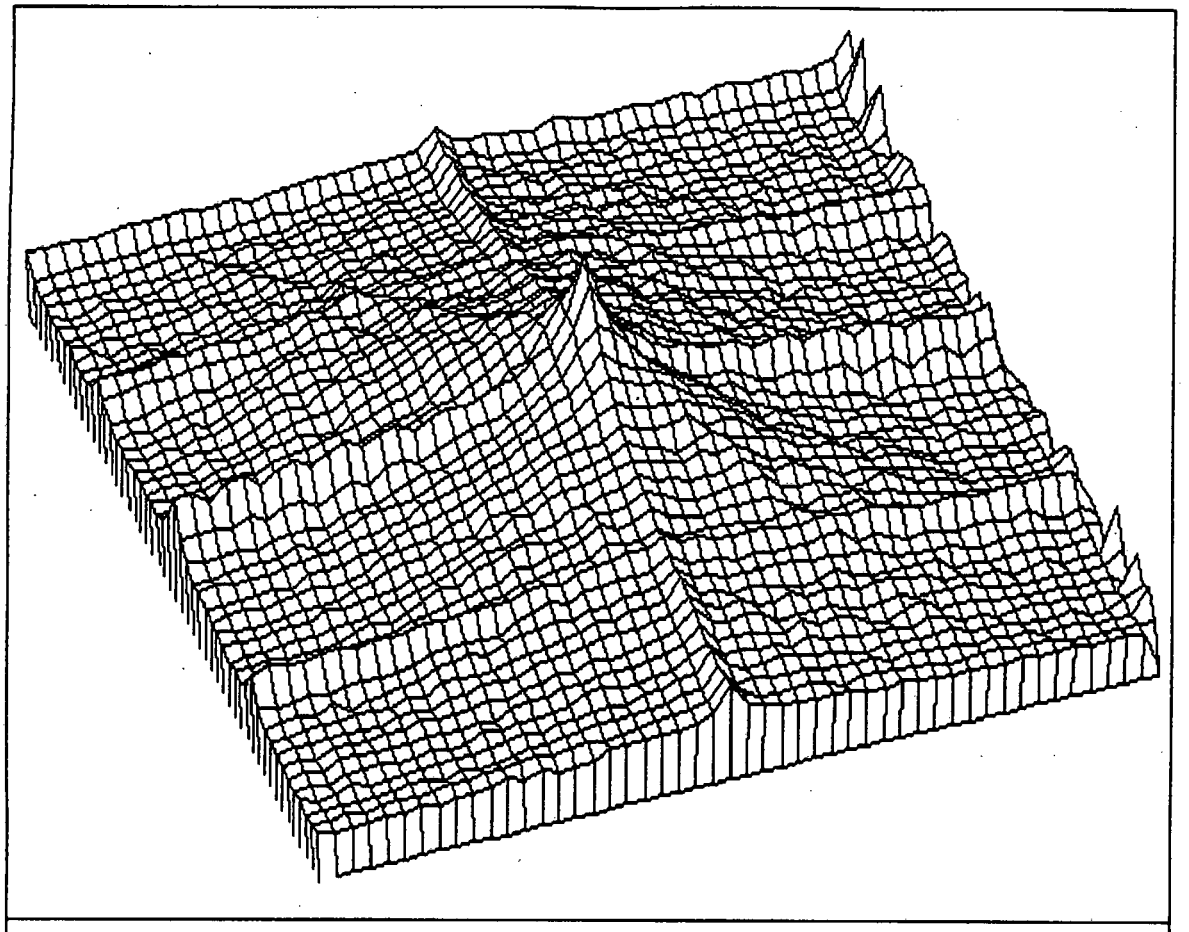

Figure 5.1. A 2D PDS of a television picture. The power is plotted on a logarithmic scale. Note the low power level in the corners (high frequencies).

This might be the case for a picture without any noise. After the addition of noise, the shape of the 2D PDS changes especially in the high frequencies. Note how much power are in the corners (high frequencies) of the 2D PDS in fig.5.2.

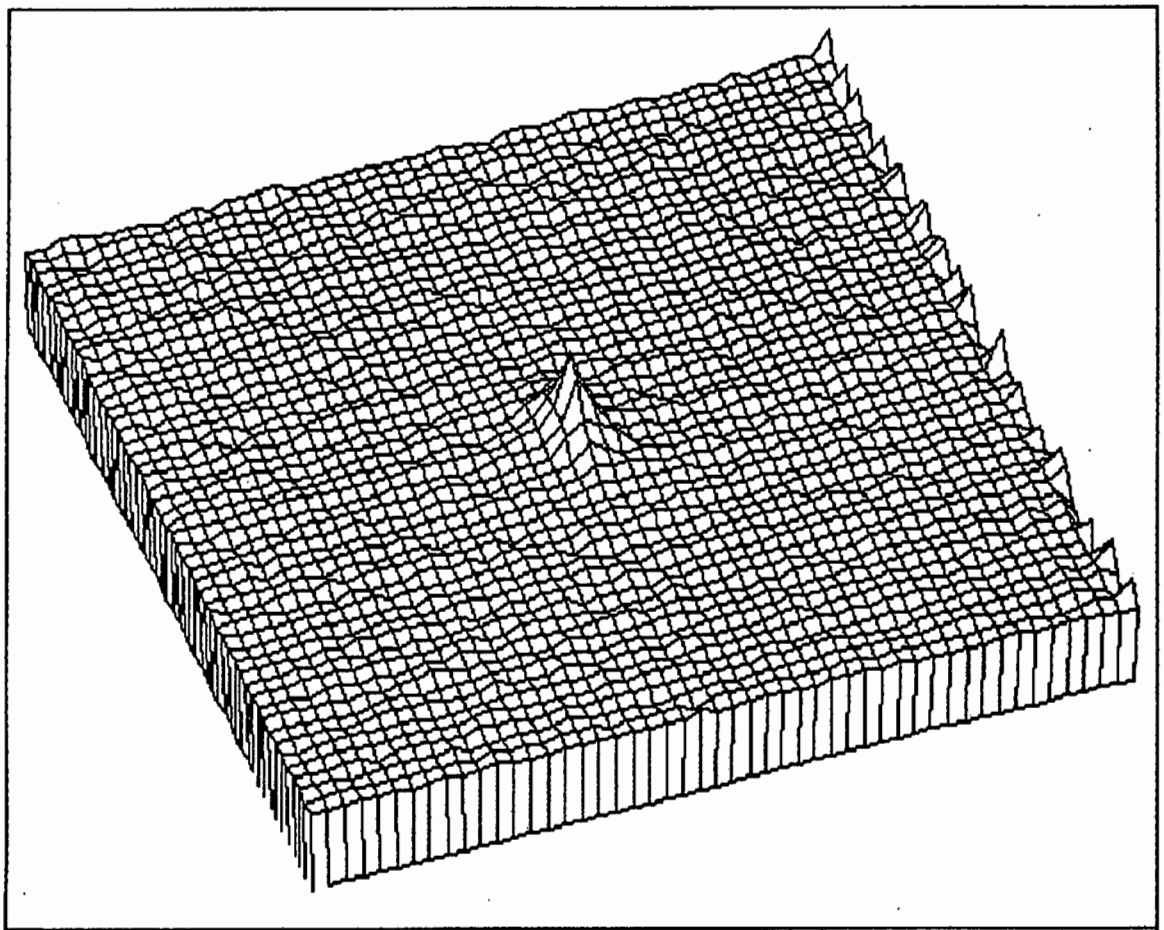

Figure 5.2. A 2D PDS of a picture to which noise has been added. Note the high power level in the corners.

Thus, an average of the minimum power at the higher frequencies may be taken as an indication of the picture noise power.

5.2 THE REASONS FOR TESSELLATING THE PICTURE

It may happen that there is much structure in a picture, like in the SABC test pattern. This will lead to a 2DS with high-frequency power which again would lead to a bad noise power estimation. The estimation by Böck et al. (1989) in equation 5.1, is a statistical approximation made by averaging spectra of more than 40 000 pictures. In order to get some statistics from one picture, the whole picture is tessellated into subimages.

5.2.1 Determining the range in the spectrum of most picture power

It is known from spectral analyses and Schreiber (1986) that the most picture information is less than 2,5 Mhz in the frequency domain. This is confirmed by the spectrum estimation in equation(5.1) by Böck et al. (1989). This formula is used to determine the ratio of power below 2,5 MHz compared to total picture power:

$$\frac{\int_{0MHz}^{2,5MHz} S_L(f)\,df}{\int_{0MHz}^{5MHz} S_L(f)\,df} * 100\%$$

$$= 98,71\ \%$$

This means that only 1,3% of picture power lies above 2,5MHz. This calculation can be repeated to determine that only 4,43% of picture power lies above 1,125MHz. The upper limit of the spectrum is 5 Mhz as will be explained in the next section. On a single scan line in an image, 5Mhz information means alternate bright and dark spots as shown in Fig.5.3.

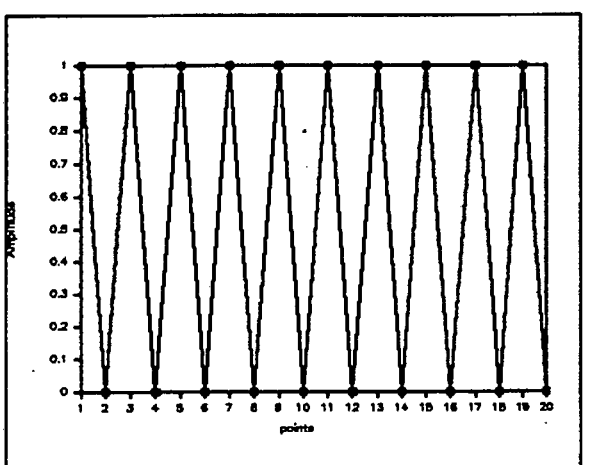

Fig.5.3. An example of 5Mhz information on a single scan line in a picture.

If the maximum frequency information on the picture is 2,5Mhz a square waveform is obtained as shown in Fig.5.4.

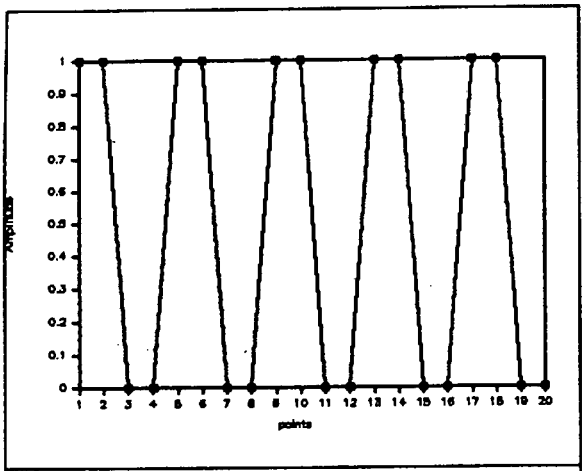

Fig.5.4. An example of 2,5Mhz information on a single scan line in a picture. This is more commonly found than that in Fig.5.3.

If this idea is extended to 2 dimensions, it would mean that the whole image consists of 2x2 (or bigger) constant luminance (flat) blocks. We can see that because there is so little picture power above 2,5MHz or even 1,25MHz, the majority of 2x2 or 4x4 sub-images will only contain flat surfaces. Again if the sub-image size is increased to say 8x8 or 16x16, the majority of these sub-images might not contain flat areas, but will probably not contain high-frequency power above 1,25MHz. A good example of this is shown in Fig.5.5, where a dithered version of an ordinary picture is displayed with an 8x8 grid superimposed, representing the sub-images. It can be seen that the majority of areas inside each sub-image are flat or slowly varying.

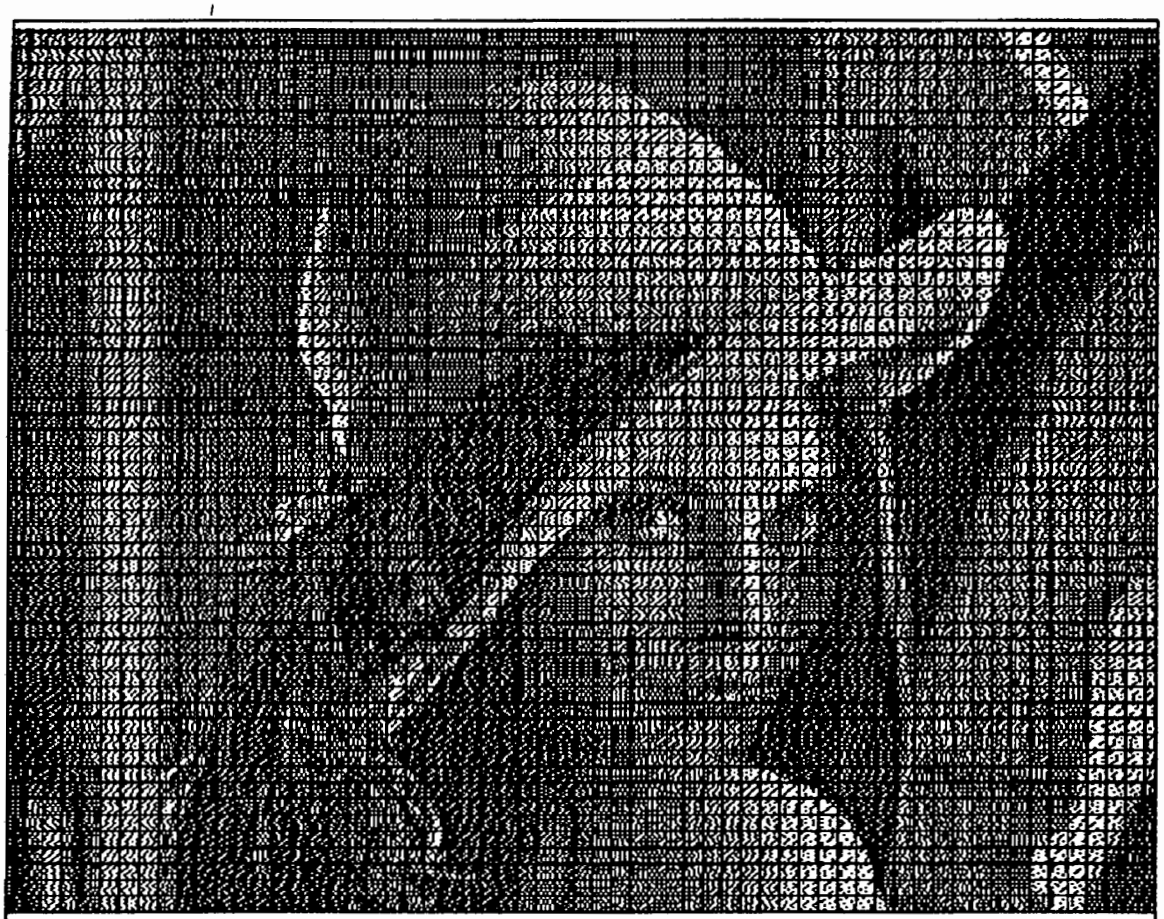

Figure 5.5 A dithered version of an ordinary picture, with an 8x8 grid superimposed, representing sub-images. Note that most of the sub-images contain flat or slowly varying surfaces.

5.2.2 Tessellation

If the whole picture is now tessellated into 256^2 blocks of size 2x2, it is a reasonable assumption that the signal inside each block to vary slowly and thus have only very low frequency information. The high-frequency information is thus mainly due to noise. This rule should apply to at least the majority of blocks in the picture. This idea is similar to that expressed by (Peter Meer, Jean-Michel Jolion, Azriel Rosenfeld, 1990). After calculating the noise variance for each block they used the 4 smallest σ^2 values as an estimation of the noise variance. They used the following formula to calculate the variance σ^2,

$$\sigma^2 = \Sigma(x(n)-<x>)^2/N$$

where

$<x>$ is the mean value of x(n) in each block.

5.2.3 The probability of flat blocks in the image

As the block size (mxn) is increased, the probability of the block containing flat areas decreases. This probability will now be calculated. It is known from chapter 4 that the correlation of a pixel with its neighboring pixels at different distances away, is an exponential function as shown in Fig.5.6.

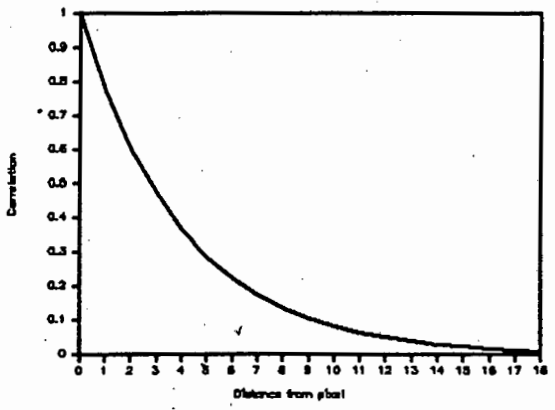

Fig.5.6. The correlation of any pixel with it's neighbors at different distances away in a picture.

If this correlation is seen as an autocorrelation function $\phi_{xx}(n,m)$ (now in 2 dimensions) of a picture signal f(n,m), then $\phi_{xx}(n,m)$ is defined by (Oppenheim and Schafer,p.384,1975) as:

$$\phi_{xx}(n,m) = E[x_n, x_m^*]$$

$$= \int_{-\infty}^{\infty} \int_{-\infty}^{\infty} x_n x_m^* \, P_{x_n, x_m}(x_n, n, x_m^*, m) dx_n dx_m$$

Where $P_{x_n, x_m}(x_n, n, x_m^*, m)$ is the probability function of f(n,m). This probability function has to be determined for a flat block of size mxn. For a flat block, $x_n = x_m$ and the product $x_n x_m$ is independent of n and m. By differentiating the above equation partially on both sides, the following is obtained:

$$\frac{\partial \quad \partial}{\partial x_m \partial x_n} \phi_{xx}(n,m) = x_n x_m \, P_{x_n, x_m}(x_n, n, x_m^*, m)$$

Since $\phi_{xx}(n,m)$ is known for the signal f(n,m) as

$$\phi_{xx}(n,m) = e^{-knm},$$

we have:

$$Px_n,x_m(x_n,n,x_m^*,m) = \frac{\partial}{\partial x_m}\frac{\partial}{\partial x_n} e^{-knm}$$

$$Px_n,x_m(x_n,n,x_m^*,m) = c_2\, e^{-kmn}. \qquad (5.2)$$

Where $c_2 = -k/(x_n x_m)$.

From equation 5.2 we see that the probability of finding flat blocks are exponentially decreasing as the size is increased.

It is therefore clear that the block size has to be a minimum in order to minimize the chance that the block would contain high-frequency picture information.

Now that the reason for blocking is explained, the 2 Dimensional Spectral Measuring Technique (2DSMT) can be explained in greater detail. A block diagram of the 2DSMT is shown in Fig.5.13.

5.3 AN EXPLANATION OF THE 2 DIMENSIONAL SPECTRAL NOISE MEASURING ALGORITHM

A detailed explanation will now be given of the 2DSMT algorithm. We will start the explanation by way of an example of the 2DSMT with an 8x8 input block. After some insight has been gained into the algorithm, the block size of 8x8 will be justified. Finally other methods of increasing the speed as well as making the algorithm more robust will be discussed.

5.3.1 Determining the 2D spectrum for an 8x8 block

An 8 x 8 sub-picture f(x,y) has a Discrete Fourier Transform (DFT) F(u,v) which, for natural scenes, shows most of the energy concentrated at low frequencies. This is indicated by stars (*) in the representation of F(u,v).

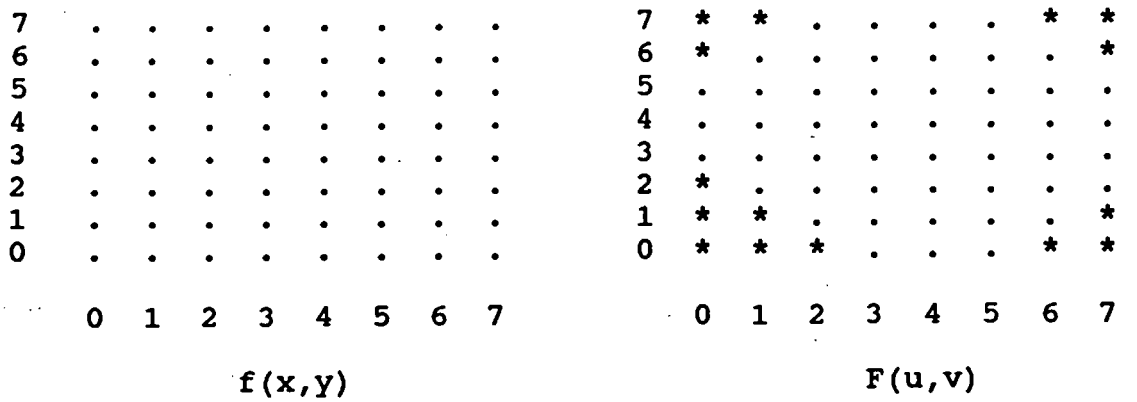

For ease of interpretation the 2-D DFT can be rearranged to give another display with the origin (+) at the center: (This step would be left out in an implementation of the algorithm.)

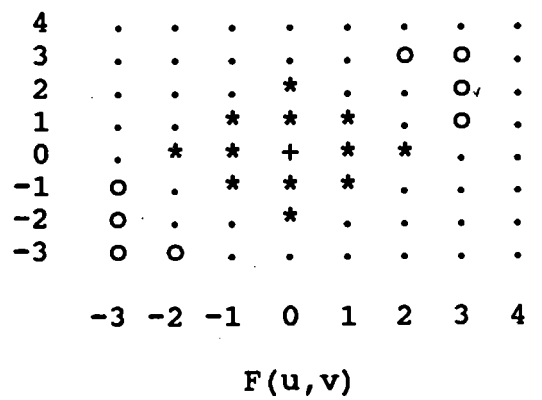

In this display the energy concentration around the origin (+) of the spatial frequency plane is now shown as a cluster of stars. The display also shows a 180 degree rotational symmetry. This symmetry arises from the Hermitian nature of the transform of the **real** values of the input image pixel intensities. The DFT has **even symmetric** real values and **odd symmetric** imaginary values. To show this symmetry the o's have been added at the corresponding spatial frequencies.

If the power spectral density, (psd) is to be calculated at each of the sample points in the (u,v) plane, complex conjugate points would yield the same values. Hence the 180 degree rotational symmetry would reduce to quadrantal symmetry as shown here:

```
 4    .  .  .  .  .  .  .  .
 3    o  o  .  .  .  o  o  .
 2    o  .  .  *  .  .  o  .
 1    o  .  *  *  *  .  o  .
 0    .  *  *  +  *  *  .  .
-1    o  .  *  *  *  .  o  .
-2    o  .  .  *  .  .  o  .
-3    o  o  .  .  .  o  o  .

     -3 -2 -1  0  1  2  3  4

           F(u,v)
```

The data was digitized with a 10Mhz Analogue to digital converter (ADC). In this representation the spacings marked 4 in one of the dimensions can be taken to represent 5 Mhz (the Nyquist frequency), the ones at sample point 1 to represent 1,25 Mhz, at sample point 2, 2,5 Mhz and at sample point 3, 3,75 Mhz. But in terms of the picture itself it, of course, represents spatial frequencies in both dimensions. Since we expect scanning effects at the Nyquist frequency which occurs at sample points 4, the values at u=4 and v=4 are not used for psd estimation. The values at u=0 and v=0 will contain too much picture energy for noise estimation. Because of the quadrantal symmetry we need to use only the average of the 9 values at u=1,2,3 and v=1,2,3. It is important to note that 9 points are used so that a more accurate Bartlett noise estimate can be made over a wider range in the spectrum. This will make the algorithm more robust against narrow band peaks or troughs in the frequency response. The average of the points marked here with an X, are used as PSD estimates:

```
 4    .  .  .  .  .  .  .  .
 3    .  .  .  .  X  X  X  .
 2    .  .  .  .  X  X  X  .
 1    .  .  .  .  X  X  X  .
 0    .  .  .  +  .  .  .  .
-1    .  .  .  .  .  .  .  .
-2    .  .  .  .  .  .  .  .
-3    .  .  .  .  .  .  .  .

     -3 -2 -1  0  1  2  3  4

           F(u,v)
```

If we do this we may include some picture energy, but we know from image spectrum models that, on average, the picture energy should be well down at these frequencies. The sub- images which contain noticeable picture energy need to be eliminated.

5.3.2 Eliminating picture Power

We therefore need to devise a method for eliminating these sub-images which have been contaminated with picture energy, in order to enable us to obtain an averaged estimate, in the Bartlett sense, of the power spectral density of the noise in the picture.

The 64 x 64 = 4096 estimates of power spectral density from the sub-images are now arranged in histogram form. Since the noise power is spread equally (with a constant PSD) over the whole picture all the high frequency PSD estimates of the flat blocks (containing no picture power) will be spread around one point on the histogram. The PSD estimates of the blocks which contain picture and noise power will be spread all over the histogram, but especially in the higher power area. We therefore assume that white gaussian noise mainly produce power estimates at one power level, while the picture + noise power estimates will be spread over the whole range. This will create a peak in the histogram showing that a gaussian noise process was present. This peak is clearly seen in the histogram obtained from actual data in Fig.5.7. In order to eliminate the effects of picture power the mode of the values in the histogram is taken. The square root of this value is calculated to yield Vrms and from this the signal to noise ratio SNR is calculated from the equation 5.14:

$$SNR = 20 \log \frac{255}{Vrms}$$

The peak corresponds to the mode in a gaussian probability density function which gives the level of the noise power. The peak is, however, a very noisy estimator and some smoothing needs to be done on the histogram. We have tested a good method of finding the peak which proved to be reliable and is also fast:

This method uses a running sum of 10 values D(i), of the histogram h(i):

$$D(i) = \sum_{i=1}^{10} h(i)$$

Find the peak in D(i). This corresponds to the peak in a smoothed version of the histogram where the smoothing was taken as the running average of 10 psd levels.

Figure 5.7 shows a histogram with the smoothed version superimposed on it. As a matter of interest, the median value is where the cumulative integral of the histogram

intersect with the horizontal bar. This value is quite different from the mode. The smoothed version has been scaled up to make the display clearer.

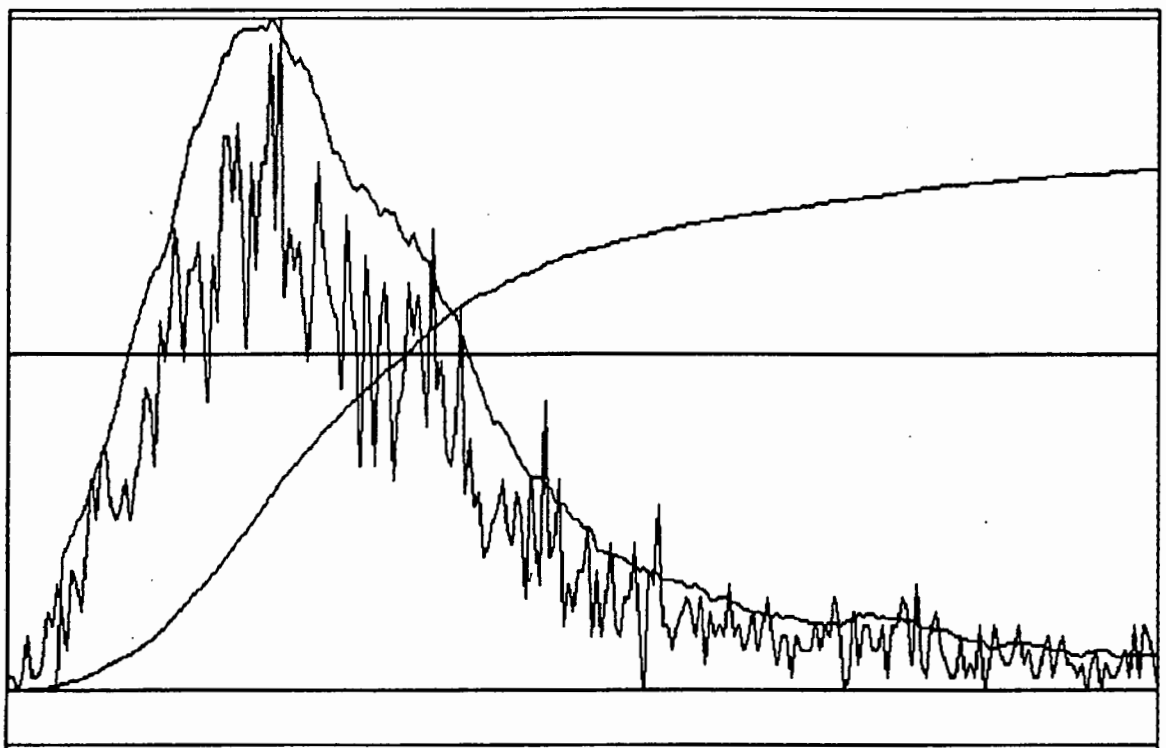

Figure 5.7 An example of a histogram with the smoothed version superimposed on it. The smoothed curve has been scaled up to make the display clearer.

5.3.3 Determining the optimum block size

For the general case the chosen block can be viewed as an NxN array (matrix). A 2DFT is taken of the matrix. Due to the symmetry of the FT quoted previously, we have (N/2+1)x(N/2+1) complex output points in the spectrum. Since the original data was digitized at 10Mhz, the one dimension of the 2DFT can be taken to represent frequencies of 0-5Mhz, the other dimension will contain purely spatial frequencies. It is the frequency dimension of the 2DFT that concerns us in selecting an optimum block size. If we take our earlier 2DFT representation of F(u,v), then we assume that the v axis corresponds to frequency. This then means that all F(u,0) represent 0Mhz and all F(u,N/2) represent 5Mhz information.

Therefore

F(u,k) represents 5k/(N/2)Mhz

where $0 \leq k \leq N/2$

In the spectrum an area should be found in which the picture power is low compared to that of the noise. The accuracy of the noise estimate will be greatest where the picture

power is least. The average of some of these points will be a representation of the noise power density in the block. An NxN block input into the 2DFT will give (N/2+1)x(N/2+1) unique complex output points in the Fourier domain. Thus it would be better to have a bigger input block, so as to get more output points which represent those frequencies between 0Mhz and 5Mhz. Due to other effects (e.g. motion blur and edge effects as described in chapter 4) in the 2DS, the highest frequency in the 2DS does not only represent noise power and thus has to be ignored in the calculation of noise power. With these constraints a minimum block size is 4x4 because in the 2x2 block case, only 2x2 unique points are available in the 2DS, and none represent frequencies between 0Mhz and 5Mhz. In the 4x4 block case, 3x3 points are available in the 2DS where only one point F(u,1) represent a frequency between 0 and 5Mhz. They are:

F(u,0) represents 0 Mhz
F(u,1) represents 2,5 Mhz
F(u,2) represents 5 Mhz

F(u,1) represents the average PSD of frequencies from 1.67Mhz (5/3Mhz) to 3.33Mhz (5-5/3Mhz). With a bigger block size it would then be possible to define a wider frequency range over which a noise power estimate can be made. The block size can thus vary from 4x4 to 8x8. A bigger block than 8x8 is not recommended as the probability of finding many flat blocks of this size is unlikely, as shown in Figure 5.6.

The trade off between a larger block, so that a greater frequency range can be used as a noise estimate, and the fact that the probability of finding many flat blocks decreases exponentially as block size increases, produces an optimum block size of 8x8. For this reason an 8x8 input block was chosen and the average of the 2DPDS points were taken from 0.625 MHz to 4.375 MHz. Thus 9 points were used out of a total of 32 points in the 2DPDS, to estimate the noise power in each block.

5.3.4 Different histogram implementations to make 2DSMT more robust

All the noise power estimates of the 4096 blocks are used to build a histogram. An example of such a histogram is shown in Fig.5.8.

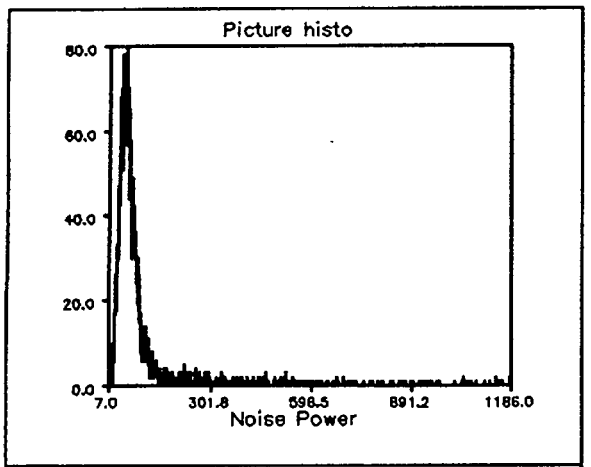

Fig.5.8 An example of a histogram built from the PD estimates of all the blocks.

A histogram can be built from a variety of inputs. In Appendix E, histograms are displayed of SNR values, median values or by not averaging the 9 points, but putting them all in the histogram. However the method which gave the best results is the one described in section 5.3.2 with the histogram in Fig.5.8. as explained in Appendix E

5.3.5 Difference pictures

Another method of reducing the effect of the picture power in the noise estimation, is by calculating the difference picture of two successive frames . We know from chapter 4 that the movement between two frames cannot be too much and that the result of differencing two successive frames would mainly be noise (which changes constantly) with a little motion. An example of such a difference picture is shown in Fig.5.9.

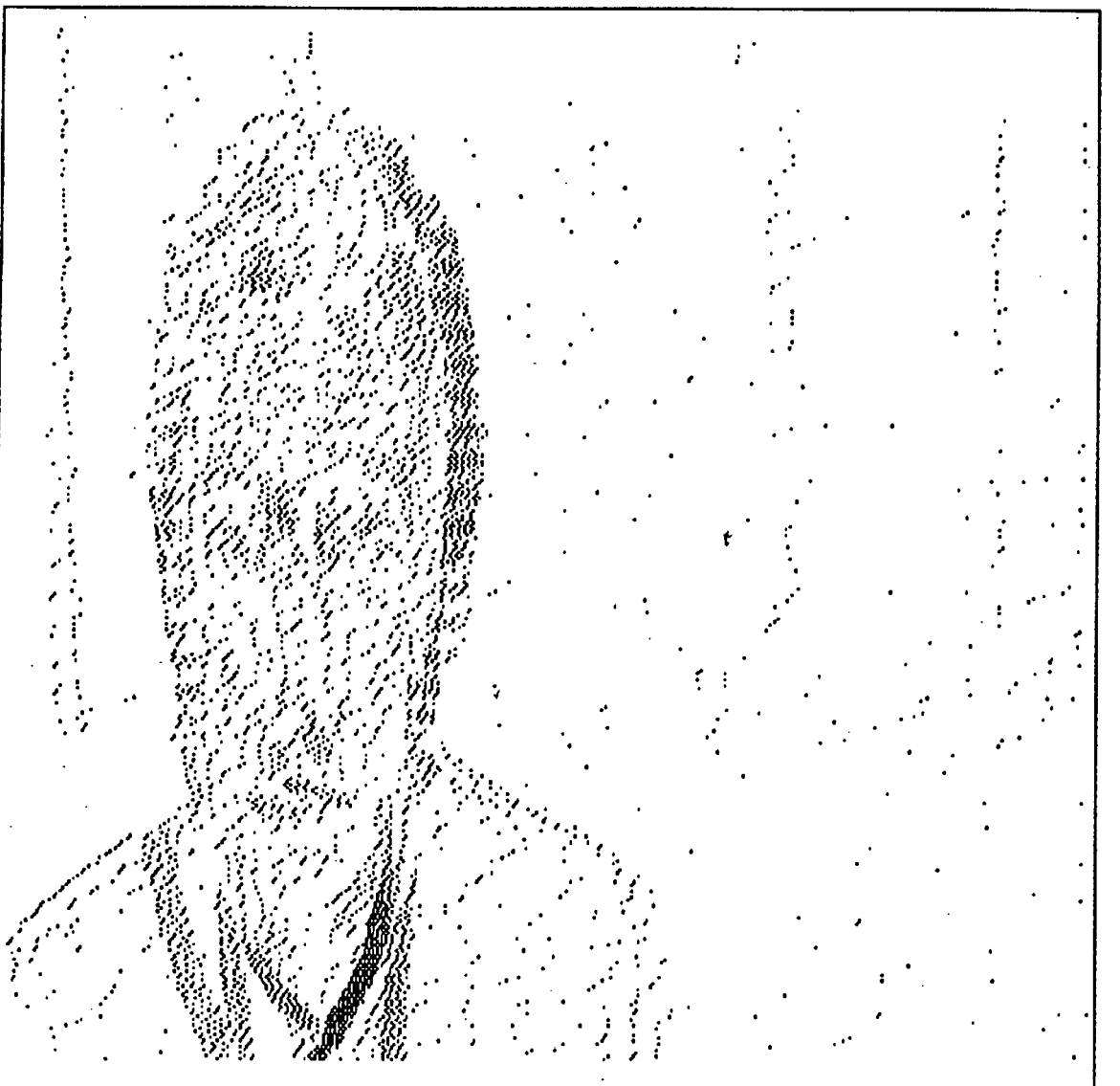

Figure 5.9. The difference picture between two successive frames. Only noise and motion is visible.

When the 2DSMT is implemented on such a difference picture, a histogram is obtained as shown in Fig.5.10.

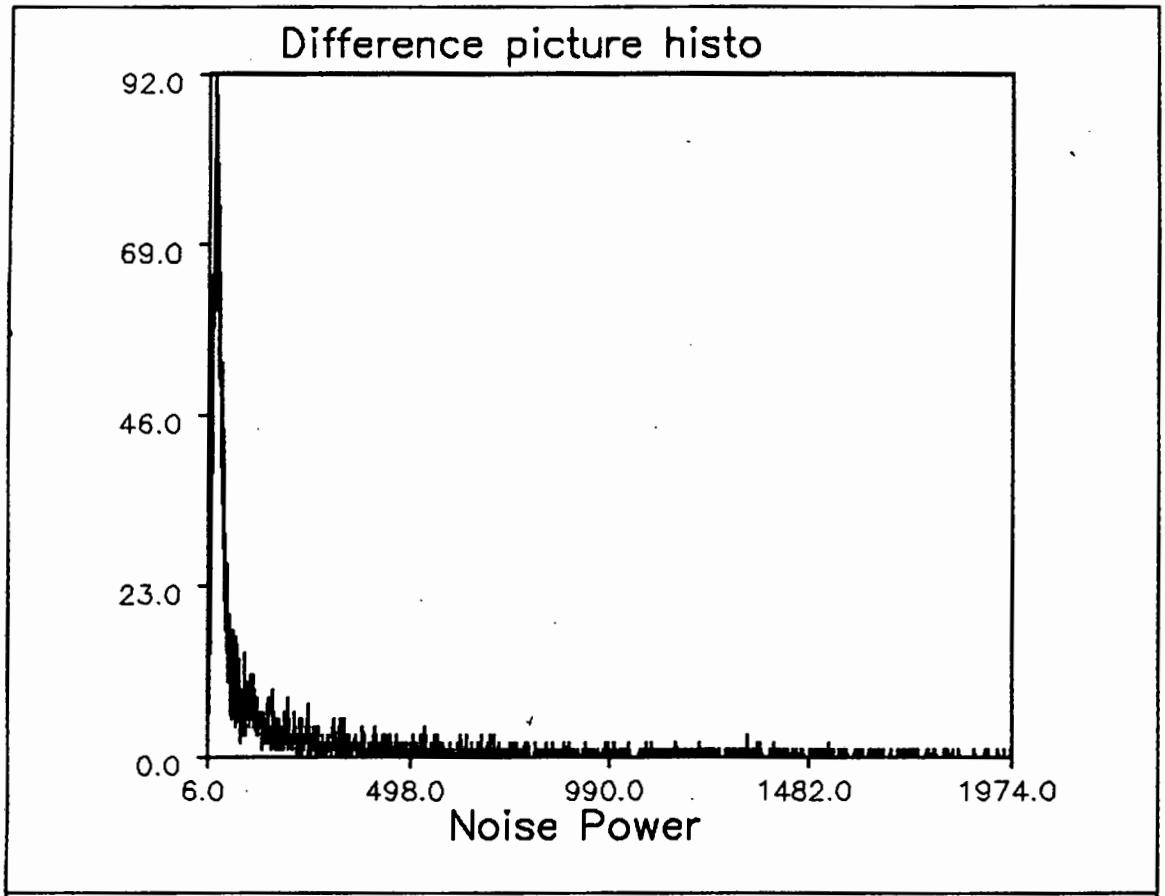

Figure 5.10 An example of a histogram obtained after the 2DSMT was implemented on a difference picture.

It can be seen from Fig.5.10 that there is more high-frequency picture power in difference pictures than ordinary ones. This is because the difference of motion causes edges which are mainly high-frequency information.

It is important to note that implementation of a picture differencing algorithm on a personal computer is virtually impossible due to the large memory required together with the speed required to capture two successive frames. However some framegrabbers have an on board facility of doing this in real-time.

5.3.6 Methods to increase the speed of the algorithm

The performance of the algorithm can be improved in a number of ways while still retaining the accuracy specifications.

(1) Good results were obtained when fewer input data were used. This means that only one quarter of the tessellated blocks be used to calculate 2D spectra. The selected blocks can form a checkered board pattern over the screen. This is justified on the

assumption that the pictures change continually and unpredictably, so that the position of the selected blocks need not change.

(2) A less accurate floating point representation in the 2D spectra calculation was used. Since the floating point values will be truncated during the histogram formation, it is best to use the least possible bit representation. Fixed point calculations have been tried as an extreme case but the accuracy is not sufficient.

(3) The optimum method for calculating the 2DS is by using FFT routines to calculate the row FT's and then to use DFT routines to calculate only the 9 individual 2D spectral points.

A Pascal version of the 2DSMT is given in Appendix F.

NB: It is important to differentiate between picture power and noise power by obtaining the histogram. This algorithm will NOT work if the average of all the high frequency PDS estimates are taken as a noise power estimate.

5.4 THE RELATIONSHIP BETWEEN THE ROOT MEAN SQUARE (RMS) VALUE, AND THE POWER DENSITY SPECTRUM (PDS) OF A SIGNAL.

Previously it was assumed that the power density (PD) is equal the mean square (MS) noise value. The proof for this is quite extensive and follows here. This proof is derived from first principles, and the definitions were obtained from Oppenheim & Schafer (1989).

5.4.1 Definitions

The average value of a signal x(n) is defined as:

$$m_x = \frac{1}{L} \sum_{n=0}^{L-1} x(n)$$

The mean square value is defined as:

$$MS = \frac{1}{L} \sum_{n=0}^{L-1} | x(n) |^2 \qquad (5.3)$$

The variance is defined as:

$$\sigma_x^2 = \frac{1}{L}\sum_{n=0}^{L-1} | x(n) - m_x |^2 \qquad (5.4)$$

The autocorrelation sequence is defined as:

$$\phi_{xx}(m) = \frac{1}{L}\sum_{n=0}^{L-1} x(n+m)\, x^*(n)$$

5.4.2 Derivation

In order to relate the autocorrelation function with the variance, we rewrite equation(5.4) in terms of the MS value defined in equation(5.3), to obtain equation(5.5)

$$\sigma_x^2 = MS - | m_x |^2 \qquad (5.5)$$

In the special case of m=0 in $\phi_{xx}(m)$, where there is a zero time delay between x(n+m) and $x^*(n)$, we have maximum correlation. In case x(n) is a white noise signal, this is the only point of correlation. We can write $\phi_{xx}(0)$ as

$$\phi_{xx}(0) = \frac{1}{L}\sum_{n=0}^{L-1} x(n)\, x^*(n)\ ,$$

which can be rewritten as

$$\phi_{xx}(0) = \frac{1}{L}\sum_{n=0}^{L-1} | x(n) |^2 = MS\ . \qquad (5.6)$$

It is seen that σ_x^2 can now be written as a function of the autocorrelation sequence, since σ_x^2 has already been written in terms of MS in equation 5.5. Combining equations 5.5 and 5.6 we have

$$\sigma_x^2 = \phi_{xx}(0) - | m_x |^2\ . \qquad (5.7)$$

The Fourier Transform of $\phi_{xx}(m)$ is $\Phi_{xx}(n)$ and is defined as:

$$\Phi_{xx}(n) = \sum_{m=0}^{L-1} \phi_{xx}(m)\, e^{-jw}$$

where $w = 2 \pi n m / L$

and the inverse is:

$$\phi_{xx}(m) = \frac{1}{L} \sum_{n=0}^{L-1} \Phi_{xx}(n) e^{jw}$$

Note that the inverse FT has the normalizing factor 1/L, but NOT the forward FT. To obtain the zero point of the autocorrelation function $\phi_{xx}(0)$, m is set to 0 in the inverse FT and the following is obtained:

$$\phi_{xx}(0) = \frac{1}{L} \sum_{n=0}^{L-1} \Phi_{xx}(n) \tag{5.8}$$

It is known that the Fourier transform of the autocorrelation sequence is equal to the power density spectrum. $\Phi_{xx}(n)$ is therefore equal to the power density $P_{xx}(n)$ of the signal. By rewriting equation(5.8) in terms of $P_{xx}(n)$ rather than $\Phi_{xx}(n)$, equation(5.9) is obtained.

$$\phi_{xx}(0) = \frac{1}{L} \sum_{n=0}^{L-1} P_{xx}(n) \tag{5.9}$$

The variance σ_x^2 can now be shown to be a function of the power density, by combining equations 5.7 and 5.9 in equation 5.10

$$\sigma_x^2 = \frac{1}{L} \sum_{n=0}^{L-1} P_{xx}(n) - | m_x |^2 \tag{5.10}$$

5.4.3 The special case of a white noise input x(n)

From equation(5.10) it is seen that σ_x^2 is equal to the average power density of the signal minus $| m_x |^2$. In the case of zero mean gaussian white noise, $m_x=0$ and σ_x^2 is equal to the average power density of the noise.

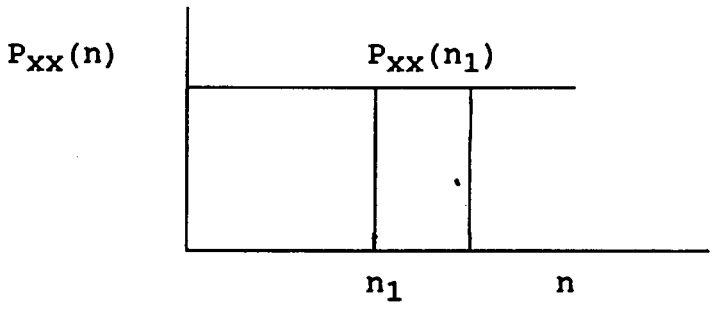

Figure 5.11. The power density function of white noise. The area under the power density is equal the power of the signal.

In Fig.5.11 it can be seen that all $P_{xx}(n)$ is constant or

$$P_{xx}(n) = P_{xx}(n_1)$$

for some n_1. Equation(5.10) can thus be rewritten in terms of $P_{xx}(n_1)$:

$$\sigma_x^2 = \frac{1}{L} \sum_{n=0}^{L-1} P_{xx}(n_1) - | m_x |^2$$

and since $m_x = 0$ and $P_{xx}(n_1)$ is a constant, we have

$$\sigma_x^2 = P_{xx}(n_1)$$

and from equation(5.5) we know that

$$\sigma_x^2 = MS ,$$

thus we see that

$$MS = P_{xx}(n_1) \qquad (5.11)$$

From equation 5.11 we can see that the MS value of white noise, is just any value on the PDS. In the 2DSMT, an estimate of a typical value of the noise PDS is obtained by averaging a few points. Alternatively this averaging is just the least squares error estimation (LSE) of the ideal white noise PDS. Therefore the LSE of the MS value of white noise is made in the 2DSMT. The RMS value is therefore calculated as follows:

$$RMS = \sqrt{P_{xx}(n_1)} \tag{5.12}$$

5.4.4 Deriving the SNR from the spectrum

With these parameters defined it is straightforward to calculate estimates for the signal to noise ratio (SNR). The standard SNR calculation in television broadcasting is, according to Weaver (1977) :

$$SNR_1 = 20 \log (0,7/E_{rms}) \tag{5.13}$$

In this expression a black to white level excursion of 0,7 volts is taken to correspond to the number 255 in an 8 bit representation of the intensities of pixels in an image. The value of E_{rms} is taken to be that calculated for RMS in equation 5.12 .

$$SNR_1 = 20 \log (255/RMS) \tag{5.14}$$

or alternatively

$$SNR_1 = 20 \log (255/\sqrt{P_{xx}(n_1)})$$

An estimation of the SNR of a picture can thus be made with the use of the 2 dimensional spectrum.

5.5 PROBLEMS

One of the most serious problems encountered in implementing this method is the presence of the colour carrier which modulates the intensities of uniform luminance areas. The effect can be seen clearly when a horizontal profile of a black and white version of a colour bar image is compared to the profile of an image with colour present. These are shown in Figure 5.12.

In the determination of the SNR of the television image we used a single colour from a colour decoded image to get rid of the colour modulation in the composite video signal.

Scaling factors are used for regenerating the full range luminance signal from the R G B signals. The smallest in magnitude of these is that for the green signal. Any noise on the green signal would therefore be multiplied by the smallest factor and the estimate of the mean from the green signal was therefore used in the analysis.

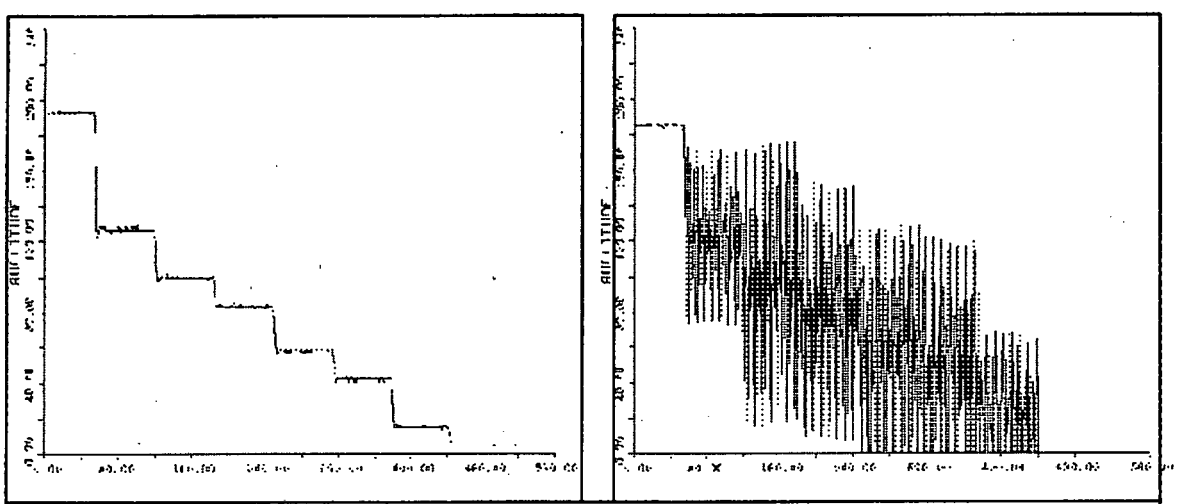

Figure 5.12. The horizontal profile of a black and white version of a colour bar image is compared to the profile of a colour bar image with colour present.

In conclusion, a summary of the noise measuring algorithm is made.

TWO DIMENSIONAL SPECTRUM NOISE MEASURING ALGORITHM

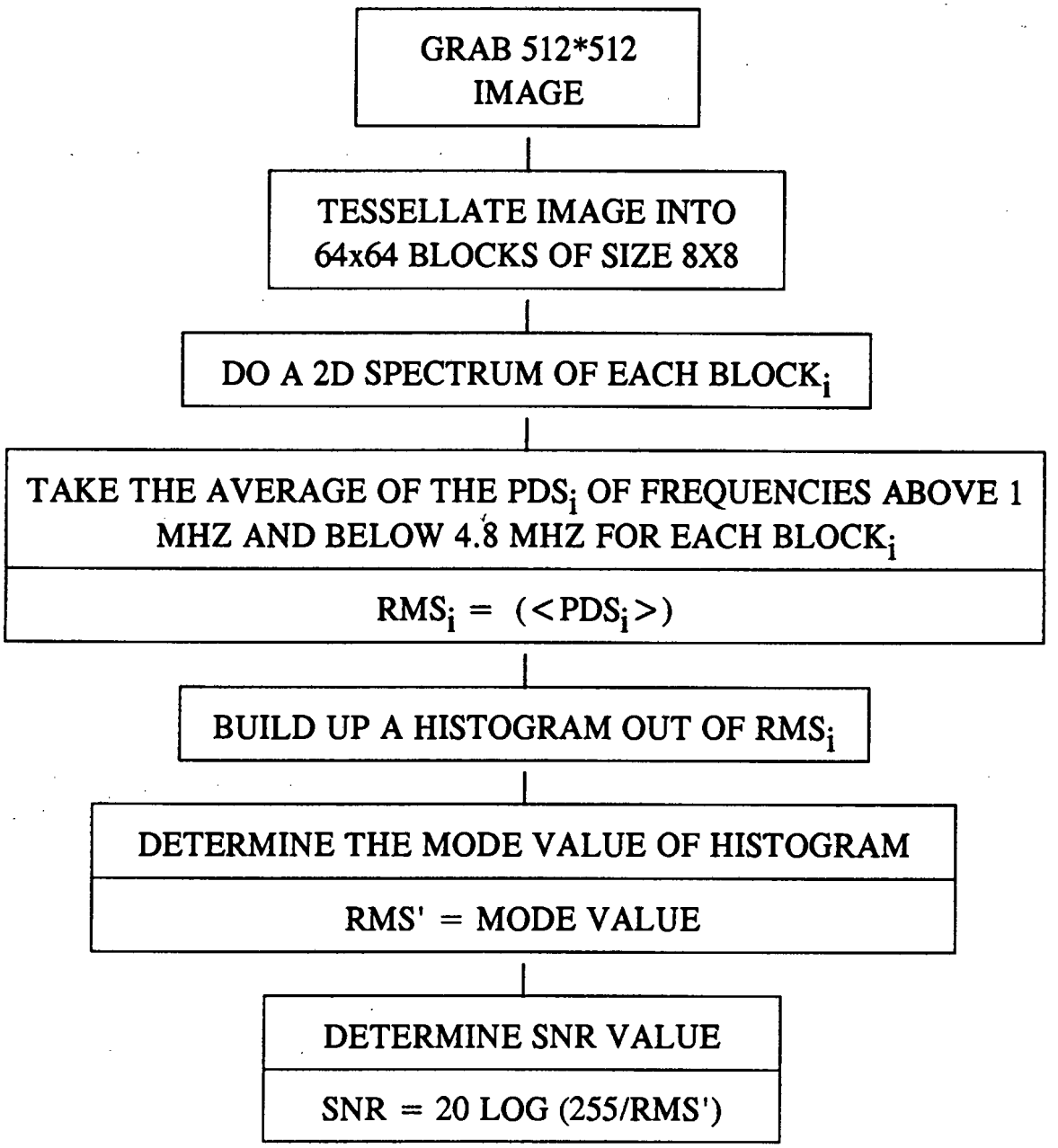

Figure 5.13. A block diagram of the 2 Dimensional Spectrum Noise Measuring Technique (2DSMT).

5.6 A SUMMARY OF THE NOISE MEASURING ALGORITHM FOR AN 8X8 PICTURE ELEMENT

1. Tessellate the image into 4096 blocks of size 8x8.

2. For an input block subimage[x,y], determine the 2DFFT, SUBIMAGE[u,v], from which the 2DPDS, SUBPDS[u,v], can be calculated for the 9 points of $1 \leq u,v \geq 3$.

3. Determine $<PDS_i>$ as the average of the 9 points calculated in SUBPDS[u,v].

4. Steps 1 to 3 have to be repeated until all 64x64 $<PDS_i>$ estimates have been determined.

5. Use $<PDS_i>$ to build a histogram h[i]. In the conversion of $<PDS_i>$ from floating point (the average) to fixed point (histogram), much information is lost. The accuracy can be improved by doing:

$$h[10*<PDS_i>] := h[10*<PDS_i>] + 1;$$

However this conversion has to be rectified later in the final SNR calculation.

6. Determine the mode of the histogram.

6.1. Let the histogram be represented by a count h(i) at $<PDS_i>$ level i. Calculate the cumulative distribution, Ch(i), for the histogram.

do for all i
Ch(i) = h(i) + Ch(i - 1)

6.2. Find the difference of two values of Ch(i) ten apart.

do for all i

$D(i) = Ch(i + 10) - Ch(i)$

This calculation yields a running sum of 10 values of h(i),

$$D(i) = \sum_{i=1}^{10} h(i)$$

6.3. Find the peak in D(i). This corresponds to the peak in a smoothed version of the histogram where the smoothing was taken as the running average of 10 psd levels.

7. Determine the SNR.

The mode of the histogram represents 10*noise_PDS of the image. Therefore

$RMS = sqrt(mode/10)$

and

$SNR = 20 \log (255/RMS)$

or

$SNR = 20 \log 255 - 10 \log (mode/10)$

$SNR = 58.13 - 10 \log (mode)$

CHAPTER 6

TESTING TECHNIQUES AND RESULTS

6.1 INTRODUCTION

The 2 dimensional spectrum noise measuring technique (2DSMT) proposed in chapter 5 is unique in the sense that there are no other readily available techniques of measuring the noise on the picture itself. Even those proposed by Meer et al (1990) and by Besl and Jain (1988), are still under development. The problem is thus how to test the accuracy of this 2DSMT. Three methods are proposed to test the 2DSMT.

(1) The 2DSMT has to be calibrated with an existing method in order to be of any use in the broadcasting industry. One of the existing methods of measuring the noise is with an analogue instrument made by Rhode & Schwarz, the UPSF1. This will be referred to as the Analogue method in future.

The limitations of (1) is that it uses frames without any picture content and is thus not a proof that the 2DSMT is independent of picture content.

(2) The second method add known amounts of noise to essentially noise free images. The limitation of this method is that it is difficult to find "noise free" images. Especially in the cases where the images are degraded with small amounts of noise, the inherent noise in the image becomes significant. The truncation noise in the A/D conversion of the framegrabber becomes significant in the high SNR cases.

(3) An interactive method was developed to measure the noise on any graphic picture. This method had to be calibrated against the analogue measurement before gaining significance. This method will be called the area of interest (AOI) method in future.

6.2 ANALOGUE METHOD

One of the existing methods of measuring noise on a television channel, is with the use of an instrument made by Rhode and Schwarz, the UPSF1. The UPSF1 only works with a constant luminance input. A midgrey bar is a constant luminance signal as shown in fig.6.1

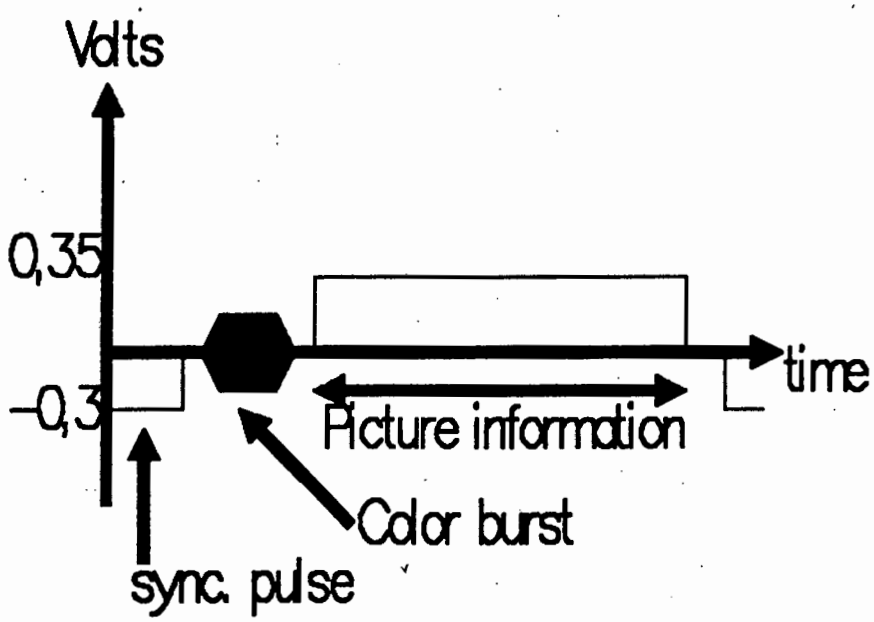

Figure 6.1 Waveform of a midgrey bar

6.2.1 Description of UPSF1 operation

According to R&S (1983) the UPSF1 fits a second order polynomial to the average luminance variation across the screen. When this signal is used it is known that any deviation from the curve (in the video area) is due to noise. The sum of the deviations squared is proportional to the noise power. Assume a signal f(t) degraded by noise n(t), f(t) is then defined as :

$$f(t) = p(t) + n(t) \tag{6.1}$$

where p(t) is the fitted second order polynomial. The power of f(t) is represented by P_f and the noise power is represented by P_n in equation(6.2) and equation(6.3).

$$P_f = \int | f(t) |^2 \, dt \tag{6.2}$$

$$P_n = \int | n(t) |^2 dt \quad (6.3)$$

$$= \int | f(t) - p(t) |^2 dt \quad (6.4)$$

Some equipment was used to generate video material with different noise levels which the UPSF1 could measure. The equipment setup that was used is shown in Fig.6.2.

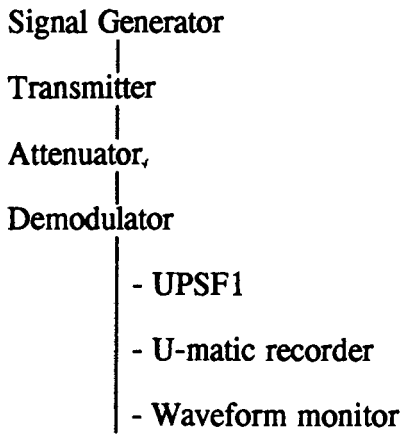

Figure.6.2 The experimental setup used to produce images with a known noise level.

The signal generator produces a baseband midgrey bar with a composite synchronizing signal. The transmitter then modulates the baseband signal to an intermediate frequency and then to radio frequency (RF). The RF signal is then attenuated with a 5dB step attenuator. The demodulator has an automatic gain control (AGC) that compensates for this attenuation and amplifies the RF signal so that the amplifier output has a constant peak-to-peak value of approximately 3 volts (Wilcox, 1987). Due to the electron movement in the amplifier of the AGC, noise is added to the RF signal. The amount of noise added is proportional to the gain of the AGC which in turn is proportional to the attenuation of the signal. The baseband output of the demodulator is fed into the UPSF1, U-matic recorder and Waveform monitor, in parallel. The UPSF1 measurement for each attenuator setting is taken down while recording the baseband signal on the U-matic recorder. The recording is played back into the UPSF1 and the new measurement taken for each attenuator setting. Due to bandwidth limitations on the U-matic the readings of signal to noise ratio (on the UPSF1), before recording differs with those when the recordings are played back into the UPSF1. Therefore the UPSF1

measurements of the playback is taken as calibrated data to test the 2DSMT and the area of interest method.

Due to CCIRR specifications the UPSF1 uses a unified weighting network. This simulates the sensitivity characteristic of the eye with respect to noise voltages, taking into account that higher frequency noise is less disturbing than low-frequency noise. The insertion loss of the weighting network is given in equation(6.5) and the frequency response is shown in Fig.6.3.(Weaver, p.70)

$$\text{INSERTION LOSS} = 10 \log_{10} \{1 + (wt)^2\} \text{ dB} \qquad (6.5)$$

where t = 200 ns,
and w = $2\pi f$.

The effect of the weighting network on a white noise input is shown in Fig.6.4.

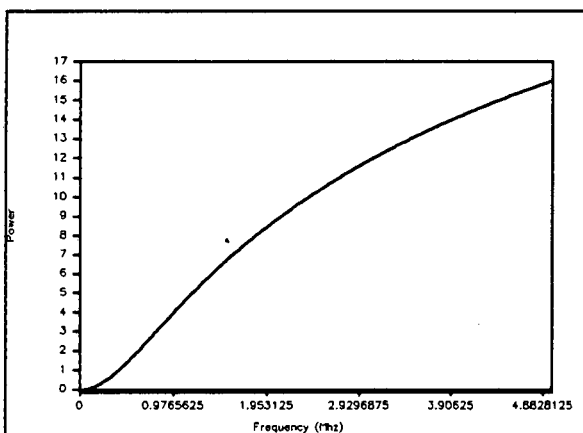

Figure 6.3 Insertion loss of the weighting network

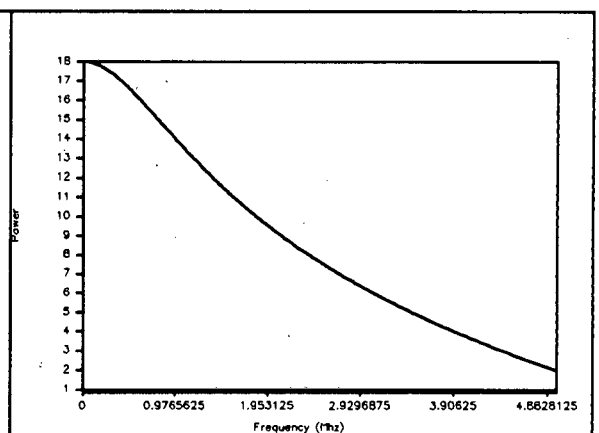

Figure 6.4 The effect of the weighting network on a white noise spectrum.

To calculate the effect of the weighting network on the measurements for a white noise input, the weighted (P_w) and unweighted (P_{uw}) power is calculated as follows:

$$P_{uw} = \int_0^B P \, df = P\,B,$$

where B is the bandwidth, of 5MHz, of the signal.

$$P_w = \int_0^B P / \{ 1 + (2 \pi 200\ 10^{-9} f)^2 \}\ df$$

$$= P\ 1{,}124\ 10^6.$$

The dB ratio between the weighted and unweighted measurements are then calculated as:

$$10 \log (P_w/P_{uw}) = 10 \log (1{,}124\ 10^6/B)$$

$$= 10 \text{ Log } (1{,}124\ 10^6/5\ 10^6)$$

$$= -6{,}48 \text{ dB.}$$

There is thus 6,5 dB less power in the weighted signal. The UPSF1 compensates for this loss by amplifying the input baseband signal by 6dB R&S (1983), then weights and measures it. This means that the 2DSMT measurements need not be converted to be equal to the analogue method .

6.2.2 Results

The results in table 6.1 were obtained by measuring the noise on the same pictures with (1) the analogue method and (2) with the 2DSMT. Since the accuracy of the UPSF1 is +/-1dB, the difference between the two sets of results may be up to 2dB to be acceptable.

Table 6.1 SNR measurements of the different methods .

ATTENUATION	UPSF1	2DSMT
0	48,2	48.6
35	47.0	47.2
40	44.0	45.0
45	40.0	41.2
50	34.7	35.6
55	29.1	29.9

By comparing the results in table 6.1, it can be seen that there is never a difference between the two sets that is bigger than 2dB. This proves the validity of the 2DSMT.

6.3 NOISE ADDITION

Another method to test the 2DSMT is to degrade pictures with known amounts of noise. The results of the 2DSMT is then compared with the RMS value of noise added to the picture.

6.3.1 Generation of gaussian noise on computer

Random numbers can be generated in the computer with the random number generator. The probability of occurrence of these numbers are shown in Fig.6.5.

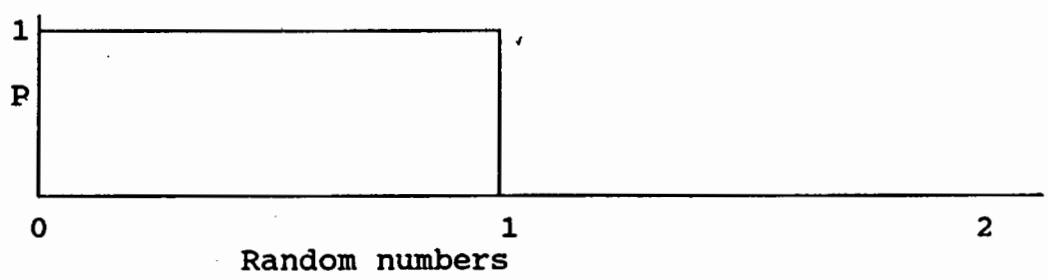

Fig.6.5. Probability of occurrence of random numbers generated by a computer.

This can also be expressed mathematically as:

$$P(x) = 1 \quad \text{for } 0 \geq x > 1$$

and

$$P(x) = 0 \quad \text{for } x \geq 1$$

Where x is the random number generated by the computer and $P(x)$ is the probability of occurence of x.

Gaussian white noise, however has a Probability of occurrence as shown in Fig.6.6.

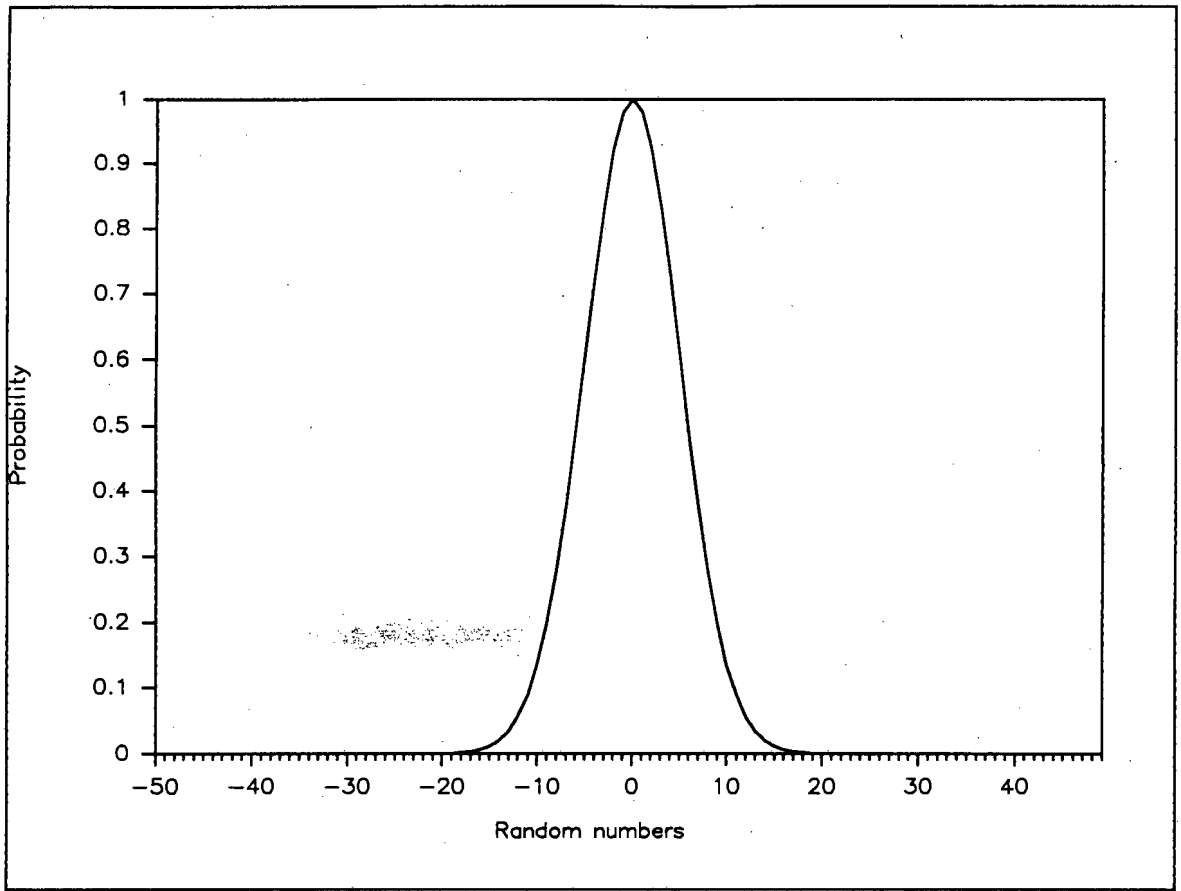

Fig.6.6. Probability of occurrence of a gaussian white noise.

In order to convert the computer generated random numbers to gaussian numbers, the following operator is used as suggested by Abramonitz and Stegan (p.953, 1964).

Assume two random numbers x_1 and x_2 .
Then

$$g_1 = \sqrt{-2 \ln(x_1)} \cos(2 \pi x_2) \quad \text{and}$$

$$g_2 = \sqrt{-2 \ln(x_1)} \sin(2 \pi x_2)$$

where g_1 and g_2 are two gaussian numbers.

A set of pictures are then degraded by adding different levels of noise to different pictures. The mean square noise value (E_{ms}) is given in equation(6.6).

$$E_{ms} = 1/N^2 \sum_{i=1}^{N} \sum_{j=1}^{N} g^2(i,j) \qquad (6.6)$$

Where g(i,j) is the added noise. The SNR is given by equation(6.7)

$$SNR = 20 \log (255/ \text{sqrt } E_{ms}) \quad (6.7)$$

The SNR in equation(6.7) is then compared with the values obtained from the 2DSMT.

This however is only true if the original image is totally noise free. If it is already degraded, the inherent noise may be significant compared to the added noise and the 2DSMT will show this.

If the amount of noise present in the original image is known, it is possible to calculate the total amount of noise in the picture. This test can then be used to test the 2DSMT.

Assume an original image f(x,y) with a known amount of noise σ_0^2. After degradation by σ_1^2 of noise there is a degraded image f'(x,y) with a total amount of noise of σ_t^2. Noise adds according to equation(6.8).

$$\sigma_t^2 = \sigma_0^2 + \sigma_1^2 \quad (6.8)$$

We therefore find the SNR of the degraded images as

$$SNR_t = 20 \log (255/ \sigma_t).$$

In this method, σ_0^2 was estimated with the 2DSMT . The 2DSMT was therefore only tested with certain degradations σ_1^2.
Seven different pictures each with different σ_0^2, was degraded with 5 levels of σ_1^2 and measured by the 2DSMT. The results are shown in table 6.2.

6.3.2 Results

The results in table 6.2 were obtained when 7 different pictures, some cartoons and a Luminance bar generated in the laboratory, were degraded with known amounts of noise.

Table 6.2 Seven different pictures degraded with 5 different noise levels, used to test the 2DSMT

(a) SNR's

Pictures	1	2	3	4	5	6	7
RMS noise levels (σ_1)							
1.6	39.0	38.7	38.3	40.0	38.7	38.0	44.0
3.6	35.0	35.0	35.1	36.0	35.0	35.0	37.0
5.6	33.0	32.0	32.4	33.0	32.0	32.0	33.0
7.6	30.0	30.0	30.1	30.0	30.0	30.0	31.0
9.6	28.0	28.0	28.3	28.0	28.0	28.0	28.0

Table 6.2(b) Errors

1.6	-0.2	0.2	-0.1	0.1	0.2	-0.5	0.2
3.6	-0.5	-0.2	-0.1	0.2	-0.2	-0.2	0.0
5.6	0.6	-0.2	0.2	0.5	-0.2	-0.2	0.0
7.6	-0.6	-0.5	-0.4	-0.7	-0.5	-0.5	0.0
9.6	0.2	0.3	0.6	0.2	0.3	0.3	0.0

Table 6.2 (a) consists of the 2DSMT SNR estimations where the RMS noise levels indicative the level of noise used to degrade the images. Table 6.2 (b) shows the difference between the expected SNR's for every image and those calculated by the 2DSMT. As can be seen the errors are all less than 1dB.

6.4 AREA OF INTEREST

This method is derived from an existing method of channel noise measurement, namely that of stimulating the channel with a constant luminance signal as in section 6.2. By measuring the root mean square (rms) value of the fluctuations of the output signal, an estimate of the noise is determined.

Similarly, it is possible to measure the noise on a constant luminance area of a picture. It is possible to find such constant luminance areas in cartoons and graphics. Pictures of natural scenes, that are generated by a camera, do not usually have constant luminance areas. Therefore this method cannot be used on pictures of natural scenes.

6.4.1 Calculating the signal to noise ratio

This algorithm, implemented on a personal computer, is used in an interactive way to find a constant luminance or "flat" surface in the image. To do this automatically would be quite difficult. A dithered version of the picture is displayed on a high resolution PC-monitor. A rectangular "area of interest" is superimposed on the image and cursor controls can change the size, shape and position of the rectangle. One can therefore visually selects an area of constant luminance. An example is given in Fig.6.7.

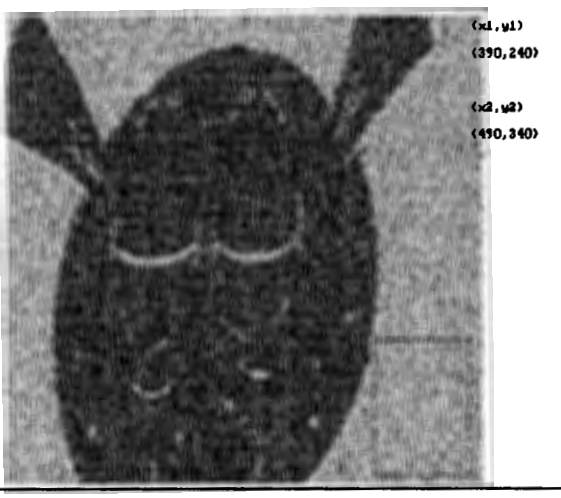

Figure 6.7. A dithered version of a cartoon, captured off the air, with the area of interest superimposed on it.

The standard deviation and mean of the signal level is then calculated for the selected pixels in a defined area of the original, undithered picture. The standard deviation is calculated from the expression :

$$\sigma^2 = \left(\frac{\sum (x_i - \langle x \rangle)^2}{N}\right) \qquad (6.9)$$

Where x_i is the intensity of any one pixel

$\langle x \rangle$ is the estimate of the mean

N is the number of pixels

With these parameters defined it is straightforward to calculate estimates for the signal to noise ratio (SNR). Two expressions can be used, one the standard in television broadcasting, according to (Weaver,p.64, 1977) :

$$SNR_1 = 20 \log (0,7/E_{rms}) \qquad (6.10)$$

In this expression a black to white level excursion of 0,7 volts is taken to correspond to the number 255 in an 8 bit representation of the intensities of pixels in an image. The value of E_{rms} is taken to be that calculated for σ.
The other expression allows for different picture energy levels, according to Brink (1987)

$$SNR_2 = -10\log \frac{[\Sigma(x_i - \langle x \rangle)^2]}{[\Sigma(\langle x \rangle)^2]} \qquad (6.11)$$

Although an area of a picture may appear to have constant luminance level, this is often deceptive. In order to check for gross "trends" or "tilt" in the data, the area of interest can be plotted as a three-dimensional display to show up any trends if these exist. Such a 3-D display is shown in Fig.6. 8.

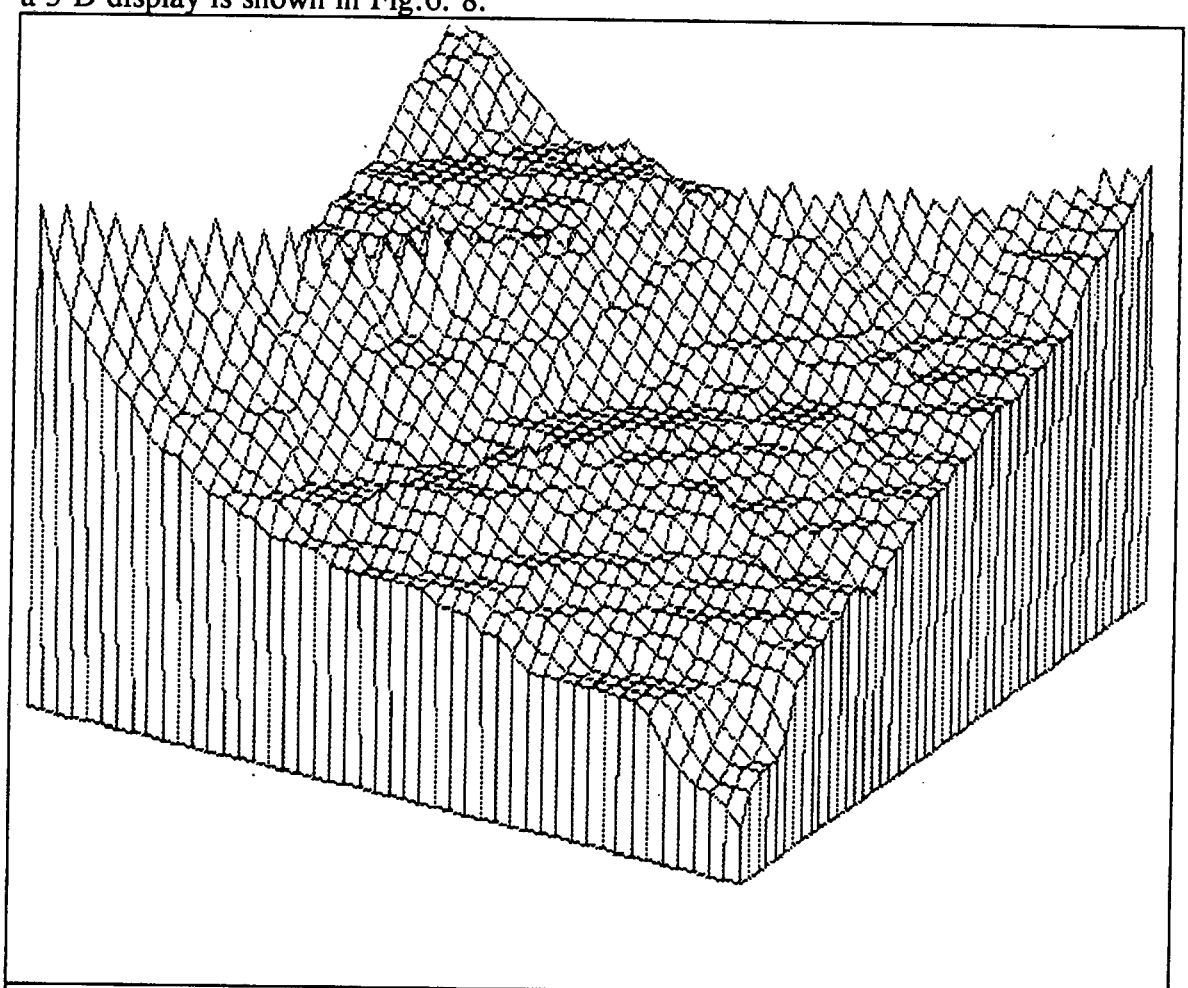

Figure 6. 8. 3-Dimensional display to show up any trends in the data.

The intensity levels in the pixels in the area of interest is used in the construction of a histogram, as shown in Fig.6.9. This histogram must not be confused with the one constructed in the 2DSMT in the previous chapter. The width of the histogram peak is

proportional to the standard deviation of the noise. The position of the peak is taken as the estimation of the signal.

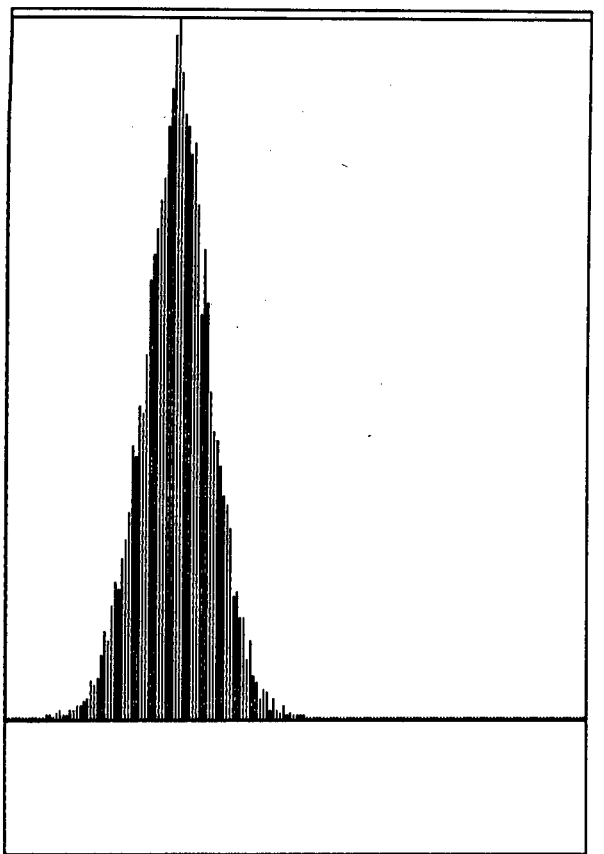

Figure 6. 9. A histogram of the pixel intensities for an area of interest. The width of the peak in the histogram is directly proportional to the standard deviation calculated from equation 6.9.

6.4.2 Results

This AOI method was used to measure the noise on 5 Television broadcast pictures and one Luminance bar waveform generated in the laboratory. These pictures were all degraded with the same amount of noise, so that they should all have the same SNR.

Table 6.3. A comparison of the SNR's of different pictures calculated with the AOI method and compared with the results of the 2DSMT.

Television pictures	SNR_1	2DSMT (dB)
1	28,0	28,0
2	28,0	28,0
3	28,1	28,3
4	28,0	28,0
5	28,0	28,0
Luminance bar	28,5	28,0

The measured SNR's in table 6.3. are constant for different pictures when the same amount of noise is added to each picture. This proves that the measurements are independent of picture content.
This method was also used on 25 different "flat" surfaces in television picture 1 and the Luminance bar, to discover how consistent the measurement was for the different areas of the picture. The Luminance bar was used as a control because it's image had the best SNR available.

Table 6.4. The variance of the rms value at different place on the picture.

Television Picture		
	mean rms	2.83
	maximum rms	3.45
	minimum rms	2.04
	variance in rms	0.28
	SNR_1	39.1dB
Luminance bar		
	mean rms	0.45
	maximum rms	0.55
	minimum rms	0.35
	variance in rms	0.07
	SNR_1	55.0dB

The information in table 6.4 proves that the measured noise value does not change significantly when the position of the area of interest is changed.

6.4.3 Comparing this method with the Analogue method

In order for this method to be valid, it has to be consistent with the Analogue method. Four different pictures were tested with both methods and the results tabled in table 6.5. 2 Different window sizes were used in the area of interest method to see the effect of different amounts of data on the results. There does not seem to be a significant difference.

Table 6.5 The noise levels measured on the flat area images using the Analogue method shown against the flat area variance digital determination of the noise levels.

Analogue method	Area of interest	
dB	128x128	10x10
48.2	47.4	47.6
40.0	40.1	41.2
34.7	35.1	36.4
29.1	29.6	30.1

The results in table 6.5 proves the consistency of the area of interest method. It is thus a valid method of testing the 2DSMT. A comparison of the results of the AOI and 2DSMT on 5 undegraded cartoons, captured off the air shows good comparison in table 6.6.

Table 6.6 A comparison of AOI and 2DSMT results of cartoons captured off the air.

	AOI	2DSMT
Television pictures		
1	39.1	40.3
2	38.4	38.4
3	37.9	38.9
4	39.6	39.7
5	37.9	38.6
Luminance bar	56	55.5

It is seen from the results that the highest SNR is 56dB. This is actually due to a limitation of the digital measuring system. This limitation will now be discussed.

6.5 LIMITATIONS TO DIGITAL MEASURING TECHNIQUES

Due to the fact that the signal is filtered and sampled, before the measurements are made, it cannot be assumed that the noise in the digital image is exactly the same as in the original analogue image. However, these differences are only significant in the high SNR case. We therefore need to determine the lowest noise level detectable on a digital system.

In the proposed context where a framegrabber is to be utilized to freeze an image, the quantization of the intensity scale will provide a lower limit to the noise that

can be detected. The CCIR recommendation 601 on ENCODING PARAMETERS FOR TELEVISION FOR STUDIOS of September 1983 states that a scale of 0 to 255 is to be used.

6.5.1 Amplitude of the quantizing noise

Assume a quantizing characteristic as in Fig.6.10, where the amplitude probability distribution is constant across each step. This is a valid approximation where the quantization error is seen as additive white noise, on a randomly changing background. Since the television picture is a complex signal that fluctuates rapidly and unpredictably this approximation becomes realistic. In that case all errors between -d/2 and d/2 are equally probable, where d is the quantization step.

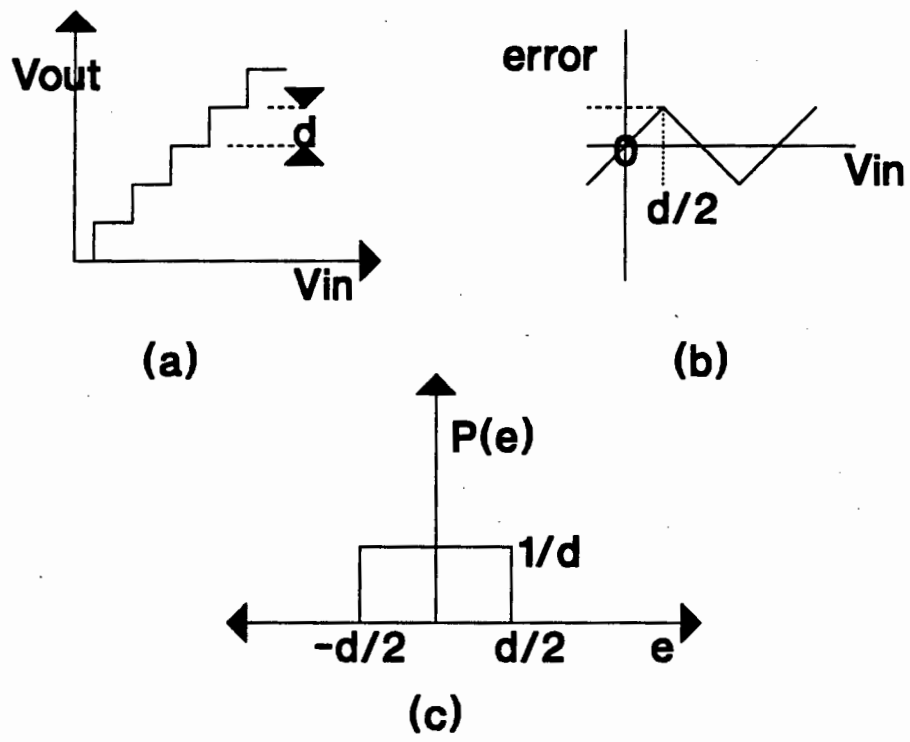

Figure 6.10 Calculation of quantization noise: (a)quantizer characteristic; (b)quantizer noise; (c)probability distribution of the quantization noise

6.5.2 Specific derivation for 8 bit quantization

With a framegrabber using 8 bit quantization, we have 256 levels between 0 to 255. We can therefore calculate the quantization noise expected from this limitation of word length because we know that d = 1, to have 256 levels in this range.

It can be seen from Fig.6.4. (c) that the quantization noise n(v), is a function of the input voltage v_{in},

$$n(v_{in}) = v_{in} \quad \text{for} \quad -d/2 < v_{in} < d/2. \tag{6.12}$$

The expected value of $n(v_{in})$, $E\{n(v_{in})\}$, is then

$$E\{n(v_{in})\} = 0$$

and the variance of the quantization noise σ_n^2, is

$$\sigma_n^2 = E\{n(v_{in})^2\}. \tag{6.13}$$

From equation (6.12) we have

$$\sigma_n^2 = E\{v_{in}^2\} \tag{6.14}$$

and from the definition of expected values

$$\sigma_n^2 = \int_{-1/2}^{+1/2} v_{in}^2 \, dv_{in} = 1/12 \, . \tag{6.15}$$

To calculate the maximum signal to noise ratio (SNR) attainable in this system, the SNR definition of section 6.5, is used. We therefore have

$$SNR = 20 \log (255/\sigma_n) \tag{6.16}$$

$$= 59 \text{ dB}.$$

This is therefore the highest signal to noise ratio attainable on a digital noise measuring technique.

6.5.3 General derivation

A more general SNR derivation is done by Oppenheim and Schaefer (1975) where d is a function of bit length

$$d = 2^{-b}$$

and the noise variance is calculated as in equation 6.15,

$$\sigma_n^2 = 2^{-b}/12.$$

The SNR is then calculated as

$$SNR = 10 \log(\sigma_x^2/\sigma_n^2)$$

Where σ_x^2 is the amplitude scaling of the input signal to fit in the dynamic range of 0 to 255. We then have

$$= 6.02b + 10.79 + 10 \log (\sigma_n^2)$$

$$= 59 + 10 \log (\sigma_n^2).$$

If the input signal does not exceed the dynamic range of the quantizer, we do not need to reduce the amplitude to reduce clipping, this means that σ_x^2 is scaled to one. Then we have

$$SNR = 59 \text{ dB}.$$

6.6 SUMMARY OF RESULTS

In conclusion, the most significant results are in table 6.7 where the results of the three measuring techniques are tabled with the same midgrey bar as input.

Table 6.7 A comparison of the results of three measuring techniques with the same input data.

Analogue	AOI	2DSMT
48.2	47.4	48.6
47.0	45.9	47.2
44.0	44.3	45.0
40.0	40.1	41.2
34.7	35.1	35.6
29.1	29.6	29.9

Table 6.8 summarizes the limitations of each method utilized. A `Y' means yes it can accommodate that input; a `N' means no, it cannot function correctly with such an input and an inc means that it can only measure incremental steps of noise added, but not absolute levels, because the inherent noise in the picture is not known. Also, Grey Bar means a constant luminance midgrey bar input, a luminance bar is an image of different constant luminance bars, the Cartoon is any cartoon captured off the air and any pic is any camera generated picture captured off the air.

Table 6.8 A summary of the different noise measuring techniques as discussed. They are compared according to the different inputs that they can accommodate.

				Add noise		
	Analogue	AOI	2DSMT	Analogue	AOI	2DSMT
GreyBar	Y	Y	Y		Y	Y
LuminBar	N	Y	Y		Y	Y
Cartoon	N	Y	Y		Y	Y
Any Pic.	N	N	Y		inc	inc

Not only does table 6.8 prove that the 2DSMT had been extensively tested, but also it shows the versatility of the 2DSMT because it can operate on such a wide range of inputs.

CHAPTER 7

CONCLUSIONS AND RECOMMENDATIONS

7.1 CONCLUSIONS

A number of conclusions can be drawn on the basis of work reported in this thesis:

1 It is possible to measure the noise on a television picture non-intrusively. Apart from the proposed method, other methods have recently been proposed independently in the literature in agreement with this conclusion

2 A noise measuring technique, the two dimensional spectral measuring technique (2DSMT) was developed. The technique is based on generally accepted signal models, as discussed by various authors in the literature.

3 The 2DSMT has been calibrated and tested against a recognized method of noise measurement in the broadcasting industry. Not only did it compare favorably with this methods, but also with a method that measures noise on cartoons, developed during this thesis.

4 The 2DSMT has been optimized for speed, by using less accurate floating point representation, as well as less input data (up to one quarter of the picture) while still maintaining a minimum accuracy of $\pm$1dB. However, it needs more optimization before it can run in near real-time.

5 The noise measurement of the 2DSMT is more indicative of picture impairment than other analogue methods. This is because the 2DSMT measures the noise in two dimensions on the screen, like the eye sees it, as compared to the analogue methods that only do it in the horizontal direction on the picture.

7.2 RECOMMENDATIONS

A few recommendations to speed up the algorithm and make it more robust are the following.

1 The 2DSMT can be optimized for speed by using less accurate fixed point calculations as well as selecting fewer sub-images to build a histogram.

2 To make the 2DSMT more robust, the mode detection in the histogram can be optimized for accuracy.

As far as future work is concerned it appears to be possible to use spectrum analysis to measure different noise types such as film-grain noise or FM-clicks.

BIBLIOGRAPHY

Abramonitz M, Stegan I.A; Handbook of mathematical functions with formulas, graphs, and mathematical tables; p.953; Washington; U S Govt. repr.; 1964.

Besl P.J, Jain R.C; Segmentation through variable-order surface fitting; IEEE Transactions on pattern analysis and machine intelligence; vol. 10; pp. 167-192; 1988.

Böck A.M, Gallois A.P, Carpenter D.C; Method for the computation of interference and distortion levels in satellite FM-TELEVISION systems; IEEE Trans. Broadcasting; September 1989

Brink Anton David; The selsction and evaluation of grey-level thresholds applied to digital images; MSc. thesis; Rhodes University; October 1987.

Caelli Terry; Visual Perception, Theory and practice; Pergamon Press; 1981.

Carpenter D.C, Gallois A.P, Mittelholtz D.K; IEEE, Transactions on Broadcasting, March 1988, Approaches to modeling FM video spectra for satellite signal interference prediction.

CCIRR RECOMMENDATIONS 601 ON ENCODING PARAMETERS OF DIGITAL TELEVISION FOR STUDIOS; SEPTEMBER 1983

CCIRR; recommendations and reports of the CCIR, 1986; vol. XII; Rec. 567-2;

Curle A.L, Conradie D; South African Broadcasting Corporation Research and Developement; Private discussion; 1989.

Dachs Andrew; de Jager Gerhard; Filtering in Hough space to enhance or detect linear features; Proceedings IEEE COMSIG90; Johannesburg 1990

Drewery J.O, Storey R, Tanton N. E; Video noise reduction; BBC research department report; Kingswood Warren; July 1984.

Efrein Joel Lawrence, Video tape production & communication techniques, Tab books, January 1971.

Gallois A.P, Böck A.M; Simulation and modeling of FM-clicks, IEEE Transactions on Broadcasting; March 1987

International Electrotechnical Commission (IEC); technical committee no. 60: recording; Sub-committee 60B: video Recording; 60B(secretariat)88; December 1981.

Isono Hiroo, Ohmaru Kenji; A New method for measuring satellite broadcasting field intensity and a measurement method for antenna gain and G/T using a satellite broadcast signal; NHK laboratories note; no. 361; September 1988.

Johnson S.P; A precise, automated test system for video tape noise evaluation; Journal of the electronic and Radio Engineers; vol. 57; no. 5; pp. 207-212; September/October 1987.

Kelly D; Spatial, temporal and chromatic relations. In spatial Contrast (spikreijse, H. and van der Tweel, L.,eds.) Akademie van Wetenschapern, Koninklijke Nederlandse, pp. 29-33; 1978.

Kretzmer E.R; Statistics of TV signals; Bell System Tech. J.; 31, 763; July 1952

Lokshin B.A, Listov I.B, Nikulin N.I; Measurement of the signal to background noise ratio of a satellite TV channel when the energy of the FM signal is dispersed; Elektrosvyaz (USSR); vol.37; no. 5; pp. 13-15; May 1983. Trans in: Telecommun. and radio eng. part 1 (USA); vol 37; no. 5; pp. 12-14; May 1983.

Lowry John D; B-MAC an optimum format for satellite television transmission; 18th annual SMPTE television conference; Montreal; 11 February 1984.

Lowry John D; SMPTE Journal, November 1984, B-MAC: An Optimum Format for Satellite Television Transmission.

Meer Peter, Jolion Jean-Michel, Rosenfeld Azriel; A fast parallel algorithm for blind estimation of noise variance; IEEE Transactions on pattern analysis and machine intelligence; vol. 12; no. 2; February 1990.

Middleton Hugh T; Television noise measurements by spectrum analyses; Broadcasting Corporation of New-Zealand; ABU Technical review; November 1983.

Moses R. A; Newman M; Adler's Physiology of the eye; Chapter 18; Visual Acuity; Saint Louis; C.V. Mosby; 1975; pp. 500-528.

Mothersole L.M; PAL color TV...The PAL system and Mullard circuits described; Mullard Limited; London; May 1967.

Nakagawa Shozo; A chrominace noise meter for videotape recorders; SMPTE Journal; April 1979; vol. 88.

Nakagawa Shozo; A method for measuring chrominace noise; NHK laboratories note; no. 208; February 1977.

Oliphant A, Taylor K.J, Misson N.T, The Visibility of noise in system I color TV, BBC Research Department Report, November 1988

Oppenheim A.V; Schaefer R,W; Digital Signal Processing, pp.548-549, Prentice Hall, 1975.

Oppenheim A.V; Schafer R,W; Discrete time signal processing, Prentice Hall, 1989

Palmer Larry C, Shenoy Ajit, Simulation of tv transmission over the communications satellite channel, IEEE Transactions on Communications, Vol COM-34, No.2, February 1986

Patchet G.N; Colour Television: The PAL system; 1970; Norman Price

Perlman Stuart S, Eisenhandler Sanford, Lyons Paul W, Shumila Michael J; Adaptive median filtering for impulse noise elimination in real-time TV signals; IEEE Transactions on Communications; vol COM-35; no 6; June 1987.

Pomerleau Andre; Sylvain Dany; Quality measurement of television picture by eye simulation; IEEE Transactions on Broadcasting; Vol. BC-28; No.1; March 1982.

Powell Steven J, Kennel Glenn L; Noise in film to video transfers; SMPTE Journal; January 1987

Rees Trevor; de Jager Gerhard; Fast 2-D correlation using simplified spatial frequencies; Proceedings IEEE COMSIG90; Johannesburg 1990

Rhodes C, Tutorial on improved systems for color TV broadcasting by satellite, IEEE, Transactions on broadcasting, March 1985

Richter Hans-Peter; Video signal noise reduction-Basic principles; BTS report; Broadcast Television Systems (BTS) GmbH; Robert-Bosch-Straße 7; D-6100 Darmstadt; Federal Republic of Germany; 1989.

Ritterman M; An application of autocorrelation theory to TV; Sylvania Technologist; pp. 70-75; July 1952

Robinson A.P; The relationship between vision carrier to noise ratio and picture signal to noise ratio in a system I television receiver; BBC research department report; Kingswood Warren; December 1987.

Rohde & Schwarz ; Automatic measurement of chroma noise with video-distortion analyzer UPF; News from Rohde & Schwarz; no. 97; pp. 21-23; 1982

Rohde & Schwarz ; Video noise meter UPSF2 for noise and chroma-noise measurement; News from Rohde & Schwarz; no. 101; pp. 17-19; 1983

Rosenfeld Azriel; Professor in Electronic Engineering; Maryland University; Private communication; 1990.

Rossouw J.F; MONOCHROOM EN KLEURTELEVISIE; University of Stellenbosch lecture notes; 1976

Rowe H.E; Signals and noise in communication systems; U.S. Van Nonstrand; 1965

Salo J, Neuvo Y, Hameenaho V; Improving TV picture quality with linear-median type operations; IEEE Transactions on Consumer Electronics; Volume 34, August 1988.

Schreiber W.F; Fundamentals of electronic imaging systems, pp. 42-46, Springer, New York, 1986

Schreiber W.F; Lippman A.B; Single-channel HDTV systems, Compatible and Noncompatible; Proc. 2nd International Workshop on Signal Processing of HDTV; L'Aquila; Italy; February 1988.

Stremler Ferrel G; Introduction to communication systems; Addison Wesley; 1982.

Tsuda M, Kimura Y; Noise reduction in real-time X-ray images; Japanese Journal of applied physics part 1; vol. 25; no. 6; pp. 891-901; June 1986.

Ulichney R.A; Dithering with blue noise; Proceedings of the IEEE; vol. 76; no. 1; pp.56-79; 1988.

Weaver L.E; Television video transmission measurements, p57-69, p60, Marconi Instruments, St Albans; 1977

Wilcox Milt; A color TV primer for the E.E.; Section1-The color TV reciever; National Semiconductor; Appendix B; p. 1201; TL/H/8740-2; 1987

LIST OF APPENDICES

APPENDIX A

ONE DIMENSIONAL LINE SPECTRA

A one dimensional line spectrum is the average of the spectra of all the horizontal lines in an image. This is similar to a Bartlett estimation of the video spectrum. System characteristics like the color subcarrier is clearly seen in the composite image spectrum.

The line spectra were generated on the micr-VAX on a program called linfft.exe. It inputs an image of byte (.cfi file) and outputs the line spectra as an image of bytes. The plots were done on the micro-VAX with a program called plotexp.exe. This program inputs a linfft.exe output file, converts the 10log() to absolute power, averages and plots. Another program plotacf.exe is similar except that it does not convert from 10log() to absolute power.

The first five spectra are of noise free images, and the last five are of images degraded with white noise. Note the high power in the high-frequencies of the spectra of the degraded images.

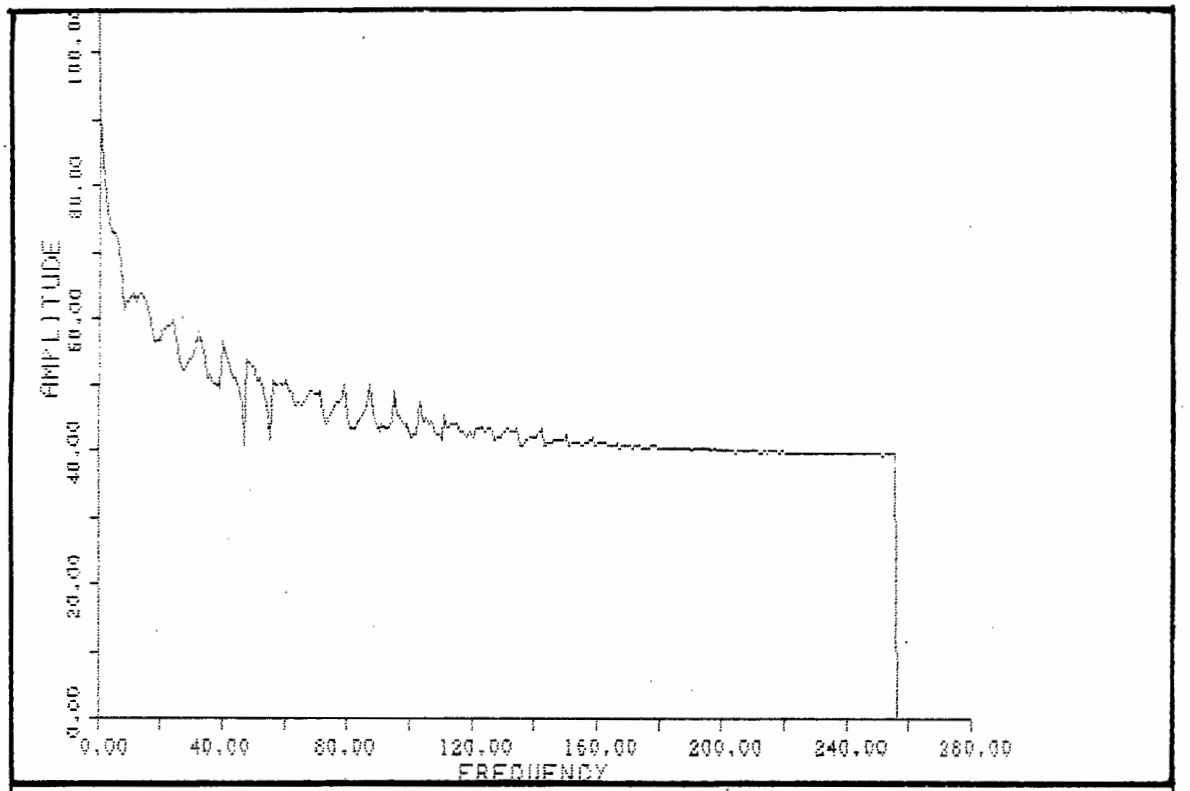

Line spectrum of a monochrome image

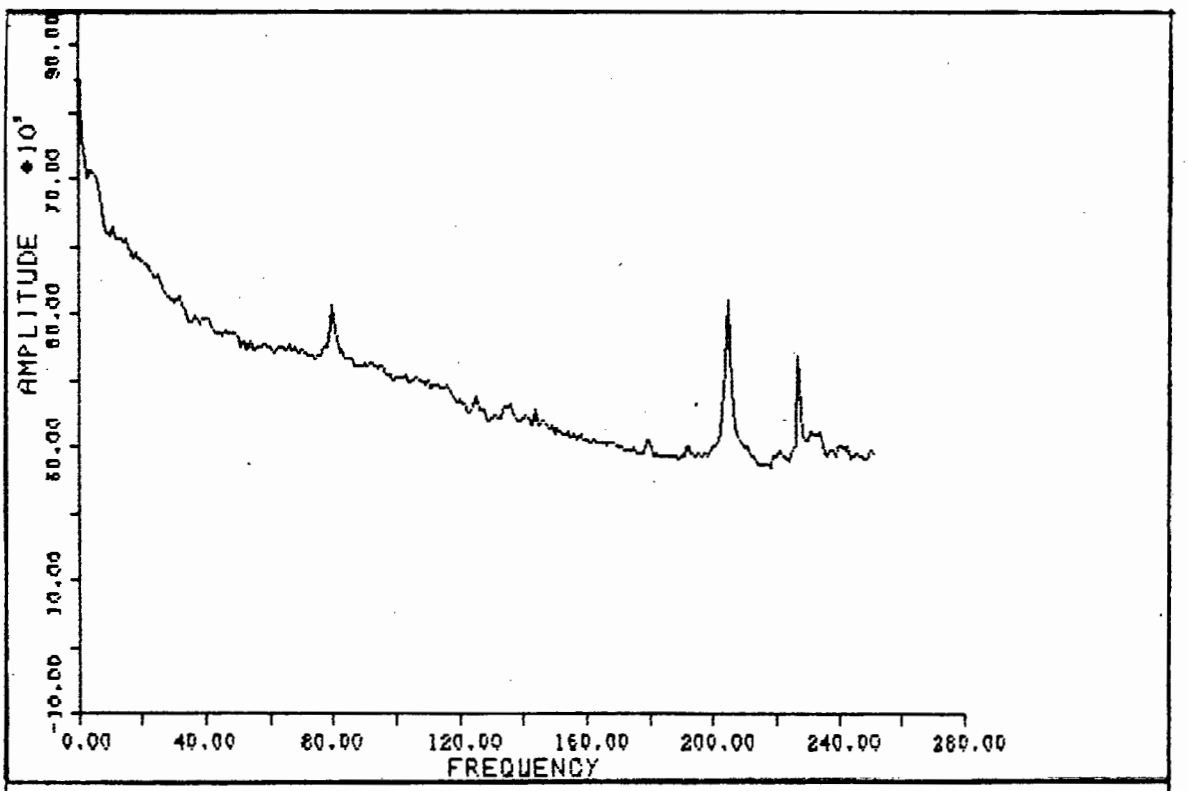

Line spectrum of a Red image

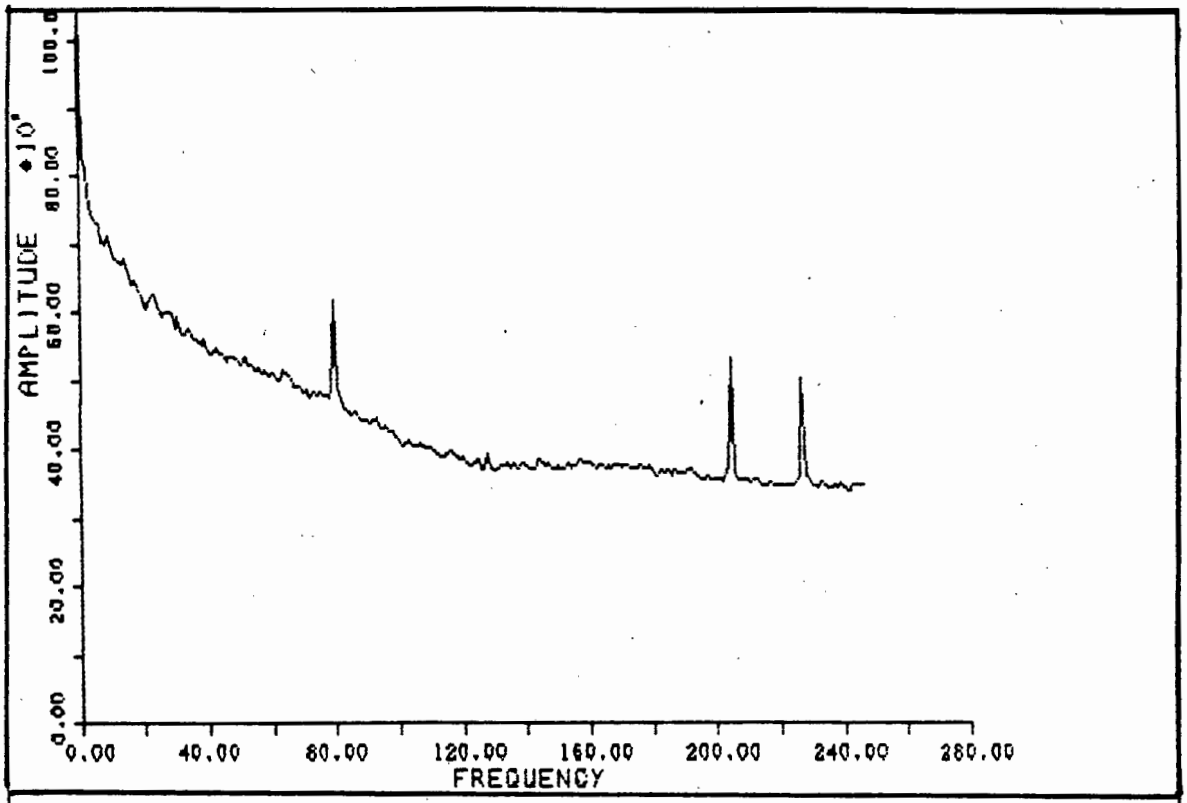

Line spectrum of a Green image

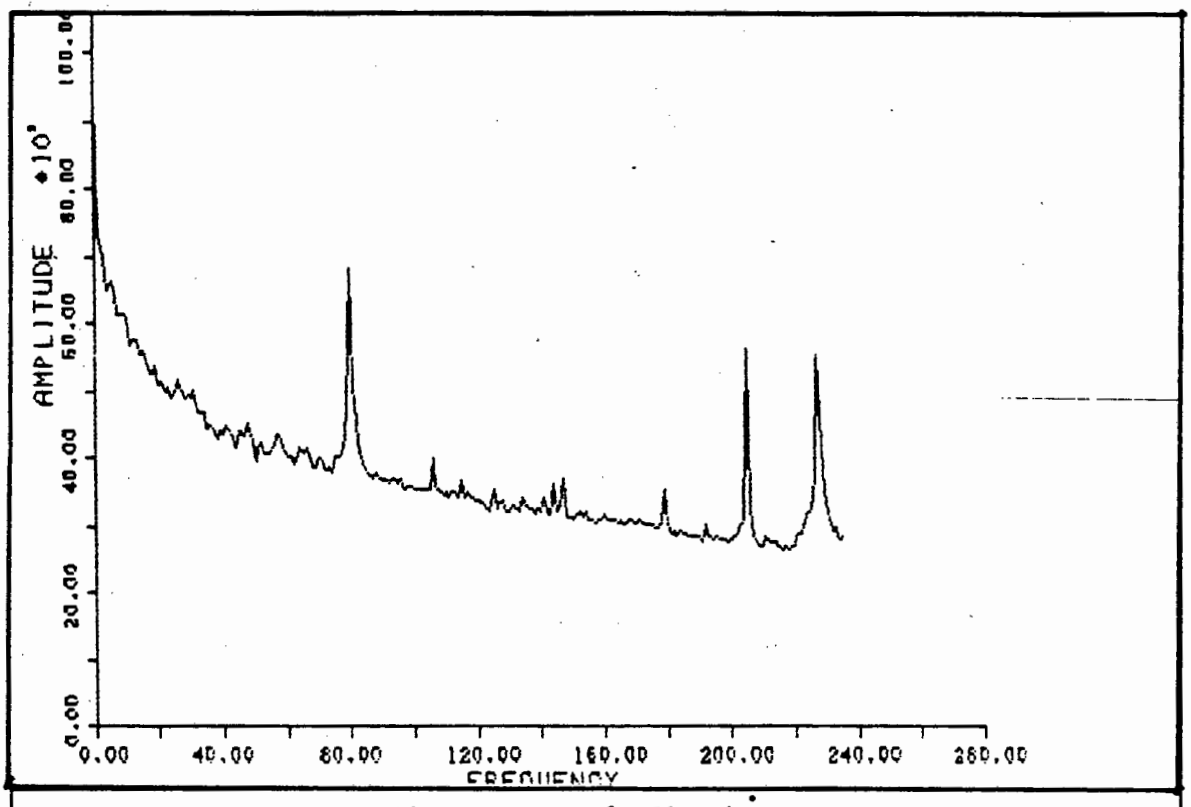

Line spectrum of a Blue image

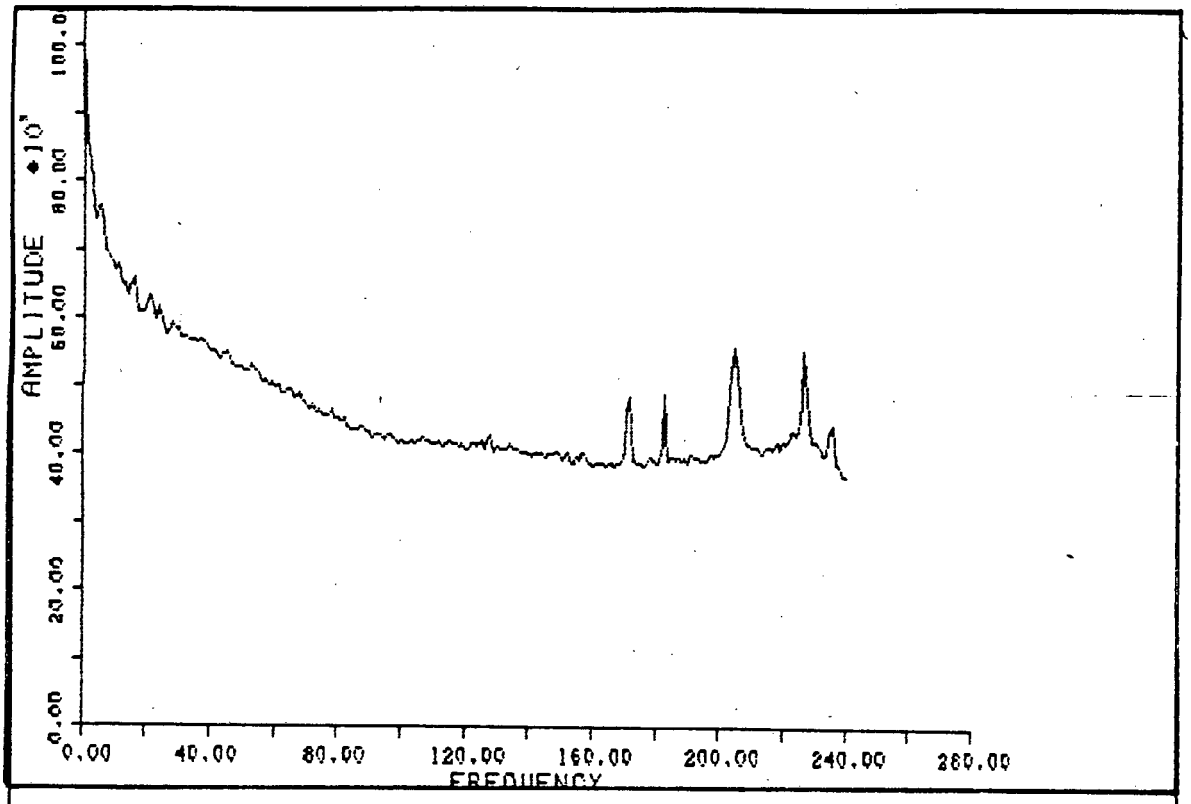

Line spectrum of a Composite image

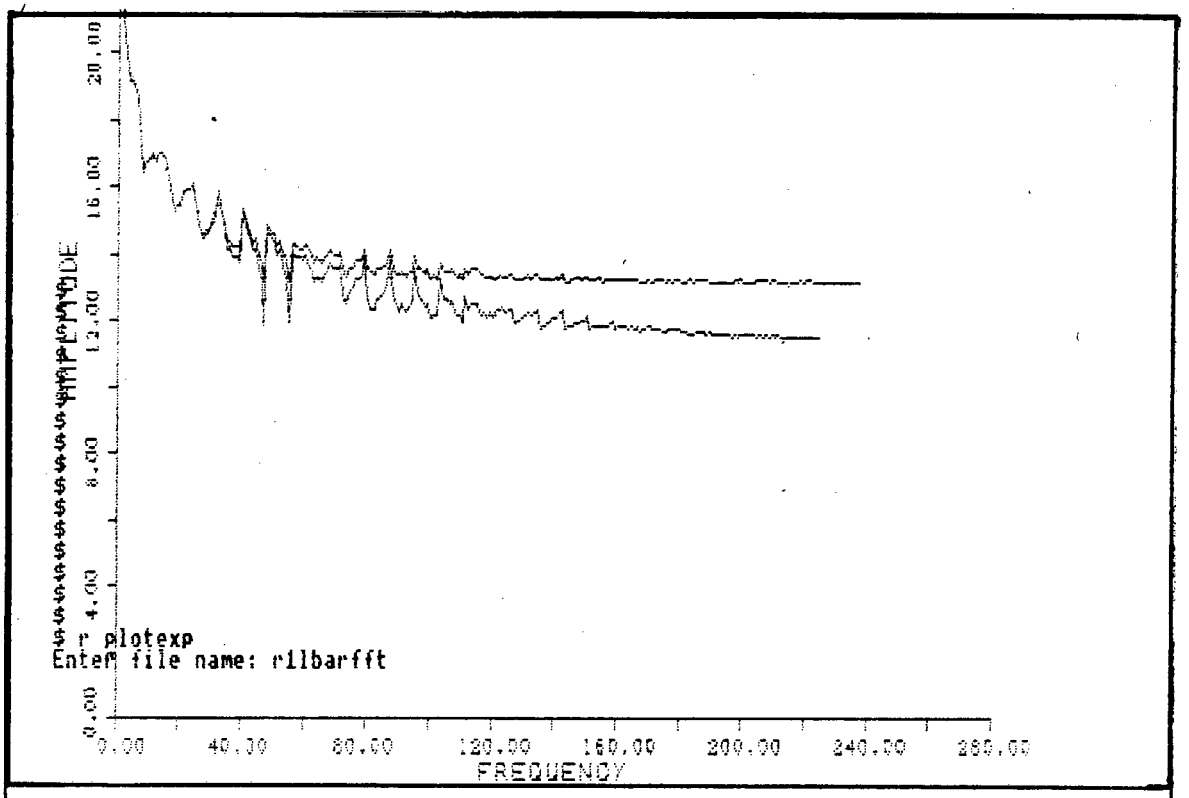

Line spectrum of a Monochrome image degraded with noise.

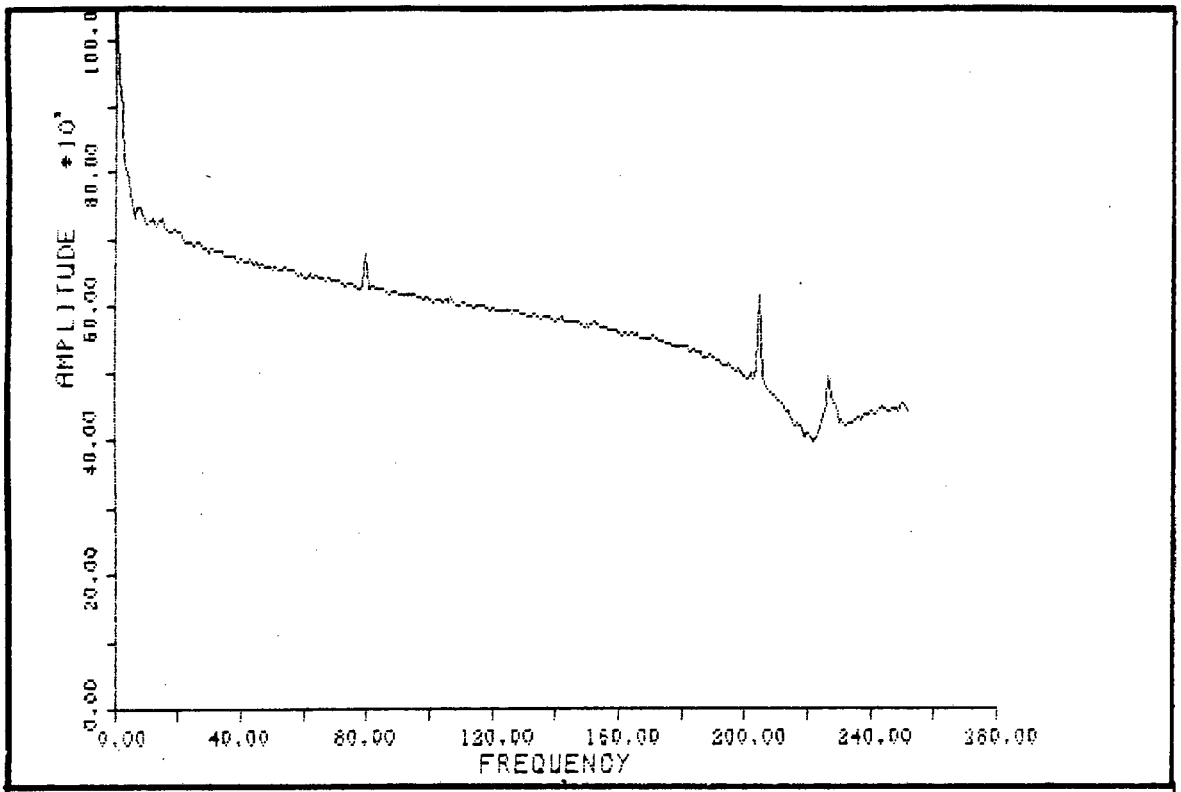

Line spectrum of a Red image degraded with noise.

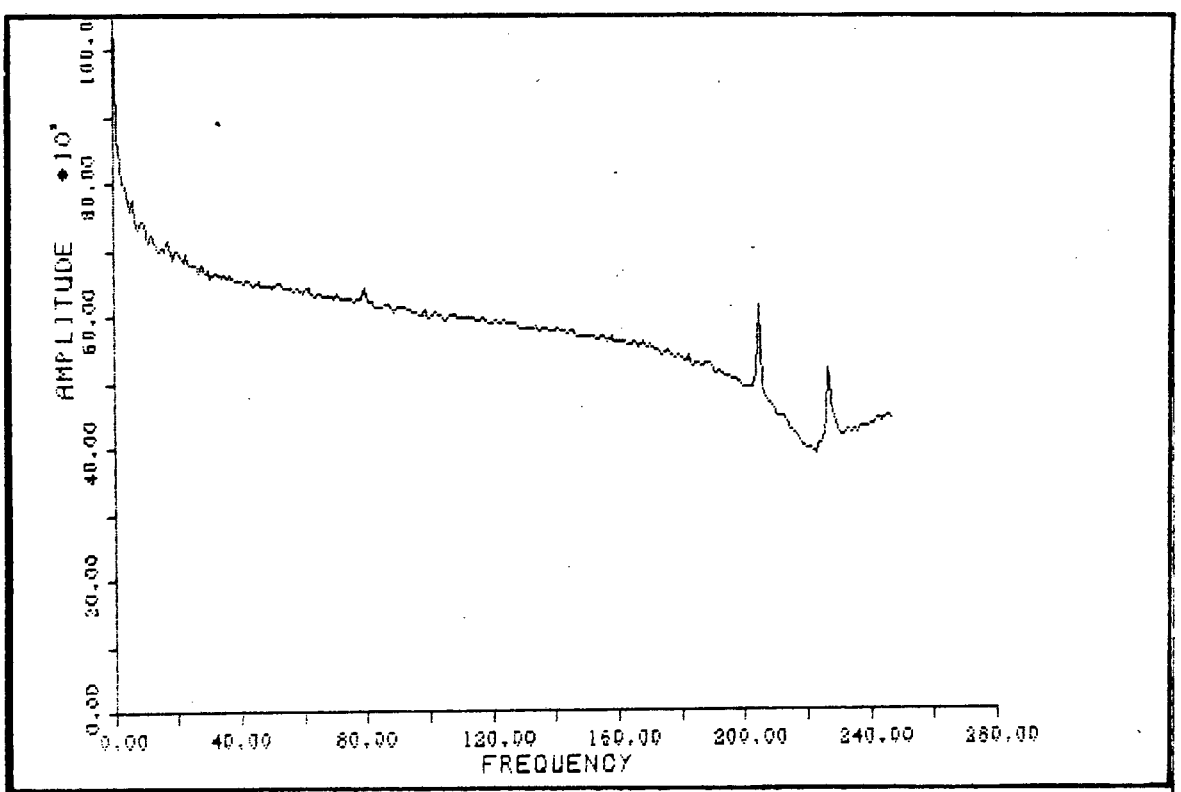

Line spectrum of a Green image degraded with noise.

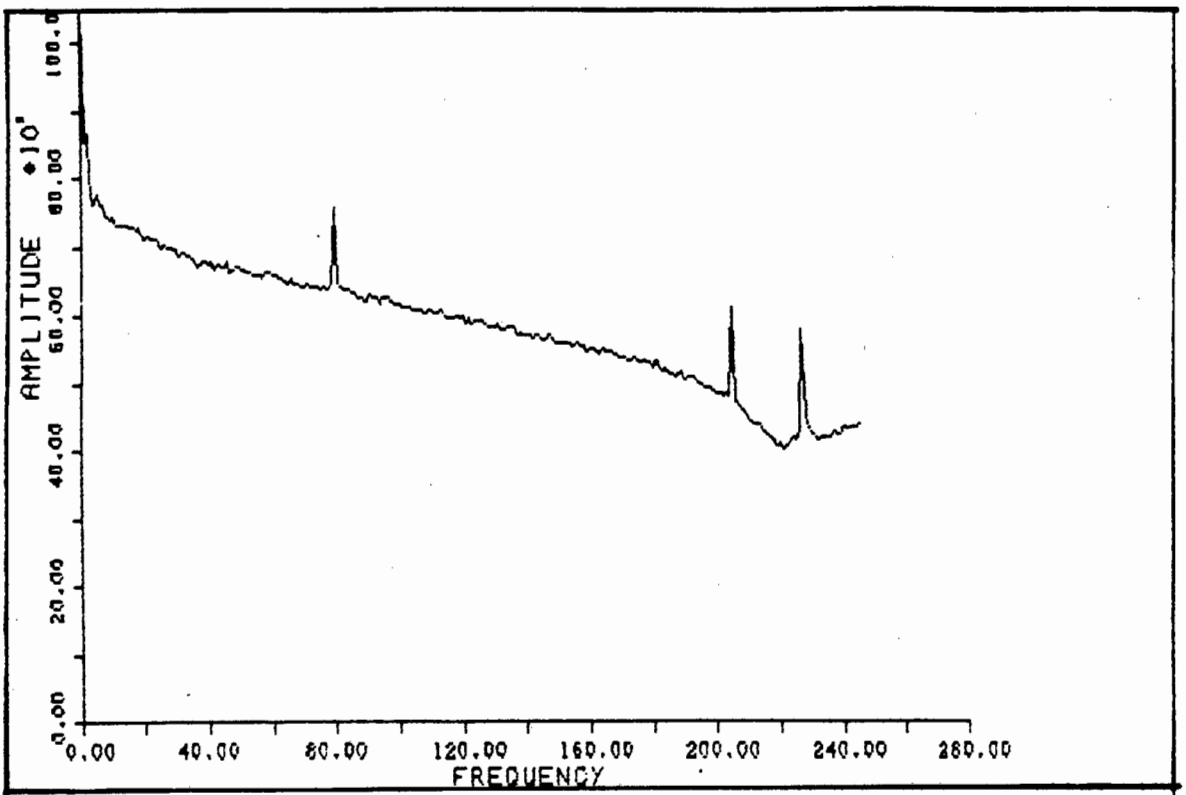

Line spectrum of a Blue image degraded with noise.

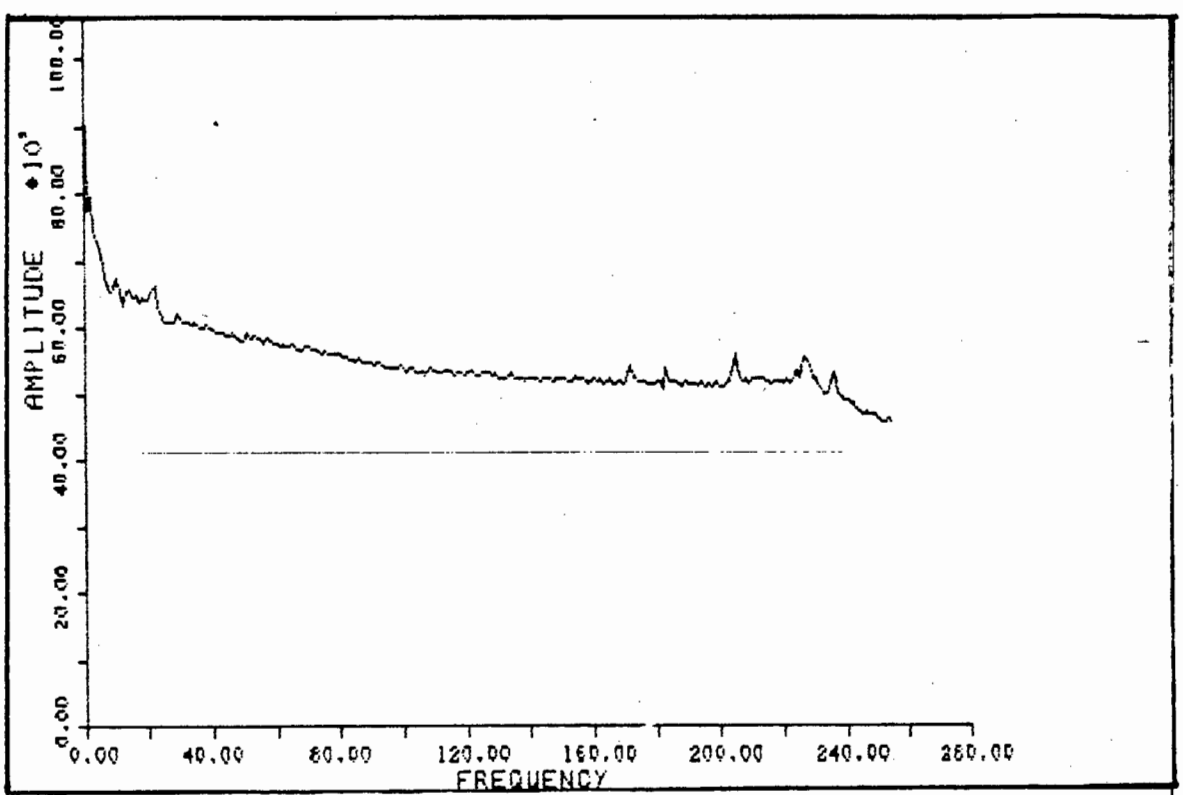

Line spectrum of a Composite image degraded with noise.

APPENDIX B

THREE DIMENSIONAL PROBABILITY PLOTS OF ONE DIMENSIONAL LINE AND COLUMN SPECTRA

A probability plot is a an estimation of the most likely shape of a one dimensional spectrum. Therefore the most likely shape of any of the following spectra is the top line (most probable) on any plot. Also is the width in the power direction an indication of how often the spectra deviates from the most likely estimation. Each point on the plot is an estimation of the occurrence of a power at a frequency of the 512 line or column spectra of 10 different pictures.

Firstly the portability plots for the noiseless line spectra are displayed, then the noisy line spectra, and then the noiseless and noisy column spectra follows

The probability plots was generated on a computer on the micro-vax called Probplots.exe. It inputs a .cfi file generated by either linfft.exe or kolfft.exe. The output of Probplot is a text file compatible with most 3D-plot software.

PROBABILITY PLOTS OF LINE SPECTRA

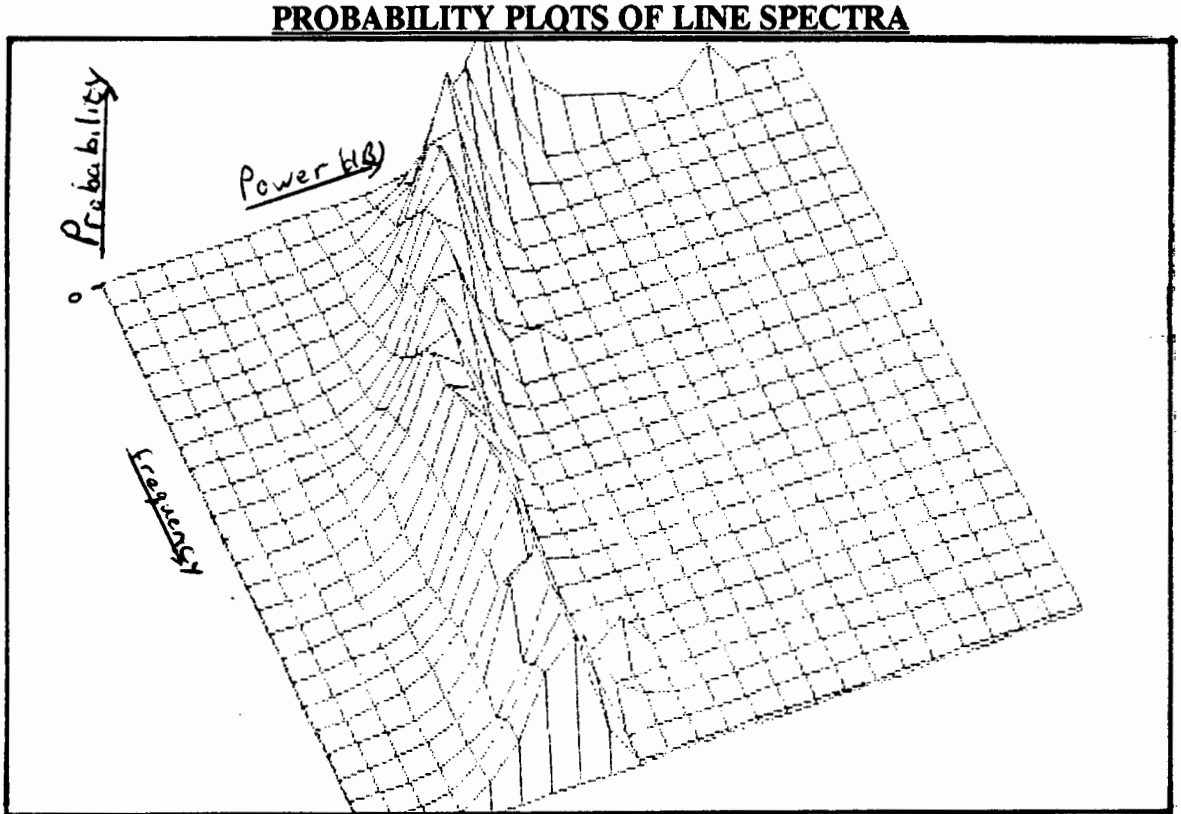

Probability plot of Line spectrum of a Red image

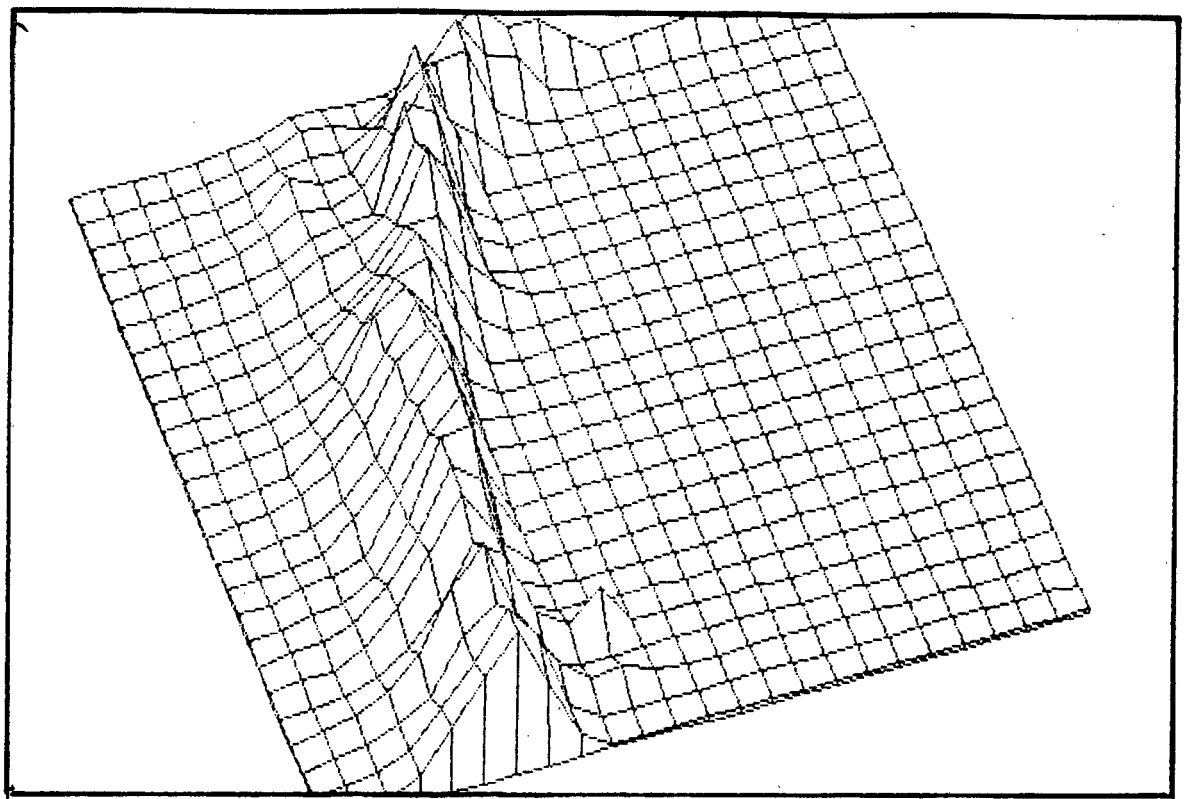

Probability plot of Line spectrum of a Green image

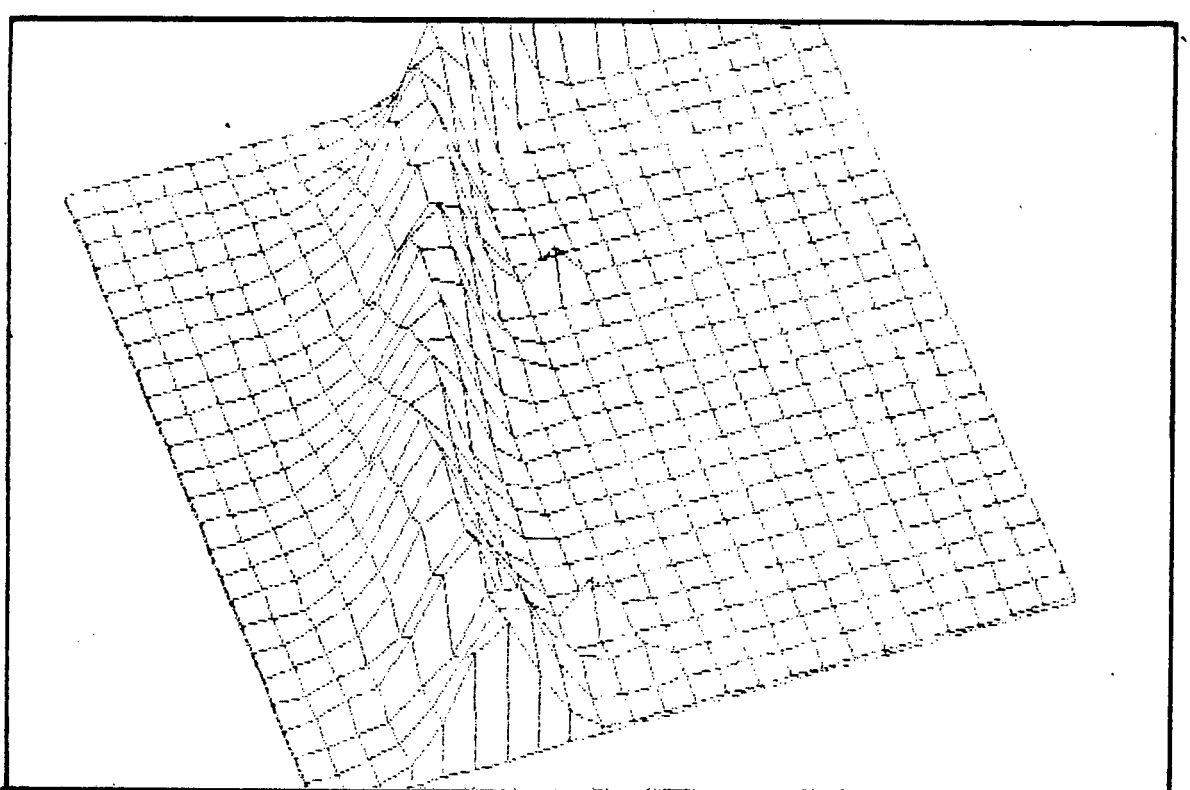

Probability plot of Line spectrum of a Blue image

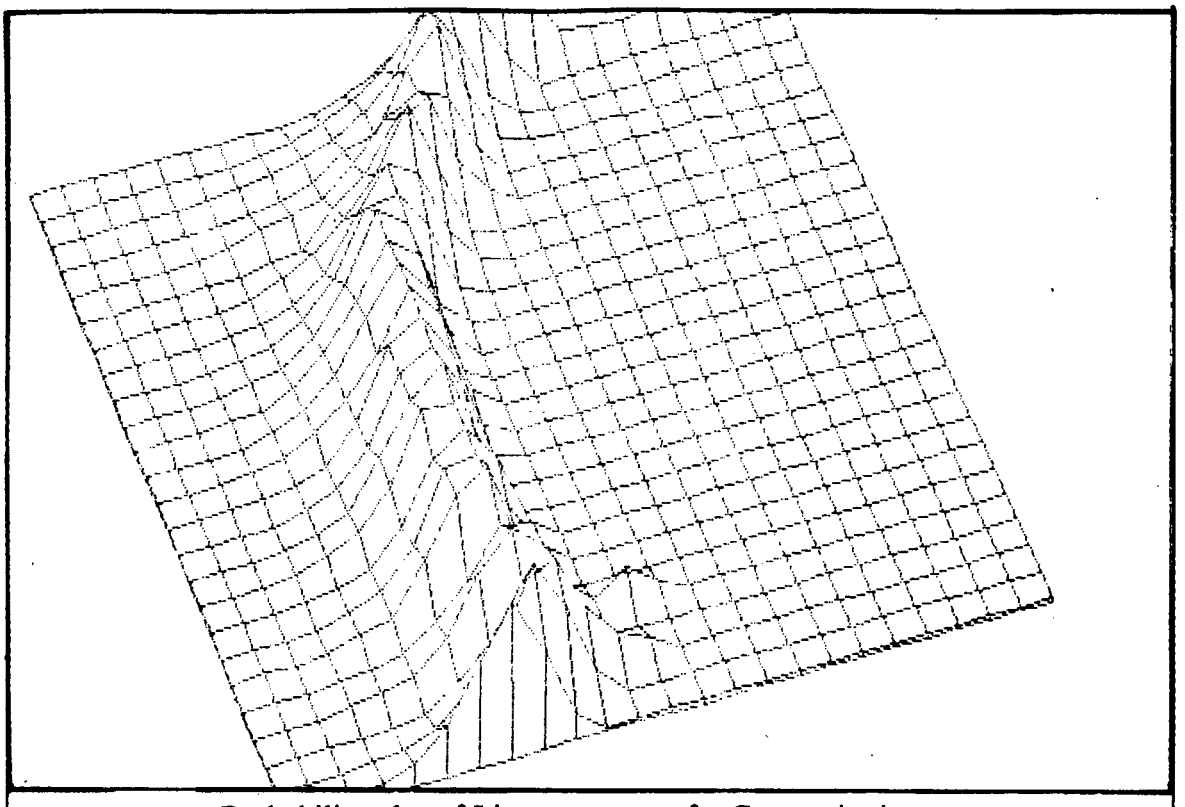

Probability plot of Line spectrum of a Composite image

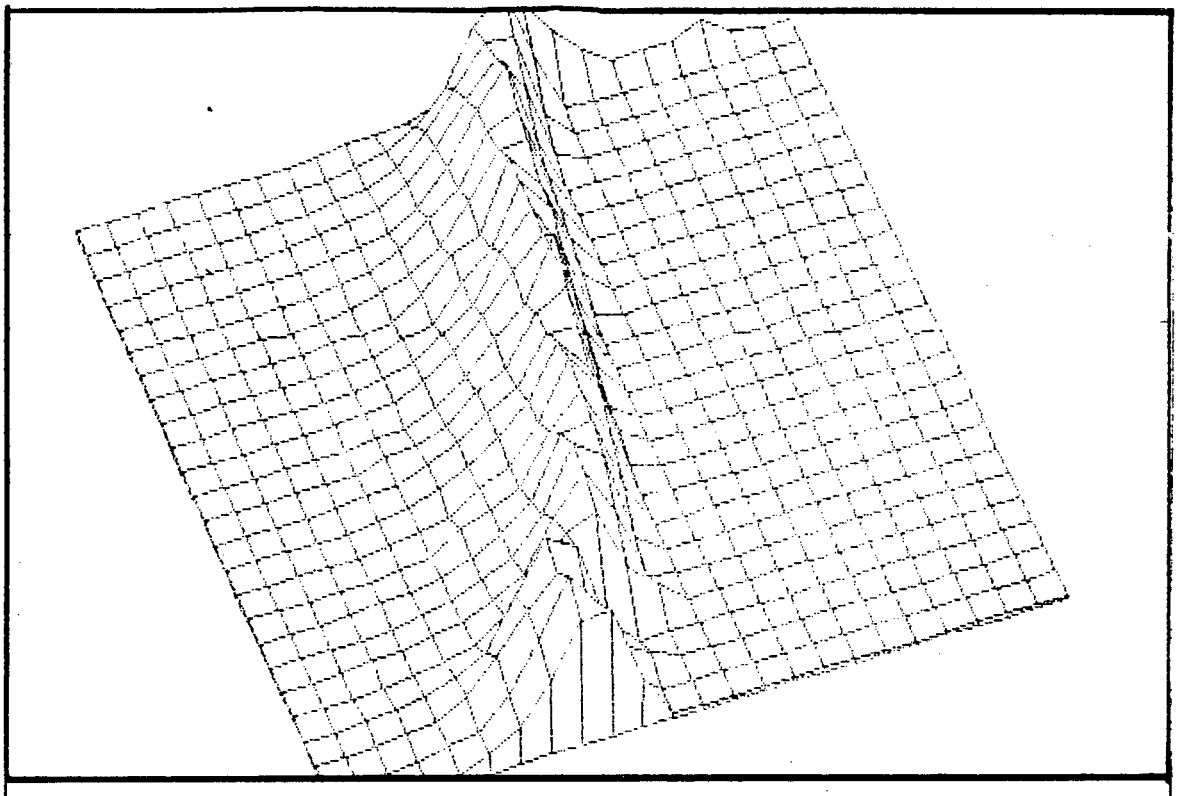

Probability plot of Line spectrum of a Red image degraded with noise.

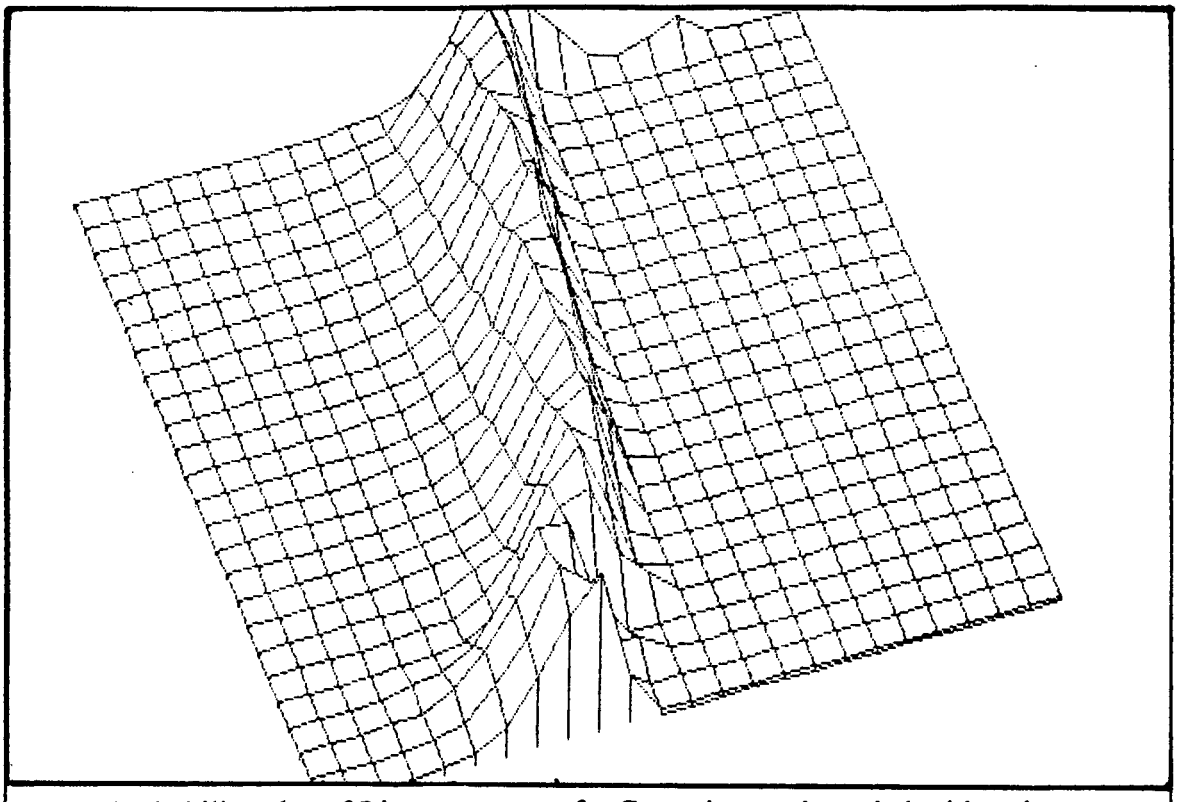

Probability plot of Line spectrum of a Green image degraded with noise.

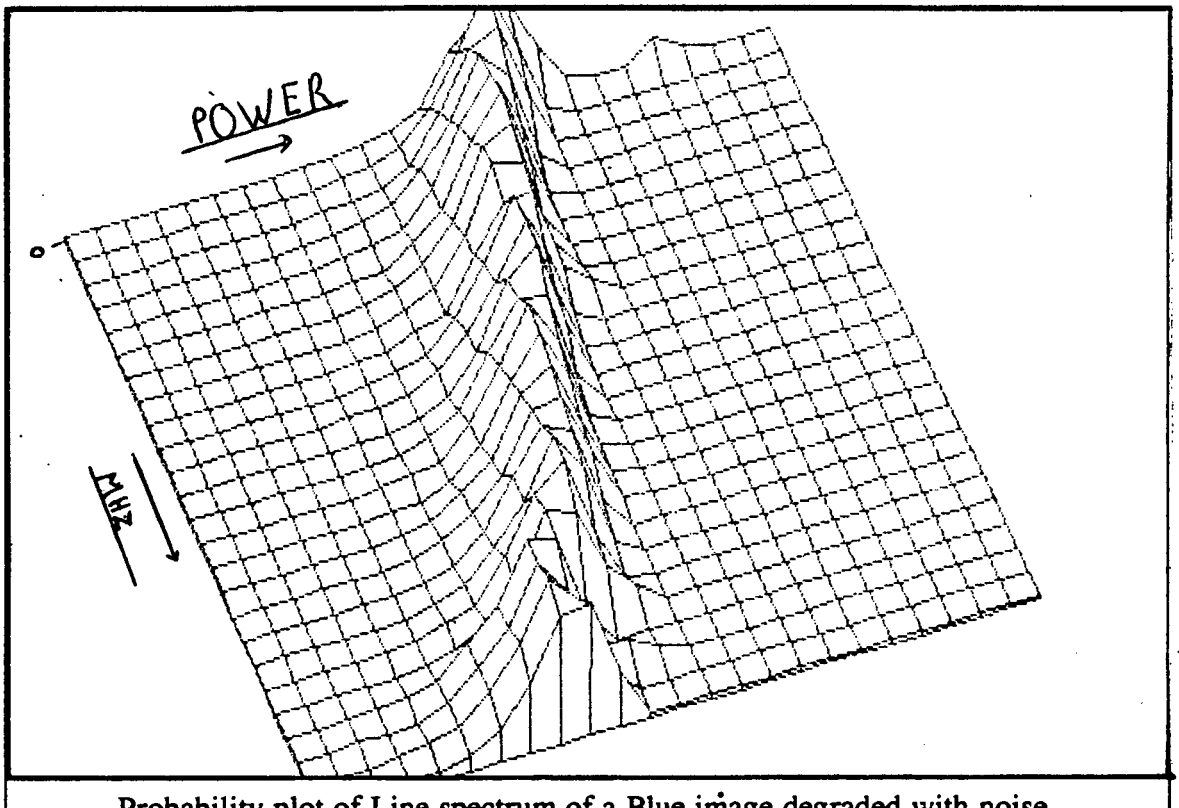

Probability plot of Line spectrum of a Blue image degraded with noise.

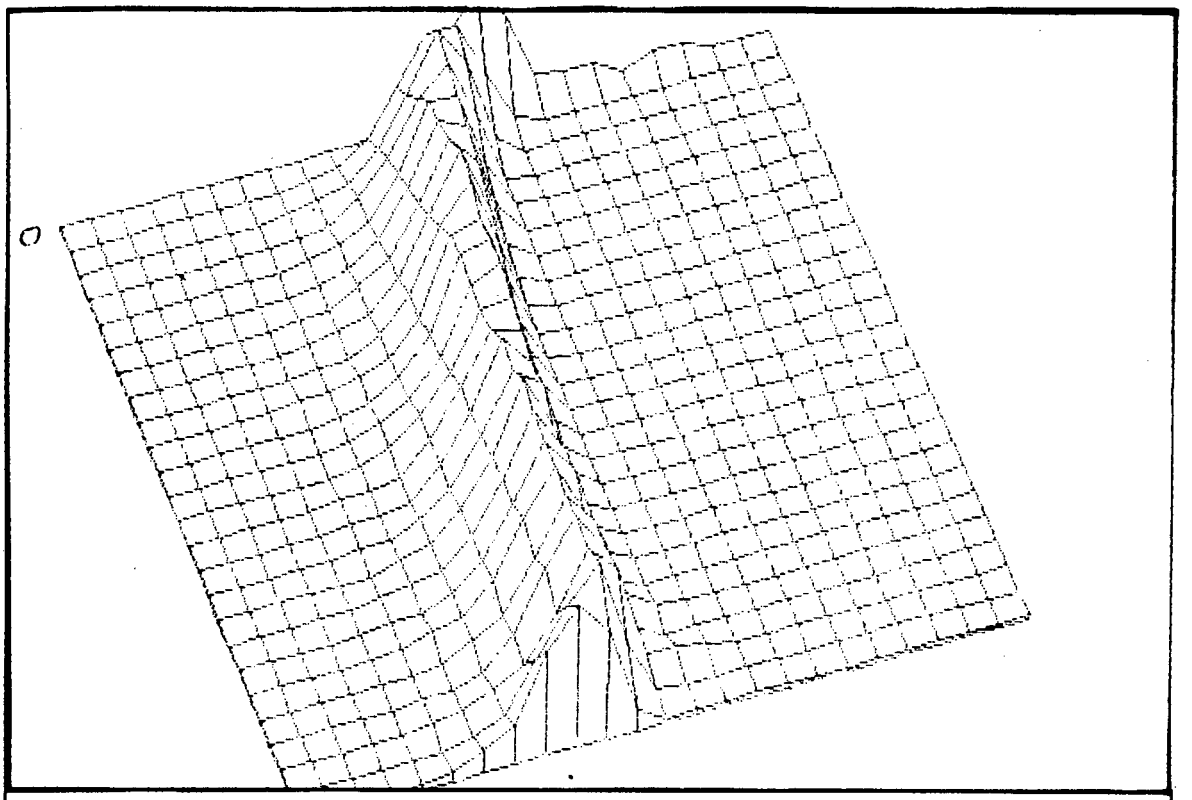

Probability plot of Line spectrum of a Composite image degraded with noise.

PLOTS OF COLUMN SPECTRA

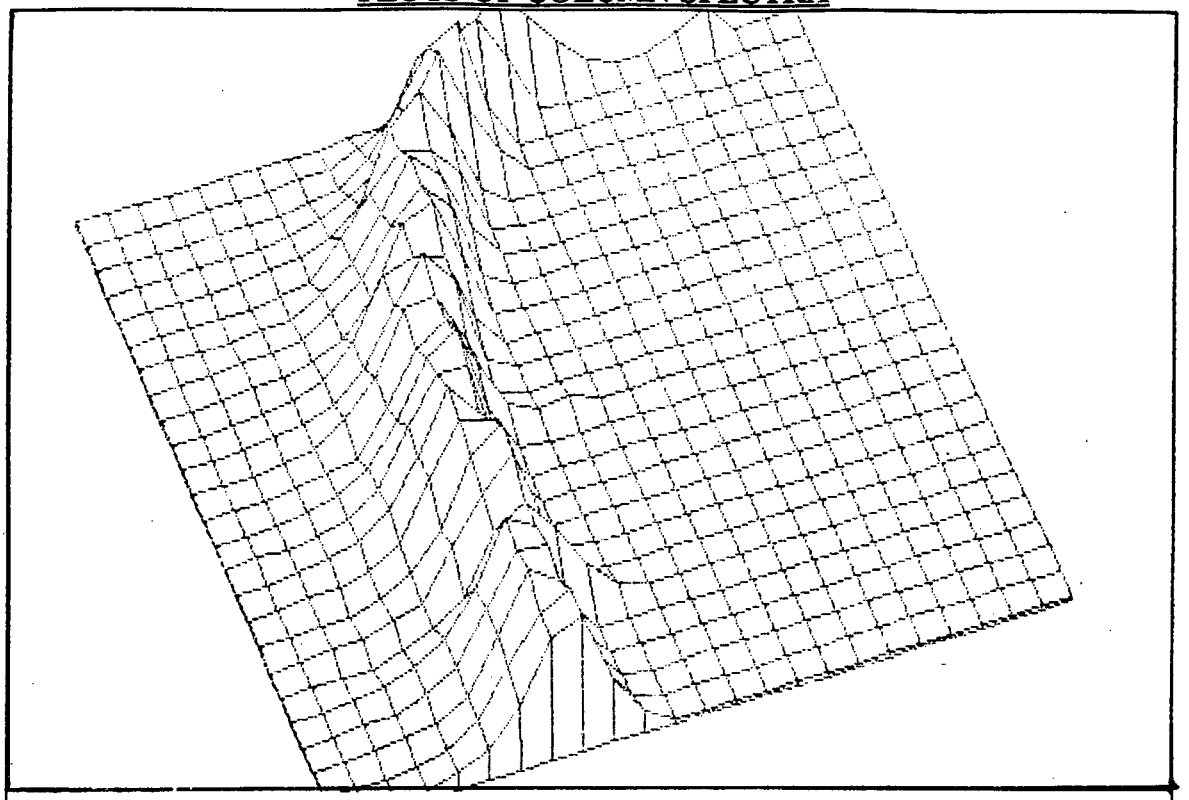

Probability plot of Column spectrum of a Red image

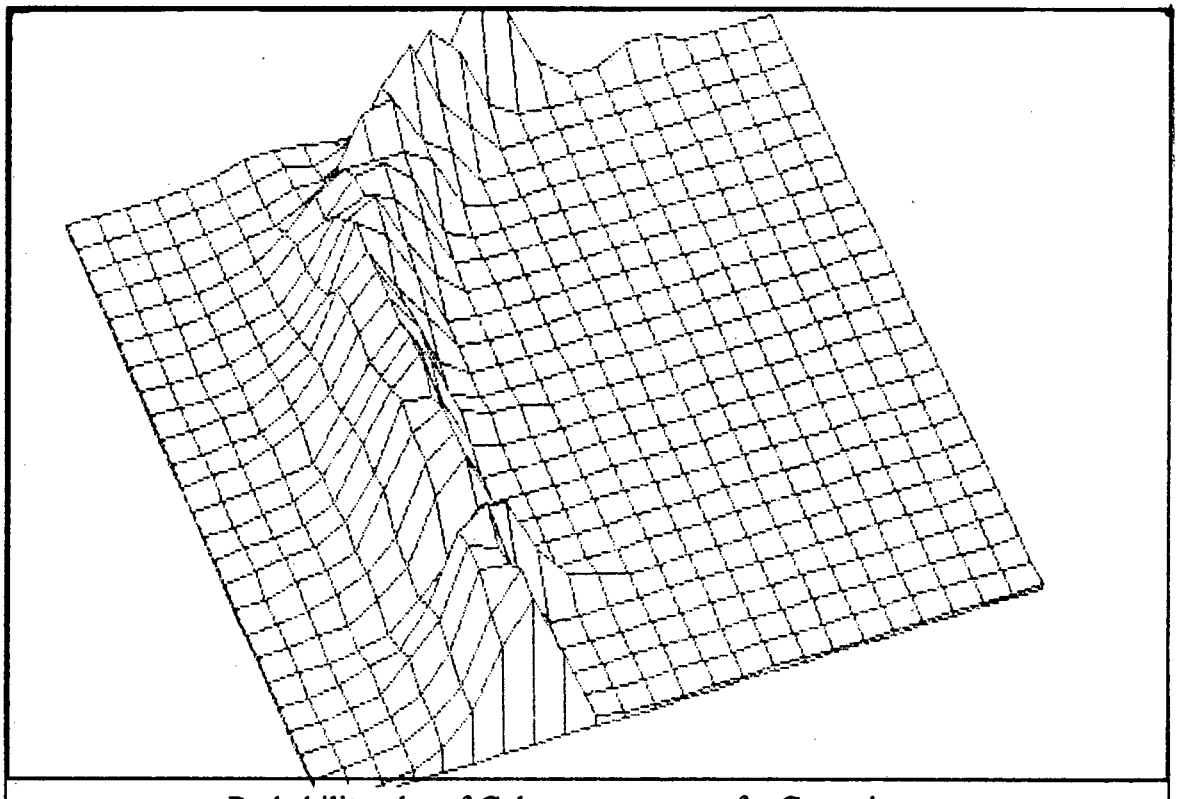

Probability plot of Column spectrum of a Green image

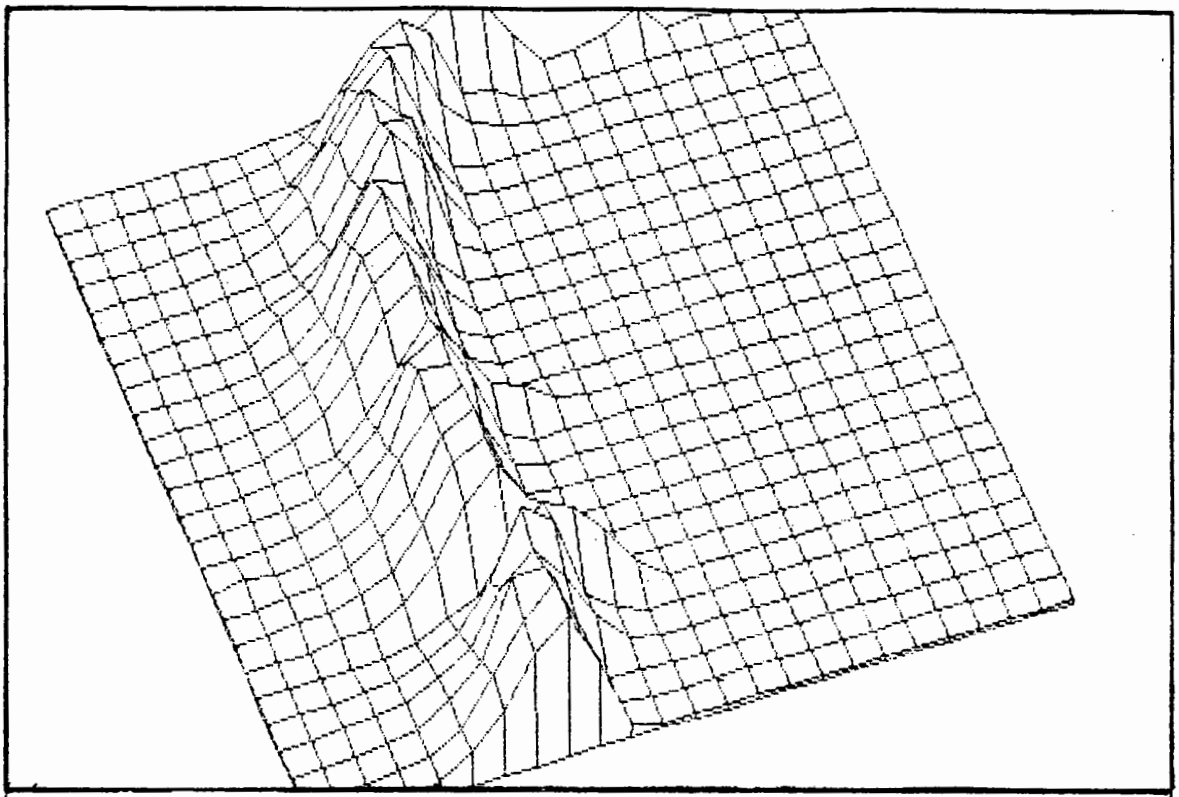

Probability plot of Column spectrum of a Blue image

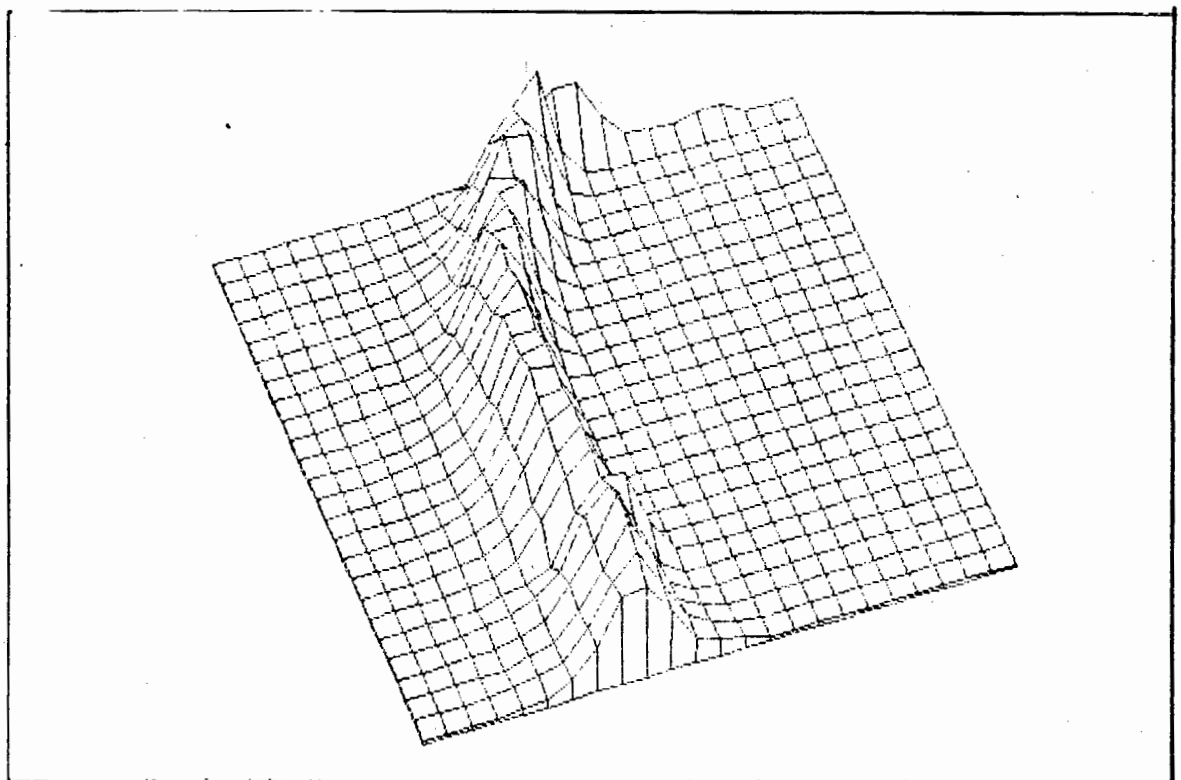

Probability plot of Column spectrum of a Composite image

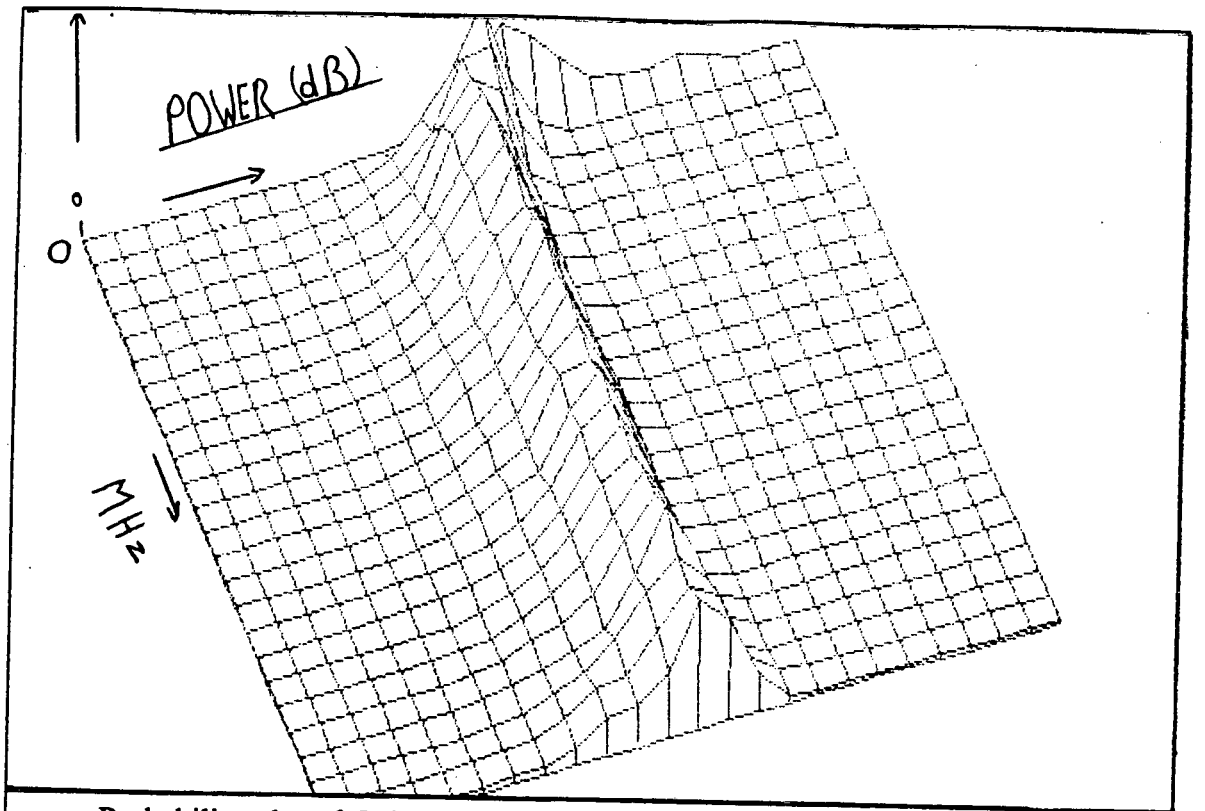

Probability plot of Column spectrum of a Red image degraded with noise.

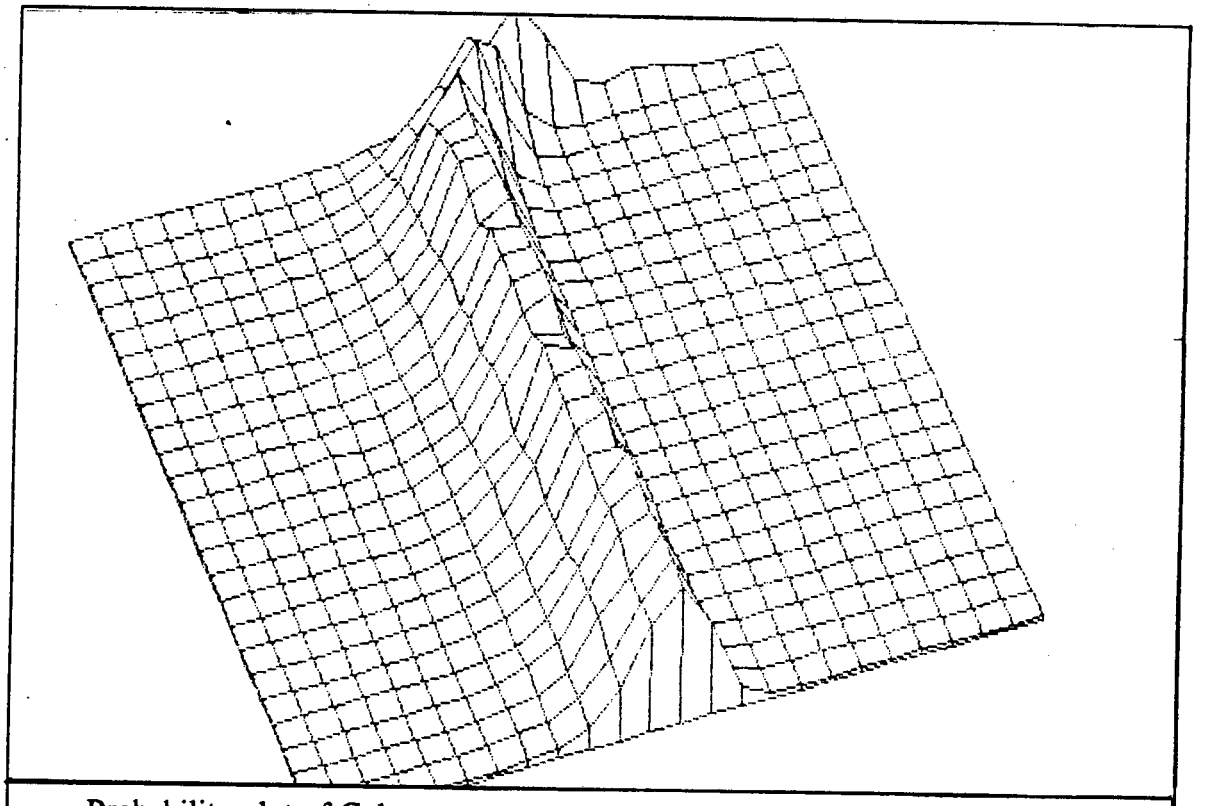

Probability plot of Column spectrum of a Green image degraded with noise.

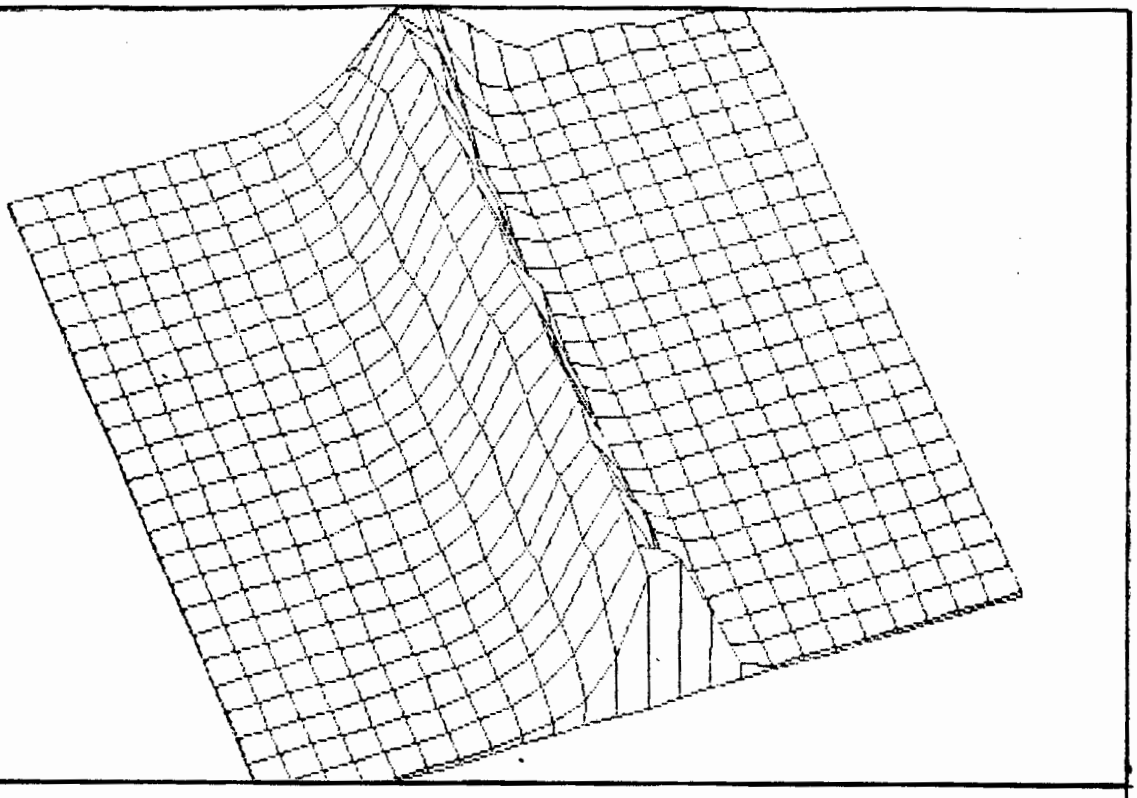

Probability plot of Column spectrum of a Blue image degraded with noise.

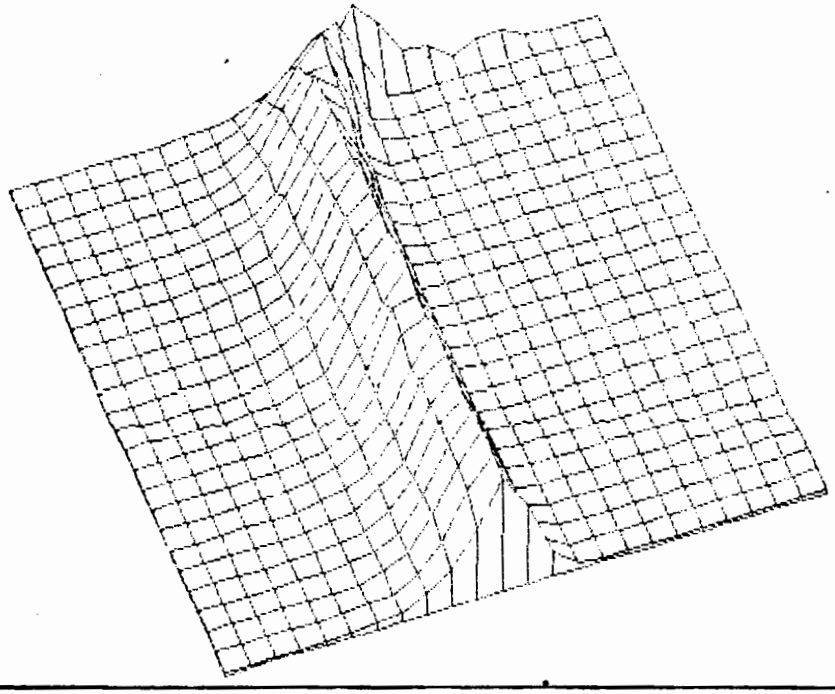

Probability plot of Column spectrum of a Composite image degraded with noise.

APPENDIX C

ONE DIMENSIONAL COLUMN SPECTRA

A one dimensional column spectrum is the average of the spectra of all the vertical lines in an image. This is similar to a Bartlett estimation of the picture spectrum. The only System characteristics in these spectra is the high-frequency motion blur.

The column spectra were generated on the micro-VAX with a program called kolfft.exe. The format is the same as that of linfft.exe.

The first four spectra are of noise free images, and the last four are of images degraded with white noise. Note the high power in the high-frequencies of the spectra of the degraded images.

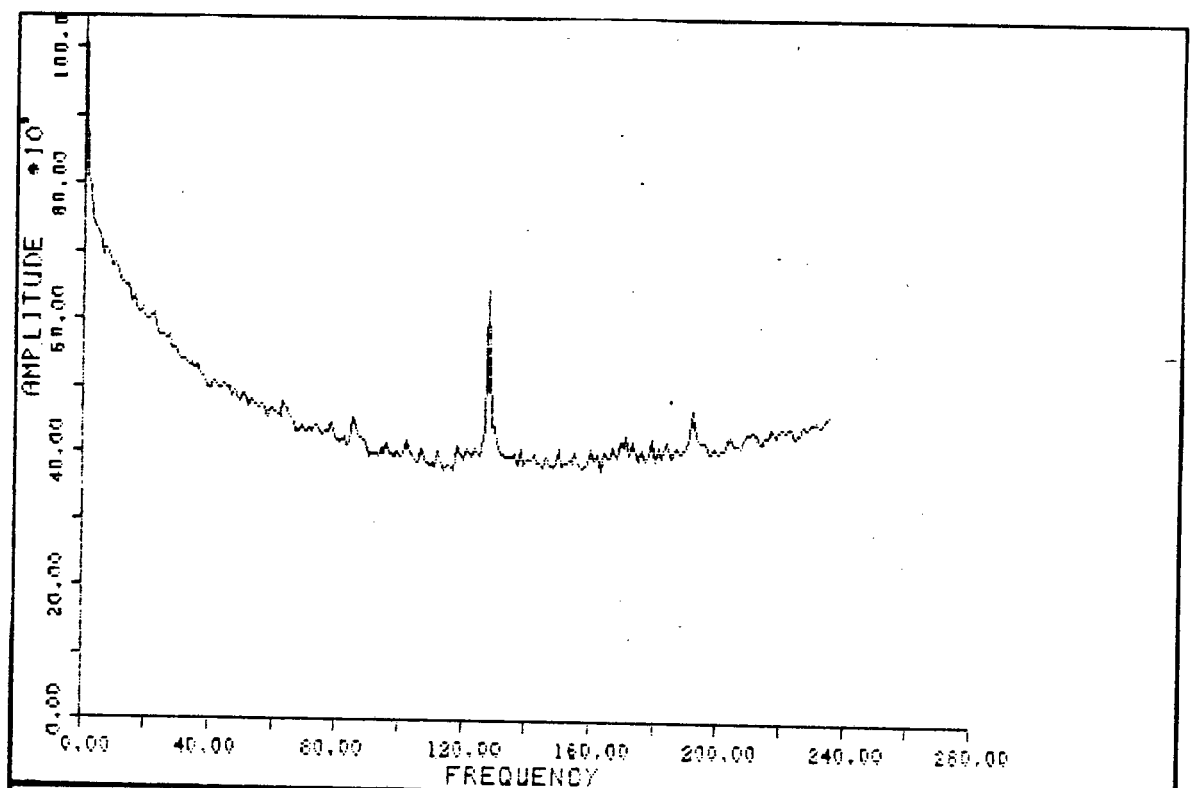

Column spectrum of a Red image

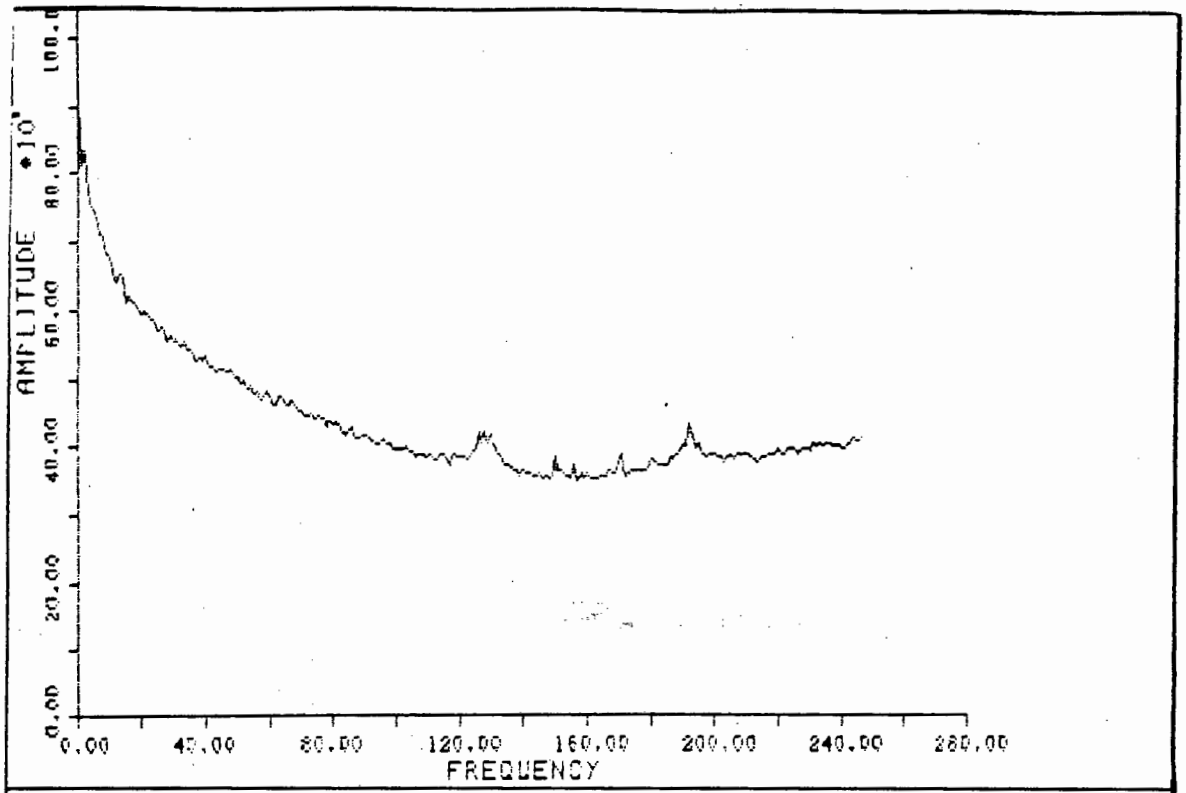

Column spectrum of a Green image

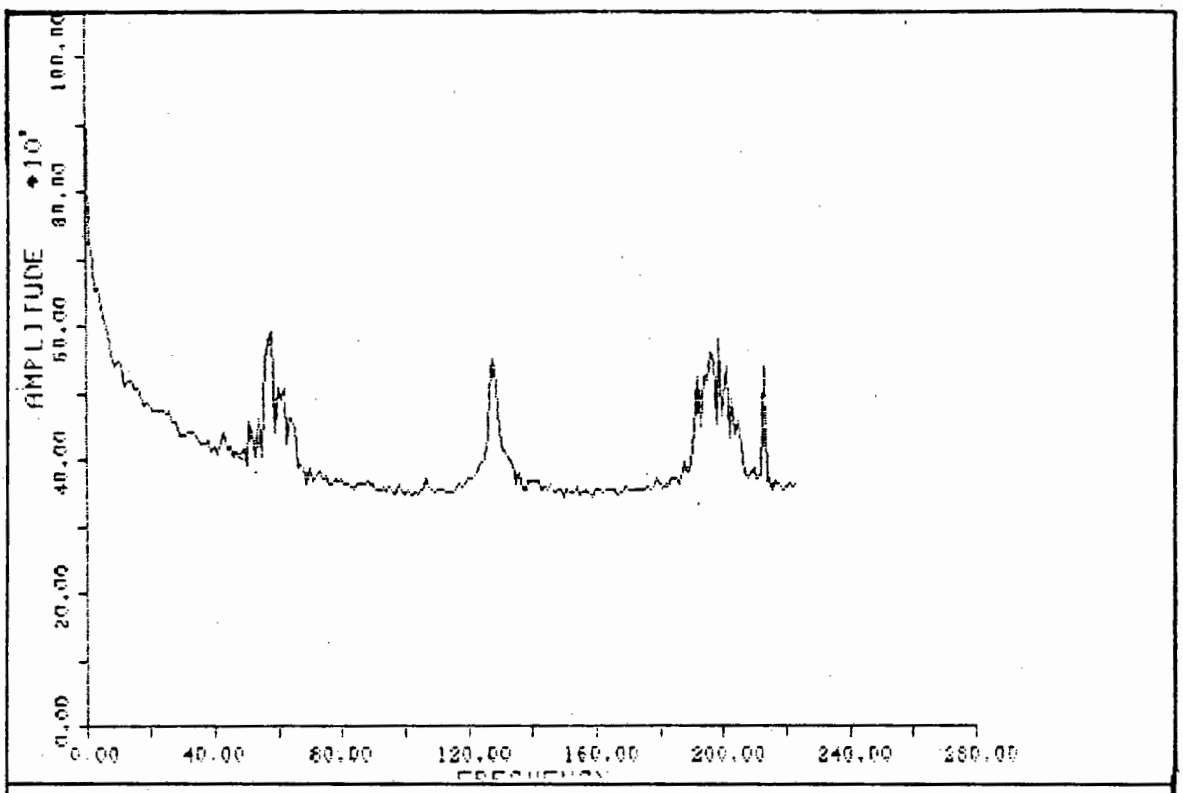

Column spectrum of a Blue image

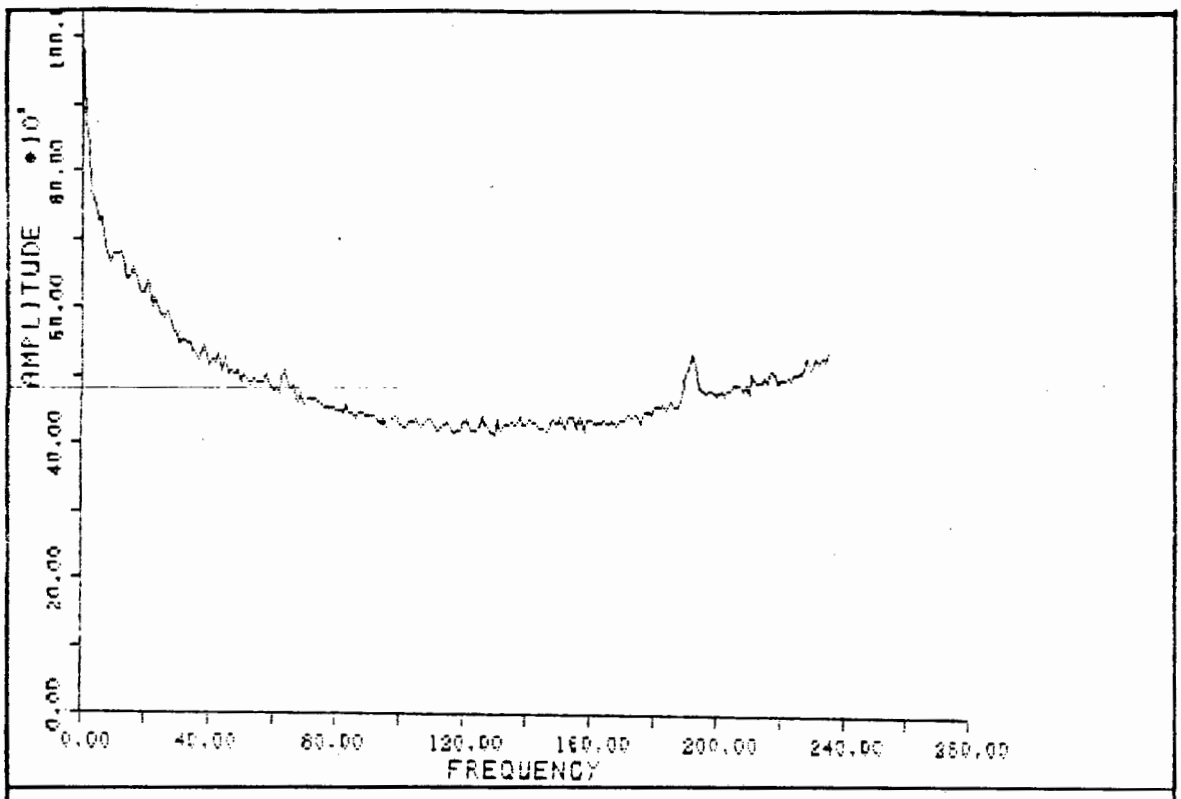

Column spectrum of a Composite image

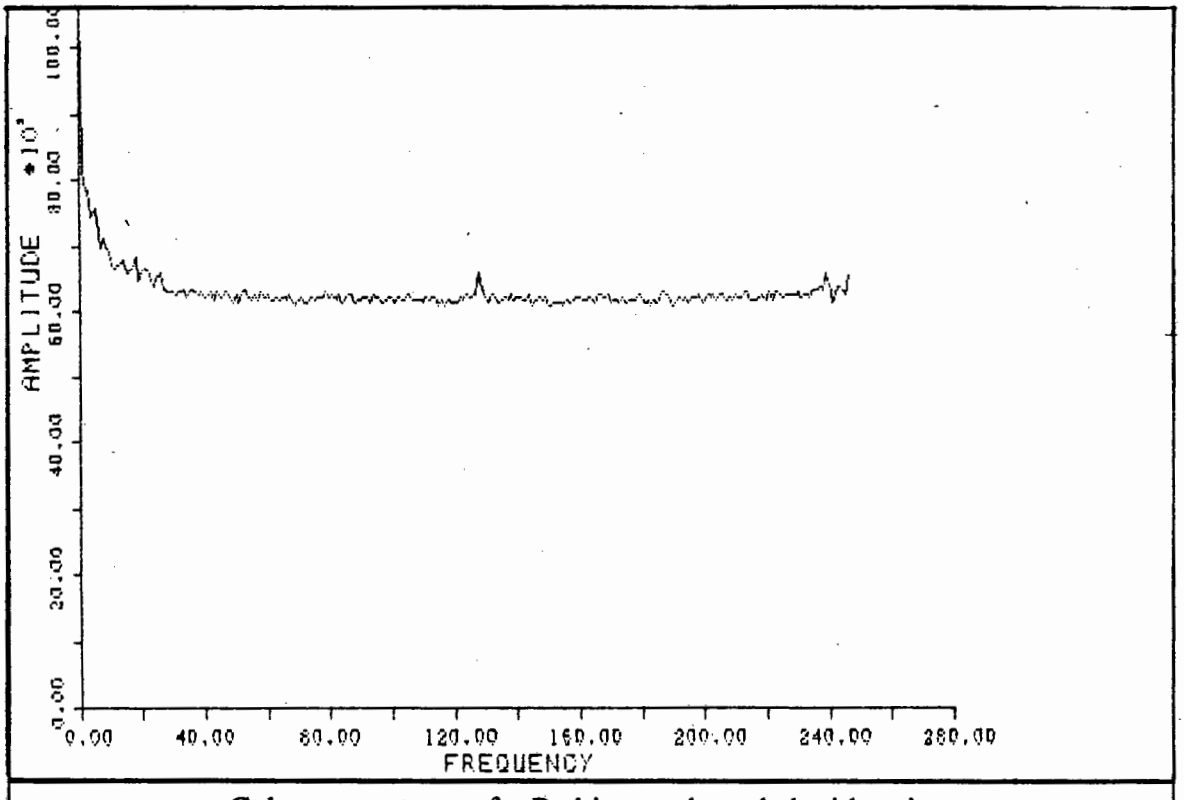

Column spectrum of a Red image degraded with noise.

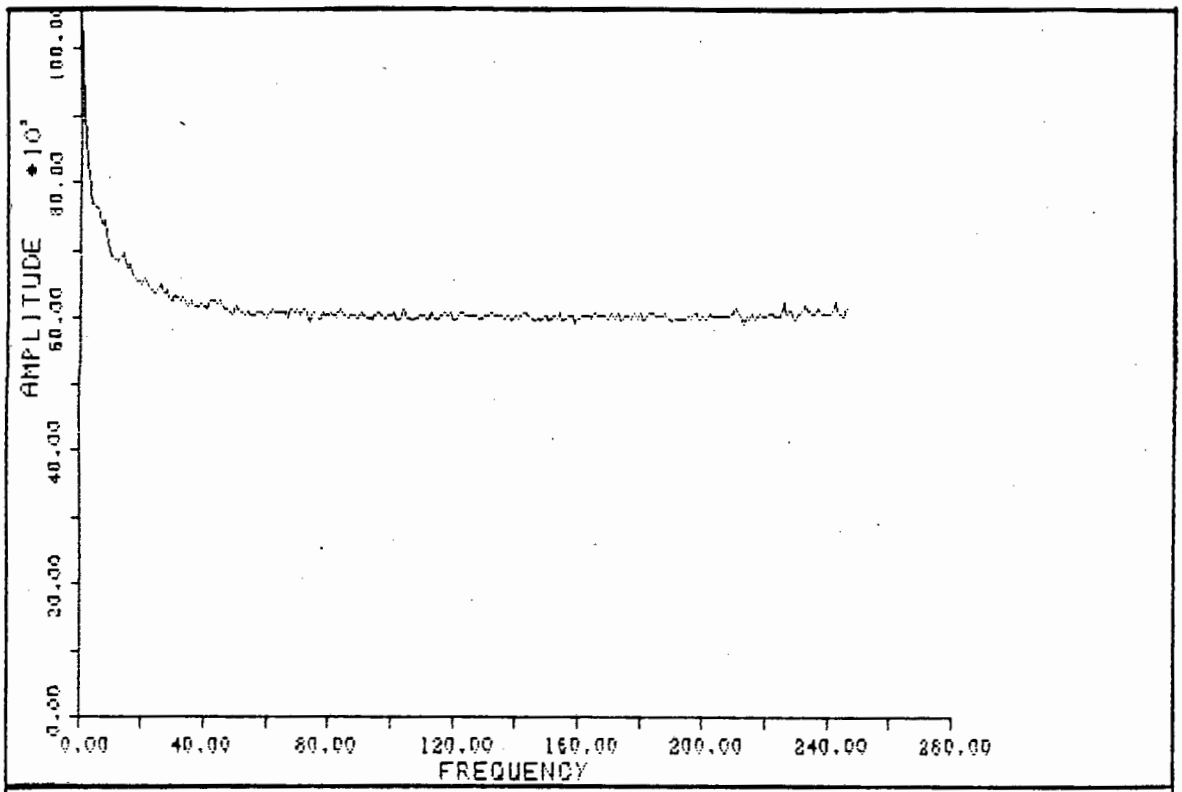

Column spectrum of a Green image degraded with noise.

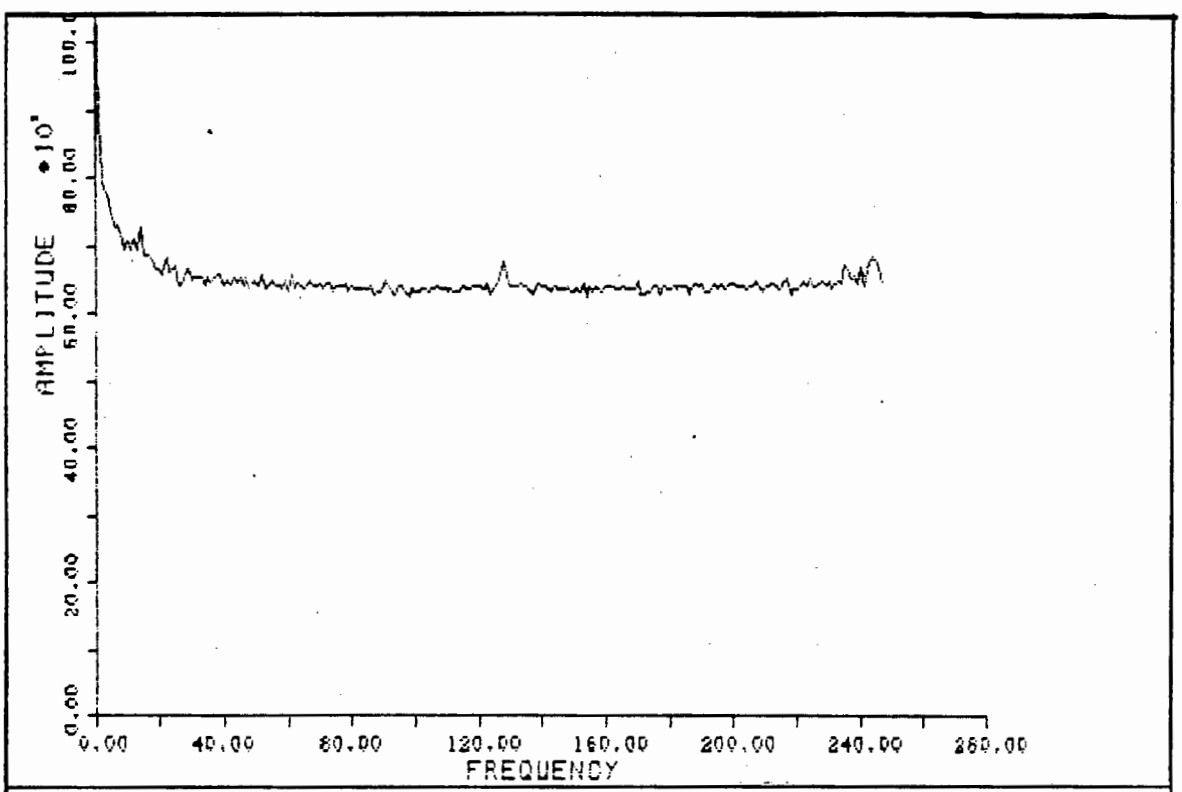

Column spectrum of a Blue image degraded with noise.

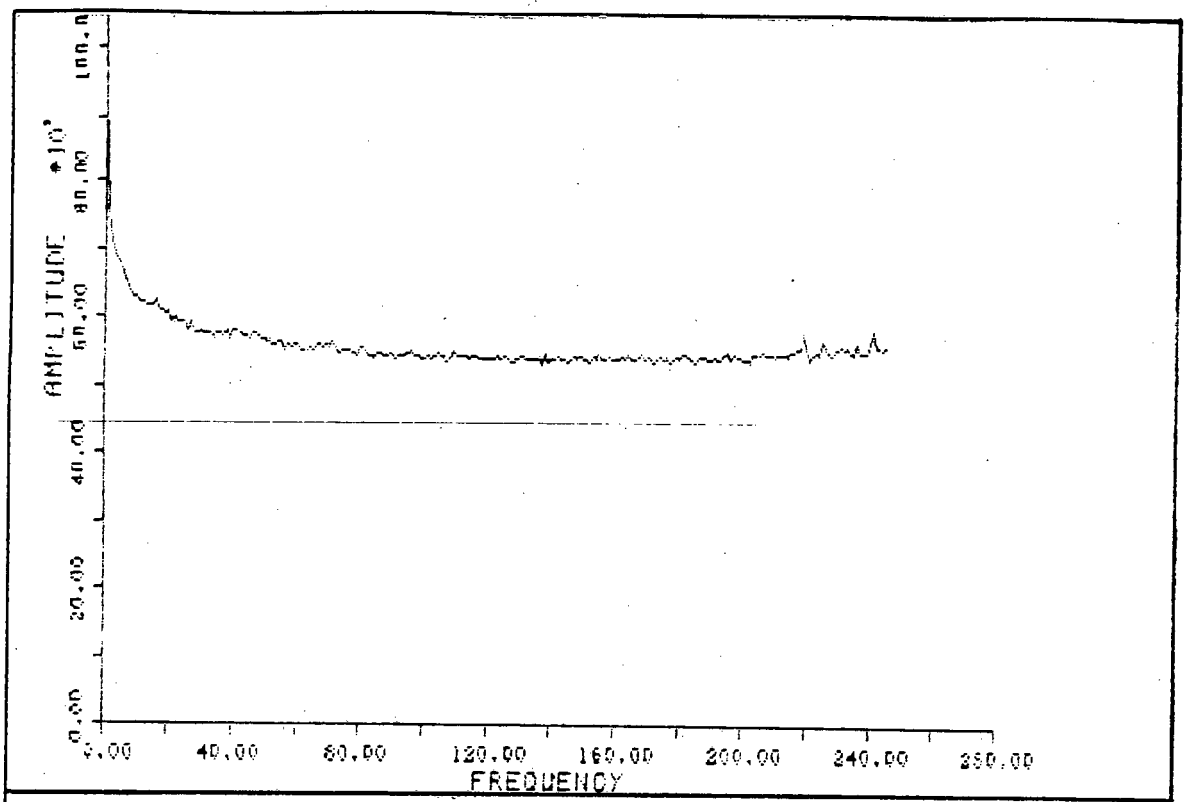

Column spectrum of a Composite image degraded with noise.

APPENDIX D

TWO DIMENSIONAL SPECTRA

The two dimensional spectra displayed are the average of 10-image-spectra. This is an periodogram estimation of the two dimensional spectrum as proposed by Ulichney (1988).

The 2D spectra were created on the micro-VAX with a program called fft2dmag.exe.

The first five spectra are of noise free images and the last five are of degraded images. Note how the composite-image-spectra conform to the 1/frequency^2 rule of Schreiber (1986), and how the Red, green, and blue images do not obey it.

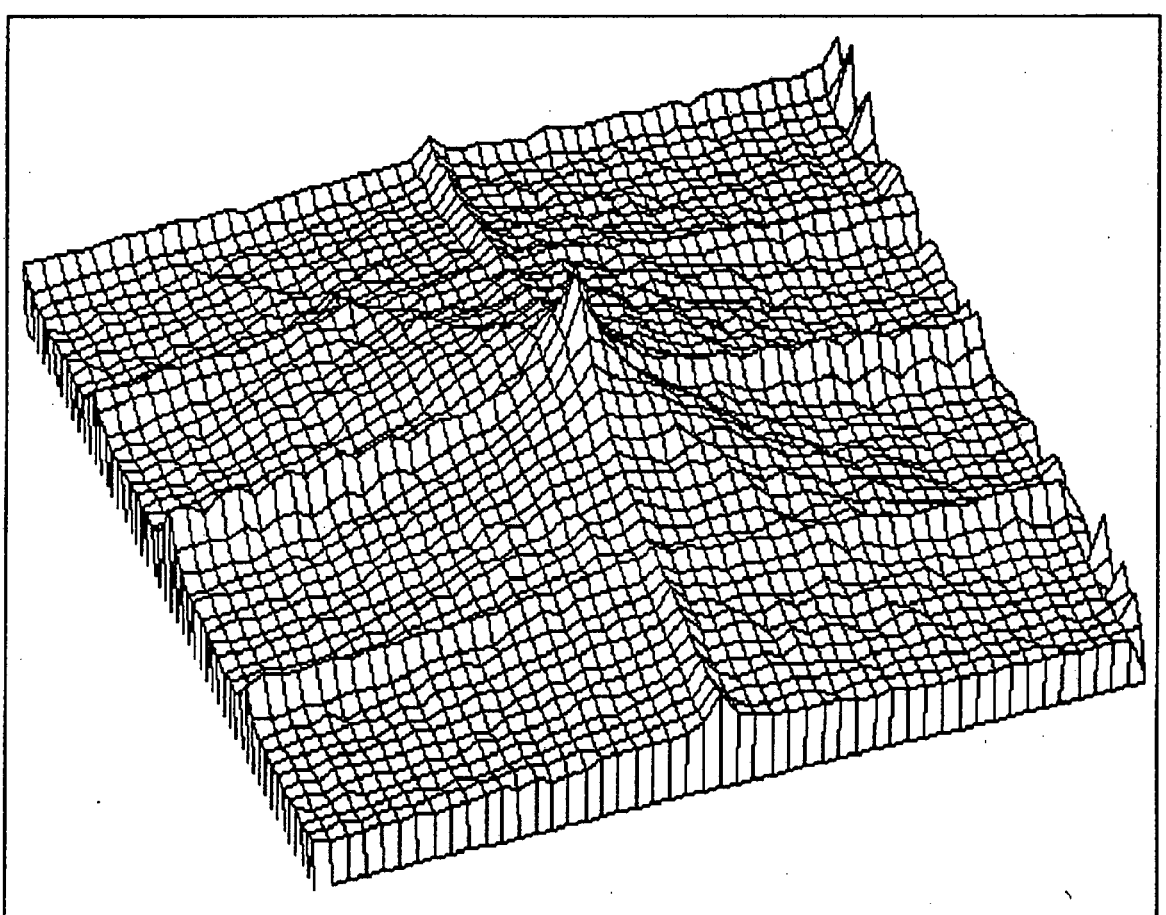

Two dimensional spectrum of a monochrome image

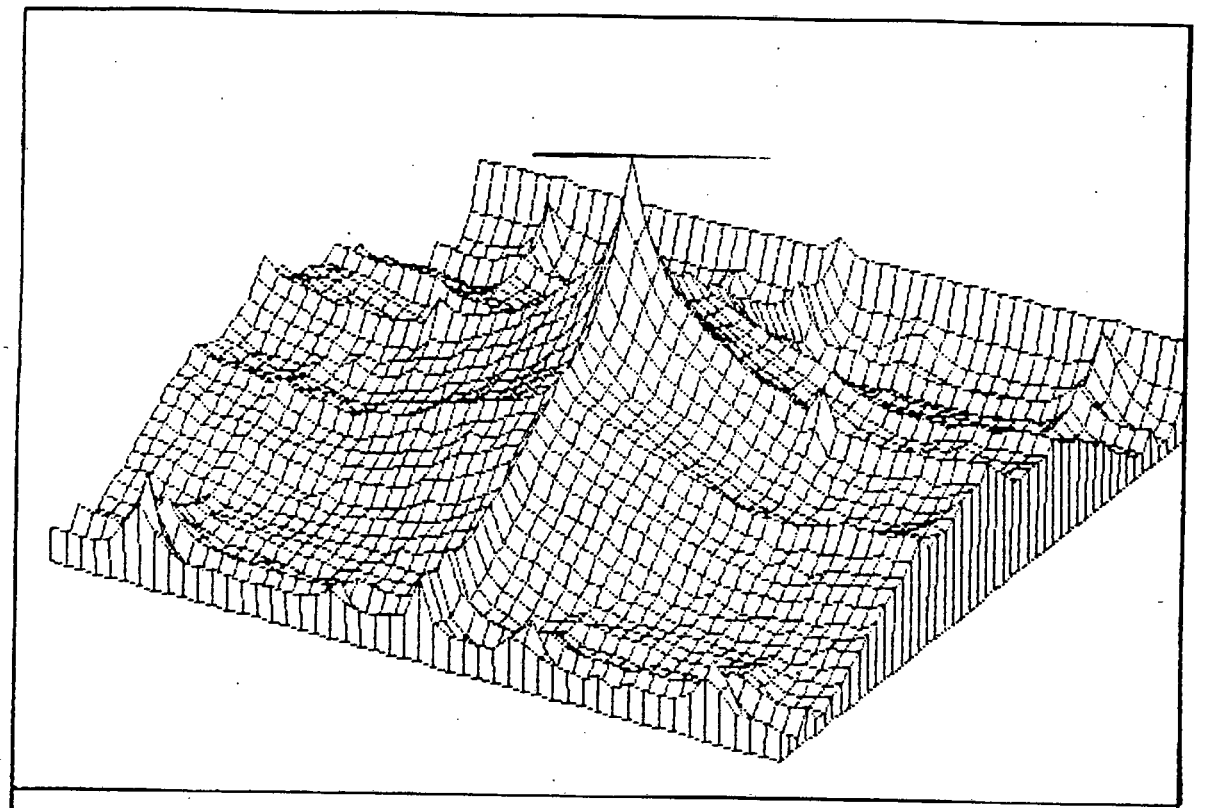

Two dimensional spectrum of a Red image

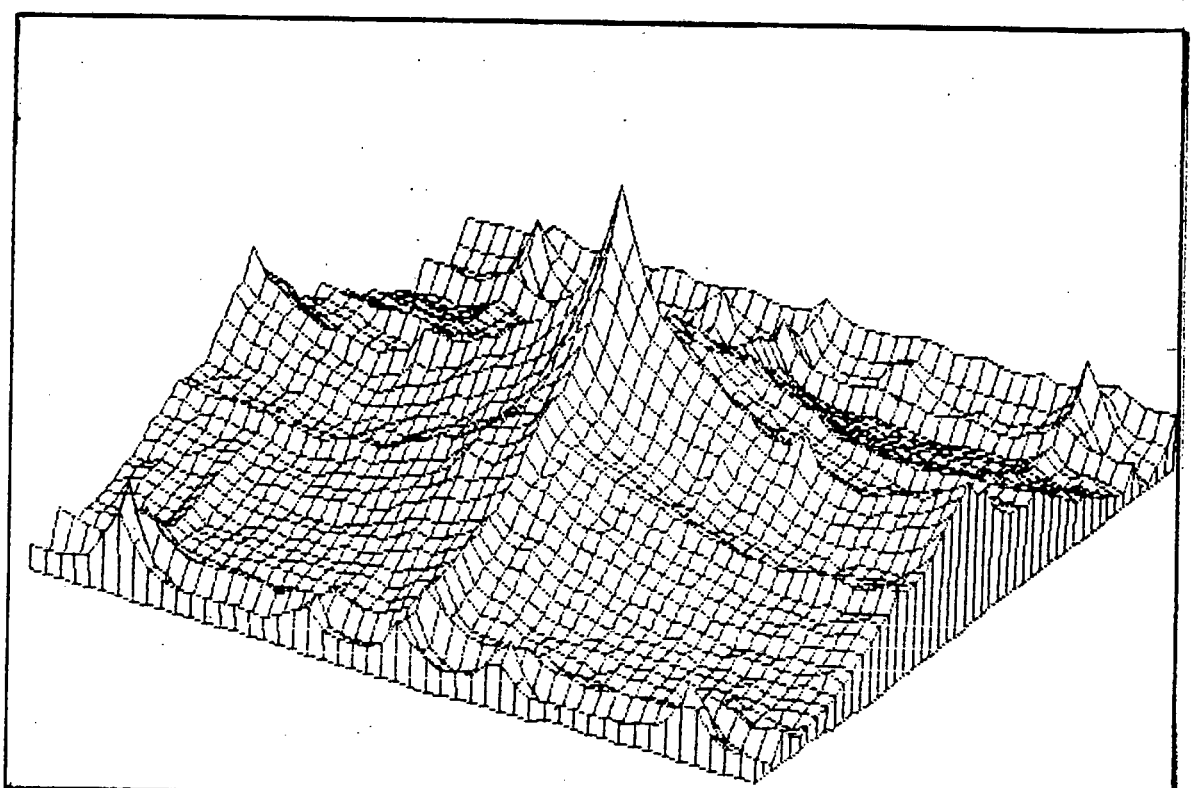

Two dimensional spectrum of a Green image

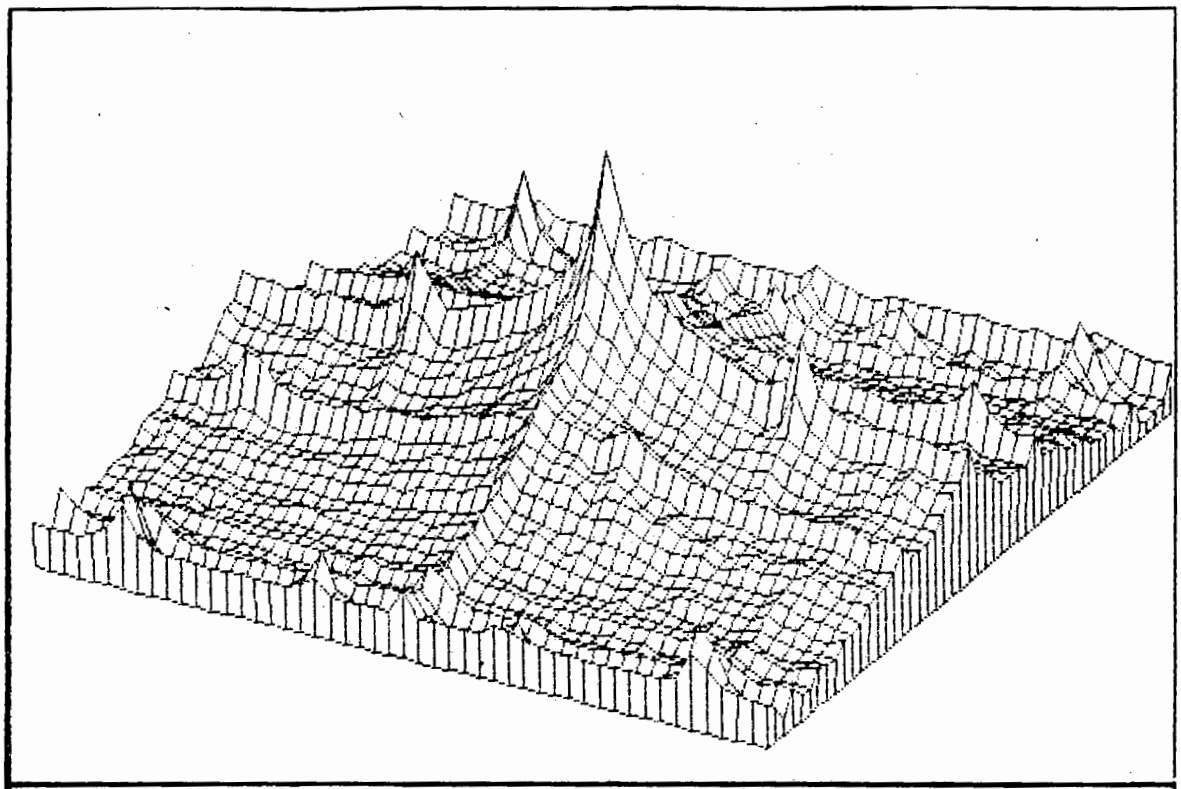

Two dimensional spectrum of a Blue image

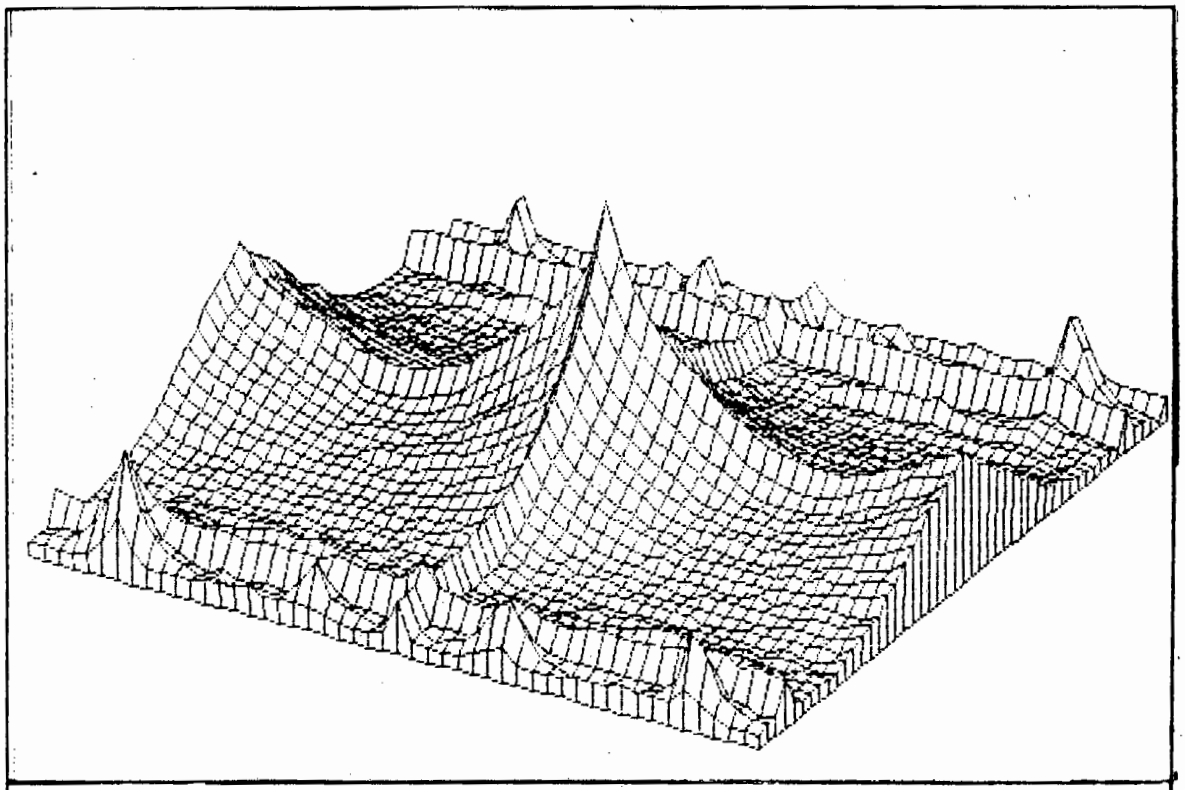

Two dimensional spectrum of a Composite image

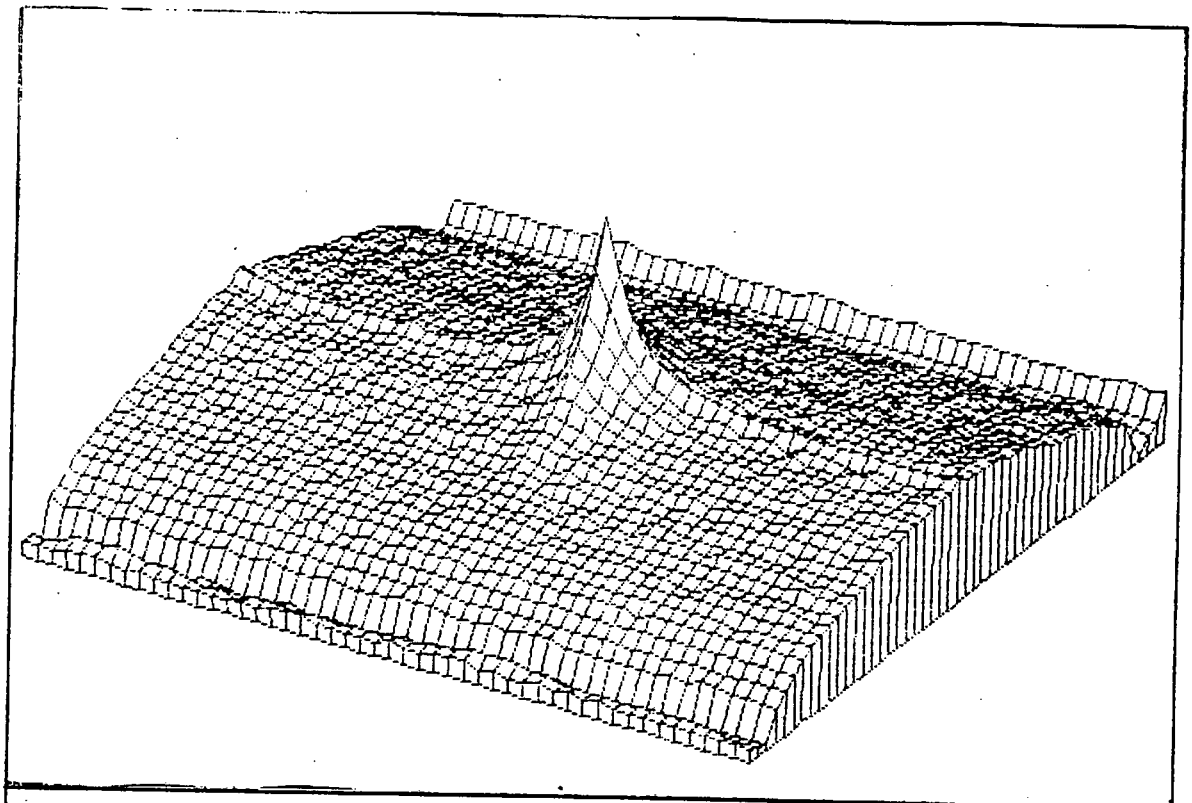

Two dimensional spectrum of a Green image degraded with noise.

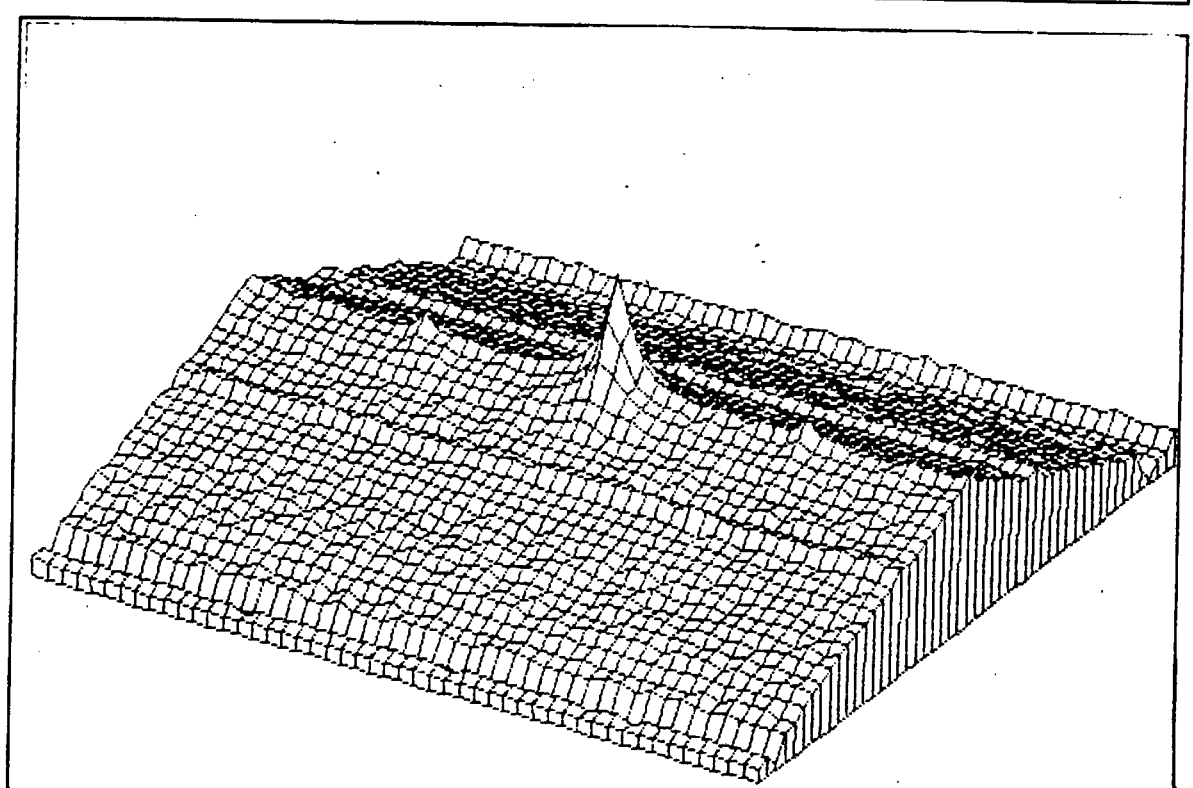

Two dimensional spectrum of a Blue image degraded with noise.

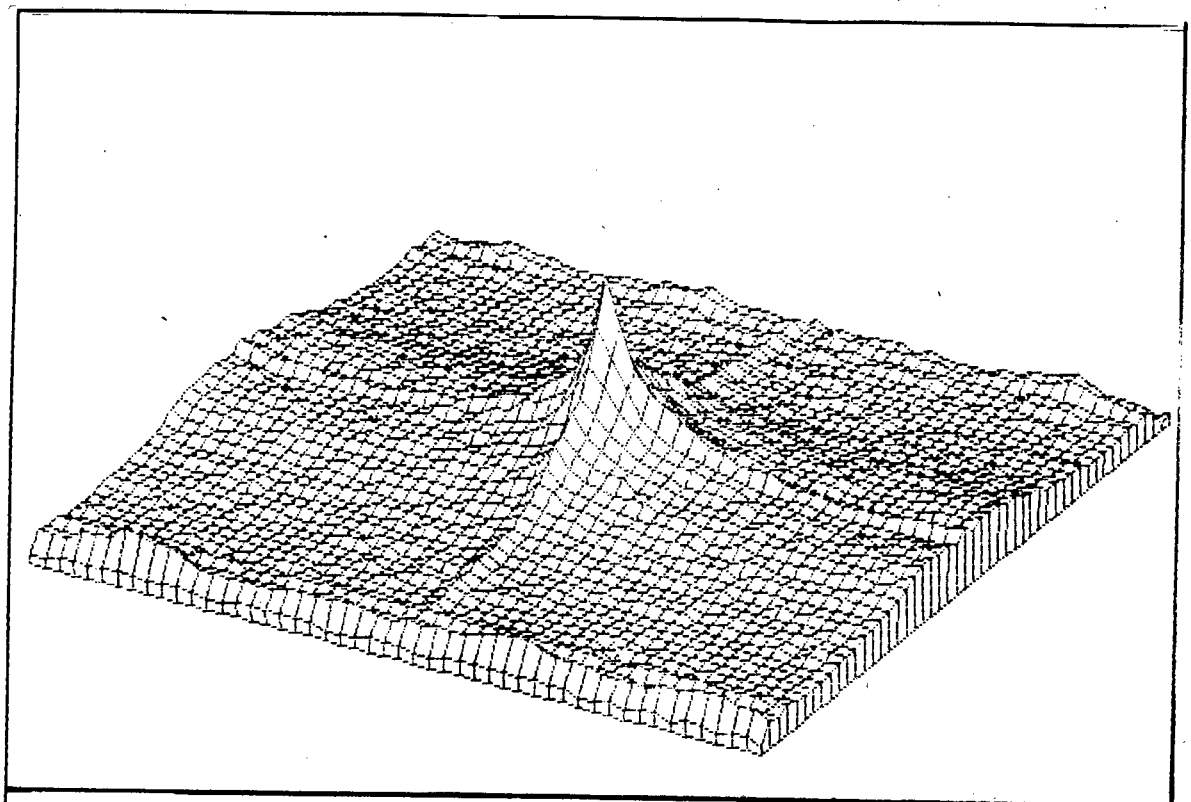

Two dimensional spectrum of a Composite image degraded with noise.

APPENDIX E

HISTOGRAMS OF NOISE ESTIMATIONS

For the Two Dimensional Spectral noise measuring technique (2DSMT) to estimate the noise power from all the estimates of the different sub-images, the estimates are arranged in histogram form. However, it is not necessary to use only noise power estimations.

E.1 SNR ESTIMATION

It is possible to determine the SNR estimate of each sub-image and arrange them in histogram form. This will increase the dynamic range of the display, making large as well as small SNR probabilities visible.

In Fig.E.1 is an example of such a histogram, and Fig.E.2 is an example where the 2DSMT was implemented on a difference picture. The difference between these figures are clear in the low SNR.

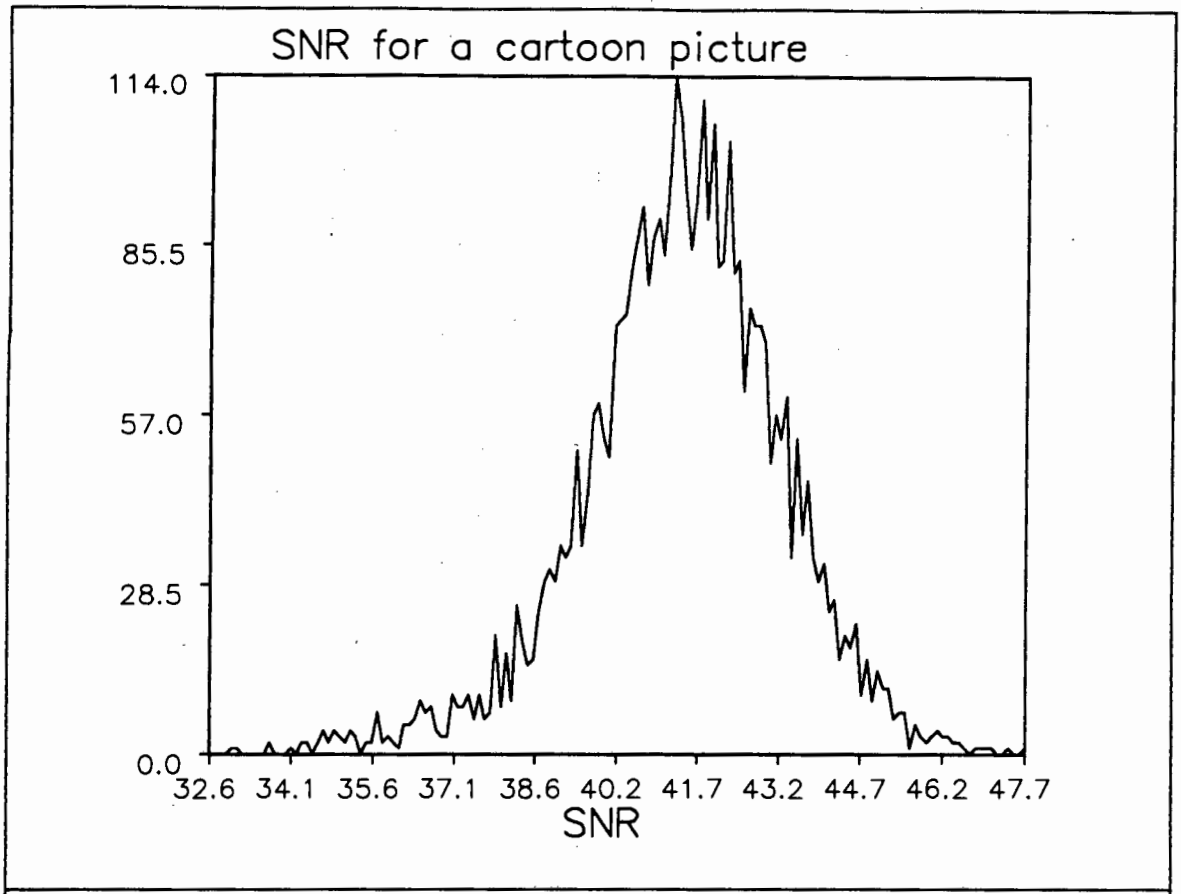

Figure E.1 SNR's arranged in histogram form.

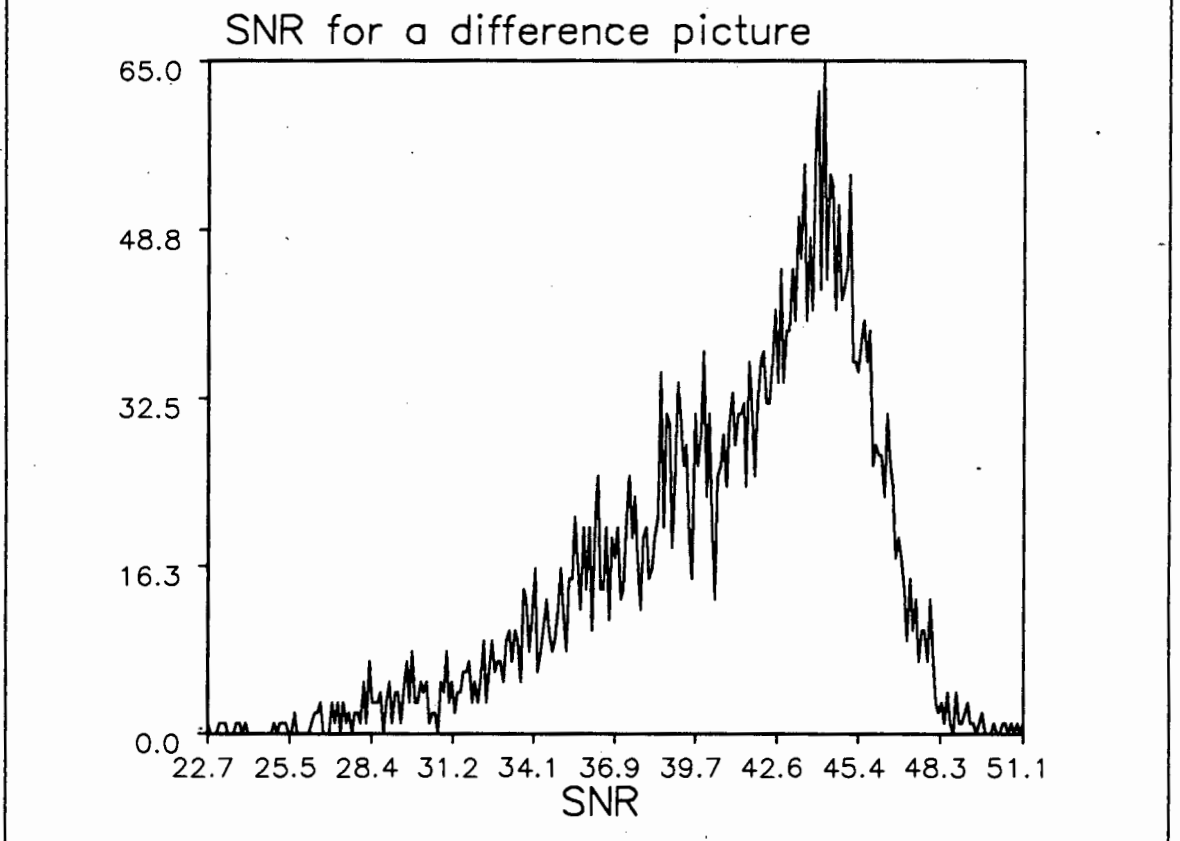

Figure E.2 SNR's of a difference picture arranged in histogram form.

E.2 POWER ESTIMATION

Another method of arranging the power estimates are by sorting all the 9 points in the 2DS in the histogram instead of taking averages. A example of such a histogram is in Fig.E.3.

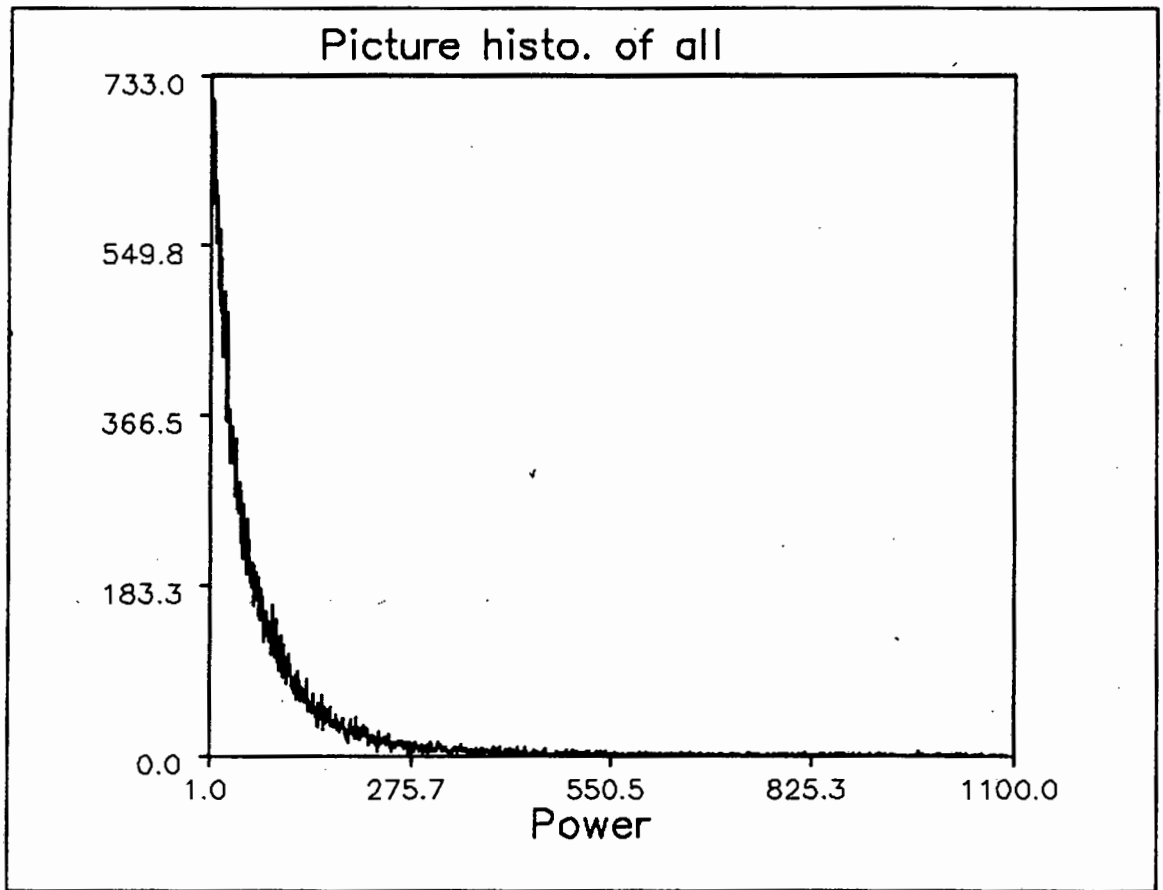

Figure E.3 All the 9 points in the 2DS are arranged into histogram form.

We can see from Fig.E.3 that all the power is concentrated at low power and also we see a very long tail of high power. The explanation for the large power concentration at zero is that when the small 2DS points are arranged into the histogram, they get truncated from floating point variables to fixed point variables. Much information is therefore lost when many different values are truncated to one value. The large values are also spread out over a wide range because there is no averaging to minimise the effect of outlier estimations.

E.3 MEDIAN FILTERING OF SNR

The SNR estimations can be median filtered before creation of the histogram. If all the SNR estimations of 9 neighboring sub-images are median filtered, and then arranged into histogram form, most of the outlier estimations should be eliminated. This is the case when observing the histograms in figures E.4-8. In Figures E.7-8 the input images were midgrey bars (no picture information) with known SNR's. The mode of the histograms do seem to correlate with the SNR's in these inputs with no picture content. Unfortunately this method did not give good results when implemented, and due to lack of time it was not investigated further.

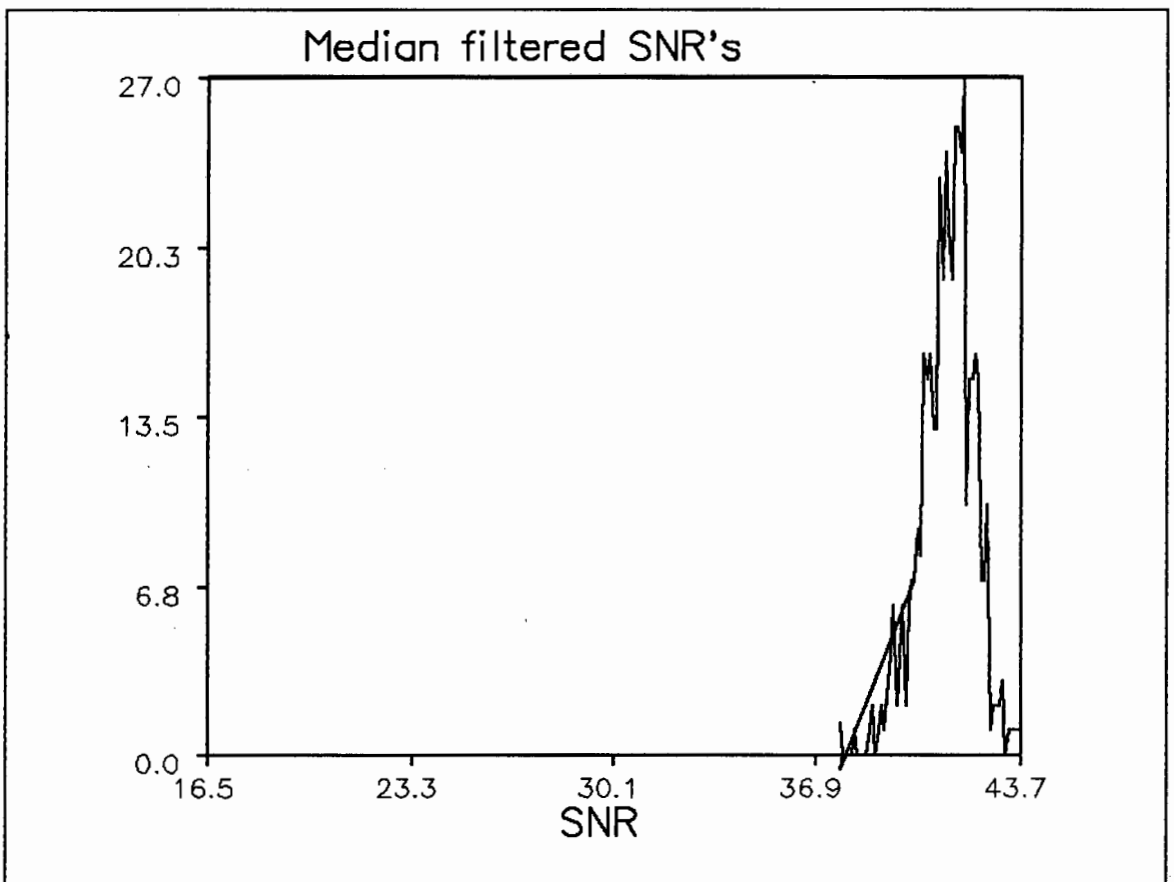

Figure E.4 Histogram of median filtered SNR estimations. Input picture is a cartoon.

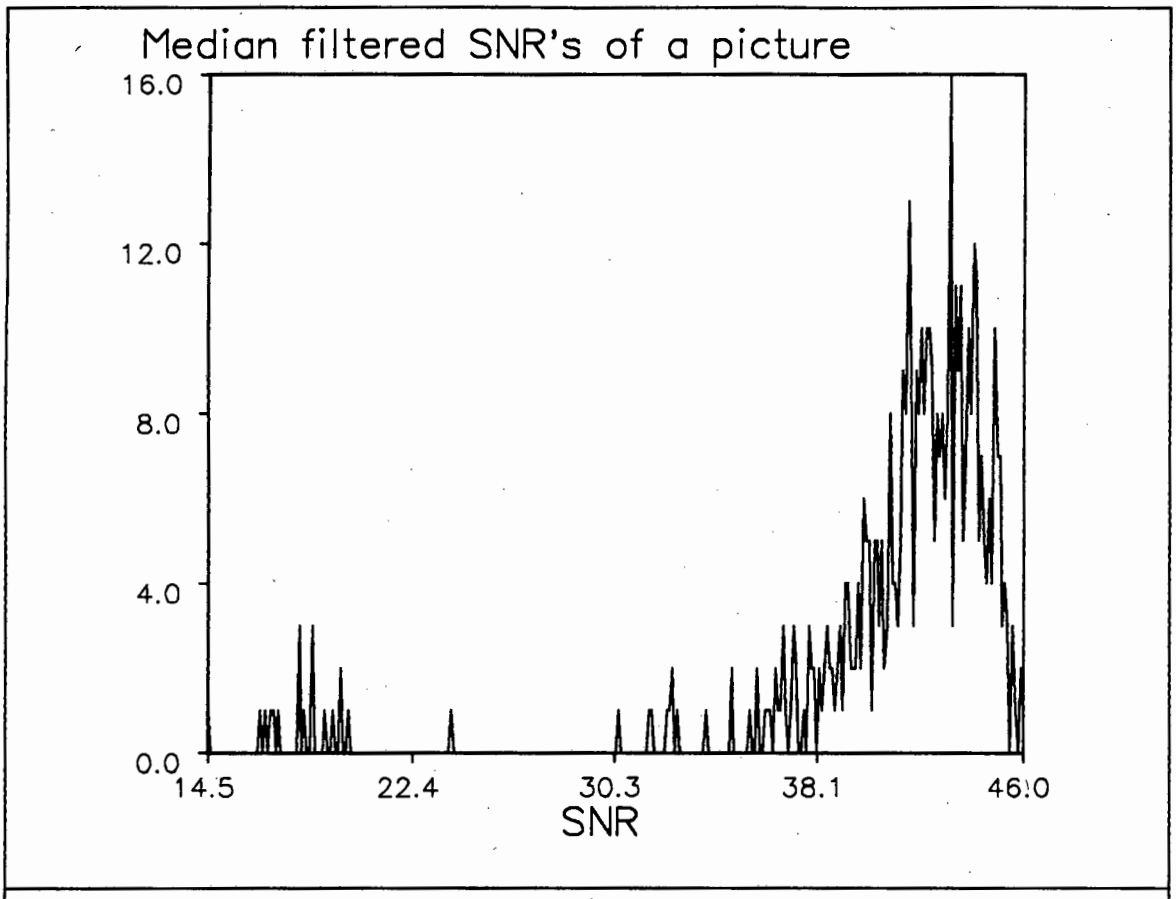

Figure E.5 Histogram of median filtered SNR estimations. Input picture is camera generated.

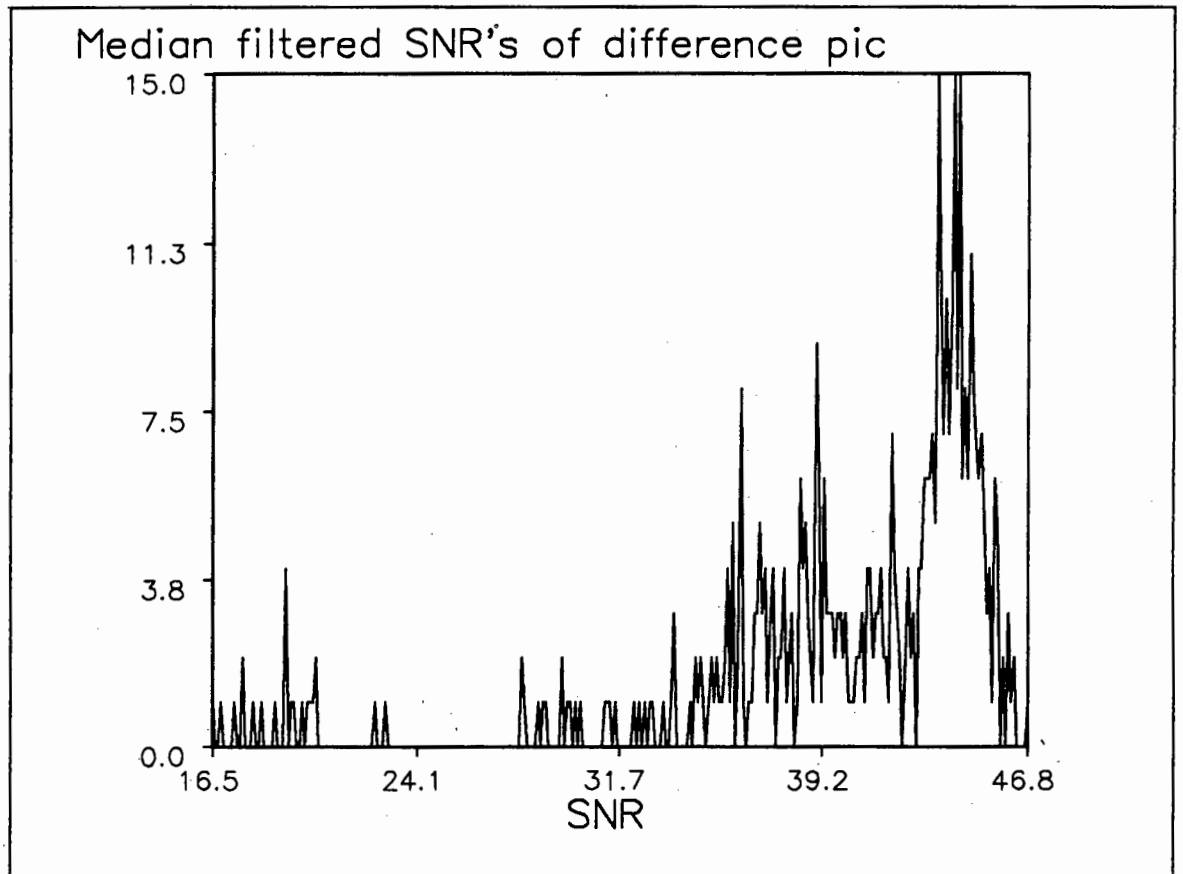

Figure E.6 Histogram of median filtered SNR estimations. Input picture is a difference picture.

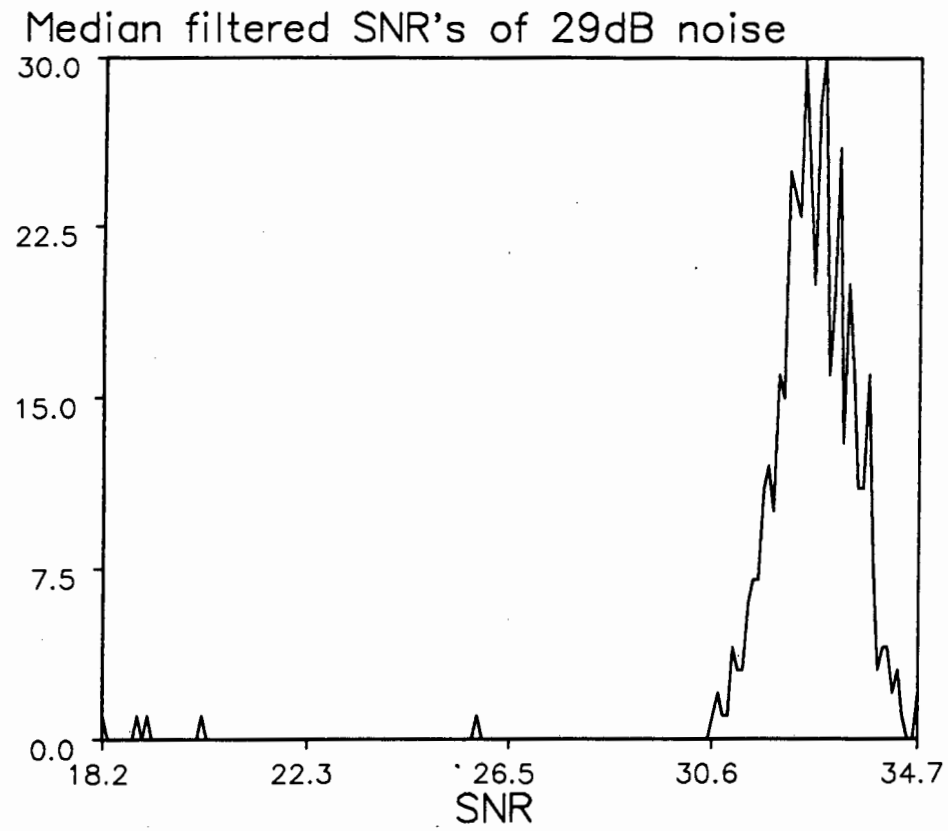

Figure E.7 Histogram of median filtered SNR estimations. Input picture is a midgreybar with SNR=29.

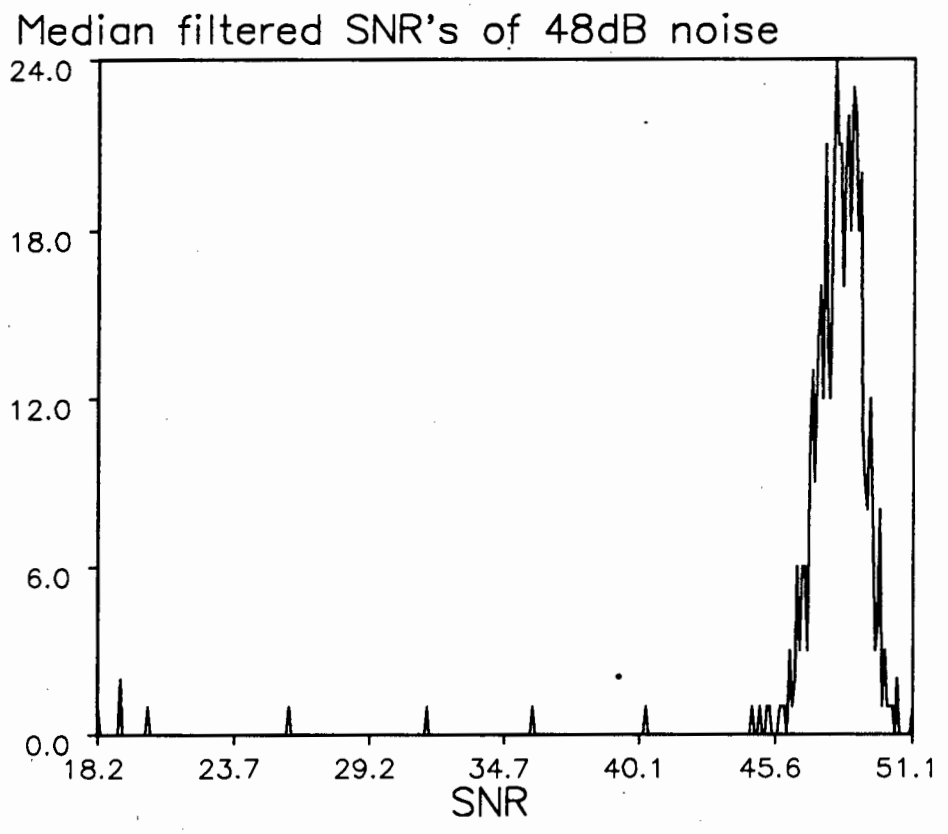

Figure E.8 Histogram of median filtered SNR estimations. Input picture is a midgreybar with SNR=48.

APPENDIX F

A DESCRIPTION OF THE PROGRAMS DEVELOPED DURING THIS THESIS

F.1 Two Dimensional Spectral Noise Measuring Technique (2DSMT)

This program runs on an IBM PC or compatible.
The 2DSMT has several versions. Namely: one uses a numeric co-processor, another uses the Numerical methods FFT and another uses its' own FFT. A program listing of the latter one is given, although the Numerical methods FFT with a co-processor runs the fastest. The include file, PC-GEN.TPU was developed by Andrew Dachs, and are only used for loading the image.

The input to the 2DSMT is a standard .cfi image file of byte. The output is a signal to noise ratio printed on the screen.

```
program pc_2DSMT;

uses pcgen;

const
N=8;
lopass=1;
highpass=4.8;
varsize=2000;
p=6.2831853072/N;

var
    variance:array [0..varsize] of integer;
    sum,maxi,min,mcollom,mrow,collom,NY,currentrow:integer;
    a,wheigt,divid,aver,snr:single;
    cfifilename:string;
    ch1,ch:char;
    s:string;
    k,z,ll,ul,x1,x2,y1,y2:Integer;
    image:matrix;
    lyn,kol,t:integer;
    image1:array [0..N ,0..2*N-1] of single;
    M:integer;
    x,y,wr,wi:array [1..N] of single;

 {**********************FFT START************************}
procedure MakeSinCosTable;
begin
M:=round(ln(N)/ln(2));
for k:=1 to N  do
  begin
    a:=(k-1)*p;
    wr[k]:=cos(a);
    wi[k]:=-sin(a);
  end;
```

```
end;


procedure FFT;

var
n2,n1,n3,i,j,k,l,ia,ie:integer;
xi,xl,yi,yl,e,xt,yt,xtc,xts,ytc,yts,c,s:single;

Begin

N2:=N;
for k:=1 to M do
  begin
   N1:=n2;
   N2:=n2 div 2;
   ie:=N div n1;
   ia:=1;
   for j:=1 to N2 do
     begin
     c:=wr[ia];
     s:=wi[ia];
     ia:=ia+ie;
     i:=j;
     while (i<=N) do
       begin
       l:=i+N2;xi:=x[i];xl:=x[l];yi:=y[i];yl:=y[l];
       xtc:= xi*c - xl*c ;
       xts:= xi*s - xl*s ;
       ytc:= yi*c - yl*c ;
       x[i]:= xi+xl ;
       yts:= yi*s - yl*s ;
       y[i]:= yi+yl ;
       x[l]:=  xtc + yts ;
       y[l]:=  ytc - xts ;
       i:=i+N1;
       end;
    end;
  end;
  j:=1;
  N1:=N-1;
  for I:=1 to N1 do
   begin
   if (i<j) then
     begin
     xt:=x[j];
     x[j]:=x[i];
     x[i]:=xt;
     xt:=y[j];
     y[j]:=y[i];
     y[i]:=xt;
     end;
   k:=N div 2;
   while (k<j) do
     begin
     j:=j-k;
     k:=k div 2;
```

```
      end;

    j:=j+k;
    end;
{************************}

 end;


 {**********************FFT ENDS ***********************}



Procedure TwoDfft;
begin     {*********2 D FFT*******}
for lyn:=0 to N-1 do
  begin
    for kol:=0 to N-1 do
      begin
      x[kol+1]:=image[lyn+y1*N]^[kol+x1*N];
      y[kol+1] :=0;
      end;
    FFT;
    for kol:=0 to N div 2 do
     begin
    image1[kol,2*lyn]:=x[kol+1];
    image1[kol,2*lyn+1]:=y[kol+1];
     end;
  end;



for lyn:=ll to z do
  begin
    for kol:=0 to N-1 do
      begin
      x[kol+1]:=image1[lyn,2*kol];
      y[kol+1] :=image1[lyn,2*kol+1];
      end;
  FFT;
    for kol:=0 to N-1   do
     begin
      image1[lyn,2*kol]:=x[kol+1];
      image1[lyn,kol*2+1]:=y[kol+1];
     end;
  end;



min:=0;aver:=0;
for lyn:=ll to z do
begin
                {******DETERMINE NOISE ESTIMATES FROM
                          HIGH-FREQUENCY SPECTRAL POINTS***}
for t:=ll to ul do
    begin
    snr:=(image1[lyn,2*t]*image1[lyn,2*t]+
    image1[lyn,2*t+1]*image1[lyn,2*t+1]);
```

```
    aver:=snr+aver;
    end;
end;
aver:=AVER/9*10;
if aver>0 then min:=round(aver)
          else min:=0;
               {******CREATE HISTOGRAM*******}
if min>varsize then min:=varsize;
variance[min]:=variance[min]+1;

end;       {******  END  FFT  *******}


procedure HISTOGRAM;
  begin
   maxi:=0;
   sum:=0;
   for collom:=0 to varsize do
       begin
       write(variance[collom],' ');
       sum:=sum+variance[collom];
       if variance[collom]>maxi then maxi:=variance[collom];
       end; readln;
   sum:=sum div 2;
   collom:=0;
   snr:=0;
          {*****  CALCULATE MEDIAN  ****}
   repeat
         snr:=snr+variance[collom];
         collom:=collom+1;
   until snr>sum;
   lyn:=collom-1;
          {****  CALCULATE SNR  ****}
   snr:=2*4.34*ln(255)-4.34*ln(lyn/10);
   write(cfifilename,'  snr= ',snr);
  end;

begin{*************   MAIN PROGRAM   ****************}
MakeSinCosTable;
ll:=trunc(N/10*lopass)+1;
z:=trunc(N/10*highpass);
if (z> (N div 2)) then z:=N div 2;
ul:=N-ll;
for t:=0 to varsize do variance[t]:=0;

  if paramstr(1)=''
    then
     begin
     write('filename  ');read(cfifilename);
     end
    else
     cfifilename:=paramstr(1);
  loadcfi(cfifilename,image);

          {******* TESSELLATE IMAGE AND CALCULATE 2DS*****}
for x1:=0 to 63 do
 begin
    for y1:=0 to 63 do
```

```
    TwoDfft;
 end;
HISTOGRAM;


end.{***END OF PROGRAM***}
```

F.2 ADDNOISE

The program Addnoise.exe runs on the micro-VAX. The input is a .cfi image file of byte and outputs an image (again .cfi file of byte) degraded with an amount of noise specified by the operator. The operator is asked for a certain RMS value of noise to be added, and then at completion gives the SNR of the output image.

F.3 LINFFT

The program linfft.exe runs on the micro-VAX. The input is a .cfi image file of byte and outputs an image (again .cfi file of byte) of the spectra of each line of the input picture. The spectra are output on a log scale.

F.4 KOLFFT

The program kolfft.exe runs on the micro-VAX. The input is a .cfi image file of byte and outputs an image (again .cfi file of byte) of the spectra of each column in the input picture. The spectra are output on a log scale.

F.5 PLOTEXP

This program runs on the micro-VAX on a tektronix 4014 screen. The input for this program is the output file of either linfft or kolfft. It plots the average of all the line/column spectra of the input.

F.6 B2LOTUS

This program runs on the micro-VAX. The input for this program is the output file of either linfft or kolfft. It outputs the average of all the line/column spectra of the input. The output is a text file compatible with Lotus .prn files. The average line/column spectrum of an image can then be displayed on a spreadsheet program.

F.7 SACLOG64

This program runs on the micro-VAX. It inputs a two dimensional fft, created by FFT2DMAG.EXE. It converts the 512x512 byte, log scale, spectrum to a 64x64 text output spectrum by averaging the values in blocks of 8x8 into one spectrum estimate. The output is used to display the spectrum on any 3D graph program. SACLAND64.exe is a similar program, except that it does input a logscale, but a linear scale. Another similar program is bytecon.exe which also converts spectra to 3D-graph standards, but it inputs 10 different spectra and averages them all to one output text file of size 64x64.

F.8 SUBTR

This program runs on the micr-VAX. It inputs two images (.cfi files of byte), subtracts them and writes the absolute value of the difference between the two input files to a third image file. The difference images mentioned in chapter 5 were created with this program.

F.9 SNRAOI

This program runs on an IBM PC or compatible. It inputs an image file (.cfi file of byte) and a binarized version of the image. The binarized image is created from the .cfi image, with a program called pc-gtoi.exe, created by Andrew Dachs. This program is described in detail in chapter 6. It has a facillity to output the selected area of interest to a text file which can be read into a spreadsheet.

```
program snraoi;
{Obtain a particular area of interest of a *.cfi file and
calculate the SNR on that area}

uses  dos,crt,pcgen,graph,listfile,DIP_Grph;

type
      bit=0..1;
      binrow=array[0..511] of bit;
      bptr=^binrow;
      bmatrix=array[0..511] of bptr;

var maxi,collom,NY,N,currentrow,totalrows,code:integer;
    sum,snr1,snr2,rms,sizem,aver,max,min:real;
    b:bmatrix;
    binfilename,cfifilename,aoifilename:string;
    invert:boolean;
    ch1,ch:char;
    s:string;
    dirname,fsmask:string;
    x1,x2,y1,y2:Integer;
    image:matrix;
    size:word;

procedure binaryload;
var binfile:file;
    row,col:integer;
    temp,mask,section:byte;
    t:array[0..63] of byte;
    i:integer;
begin
{$I-}
  assign(binfile,binfilename);
  reset(binfile,1);
  i:=ioresult;
{$I+}
  if i<>0 then
    begin
      RestoreCrtMode;
      writeln('File error');
    end
  else
```

```
  begin
  row:=0;
  while (row<totalrows) and (row<maxy) and
(not(eof(binfile))) do
   begin
    blockread(binfile,t,64);
    for col:=0 to 63 do
      begin
        mask:=1;
        for section:=0 to 7 do
           begin
             temp:=t[col];
             if not invert
               then
                 begin
                   if (temp and mask)<>0 then
putpixel(col*8+section,row,15);
                 end
               else if (temp and mask)=0 then
putpixel(col*8+section,row,15);
             mask:=mask*2;
           end;
      end;
     inc(row);
    end;
   close(binfile);
  end;
end;
procedure display3d;

const
NN=256;
offset=310;
gridsize=3;
gridsizex=3;
var
    angle:real;
    lyn,kol,y,x,t,k,w1:integer;
    ch:char;
    max:array [0..2*NN-1] of integer;
    gd,gm:integer;


begin {**********************MAIN************************}
writeln('init');

  angle:=pi/4; angle:=sin(angle)/cos(angle);
   detectgraph(gd,gm);
   initgraph(gd,gm,' ');
   for kol:=0 to 2*N-1 do max[kol]:=-400;

   for lyn:=0 to NY-1 do
   begin
   x:=lyn;
   y:=round(x*angle);
   moveto(gridsizex*x,offset-max[lyn]);
     for kol:=0 to N-1 do
     begin
```

```
      x:=round(angle*lyn)+kol;
      if max[x]<(image[lyn+y1]^[kol+x1]+gridsize*y) then
                  begin
                  max[x]:=image[lyn+y1]^[kol+x1]+gridsize*y;
                  lineto(gridsizex*x,offset-max[x]);
                  end
                  else
                  moveto(gridsizex*x,offset-max[x]);
      end;
    end;
    line(0,offset+10,gridsizex*N,offset+10);
    repeat until keypressed;
    ch:=readkey;
    closegraph;

end;


procedure histo;

var
 max:array[0..255] of integer;
 gd,gm,maxx:integer;
 sig:real;
procedure display;
  begin
   detectgraph(gd,gm);
   initgraph(gd,gm,' ');
   for collom:=0 to 256 do
     line(2*collom,300,2*collom,300-max[collom]);
   rectangle(0,0,512,301);
   readln;
   closegraph;
  end;

 begin {*******HISTO*******}
 for collom :=0 to 256 do max[collom]:=0;
 maxx:=0;
 sig:=0;
 maxi:=0;
 for currentrow:=y1 to y2-1 do
   for collom:=x1 to x2-1 do

max[image[currentrow]^[collom]]:=max[image[currentrow]^[coll
om]]+1;
sum:=0;
 for collom:=0 to 256 do
      if maxx<max[collom] then
          begin
          maxx:=max[collom];
          maxi:=collom;
          end;
 for collom:=0 to 256 do
      begin
      max[collom]:=round(max[collom]/maxx*300);
      sum:=sum+max[collom];
      end;
 collom:=maxi;
```

```
 sum:=sum/3;
 sig:=0;
   repeat
     sig:=sig+max[collom];
     collom:=collom+1;
   until (sig>sum);
 display;
 writeln('sigma = ',sig,'  at intensity (0..255) =',maxi);
 sig:=4.34*ln(255/sig);
 writeln('snr = ',sig,'  at intensity (0..255) =',maxi);
 readln;
 end;  {*******HISTO*******}

procedure title1;
begin
  clrscr;
  writeln('PC-HISTO - obtain an area of interest of a
*.cfi'+
          ' file using a *.bin file.');
  solidline(2);
  gotoxy(1,22);
end;

procedure title2;
begin
  ClrScr;
  WriteLn('PC-AOI - adjusting *.cfi file.');
  SolidLine(2);
  GotoXY(2,4);
  Write('Selected area of interest :');
  GotoXY(30,4);
  Write('(x1,y1) = (',x1,',',y1,')');
  GotoXY(30,5);
  Write('(x2,y2) = (',x2,',',y2,')');
end;

function byte_to_str(Number:Byte):String;
var S:String;
begin
    str(number,S);
    byte_to_str:=S;
end;

procedure saveaoi(aoifilename:string;image:matrix;
                  VAR x1,y1,x2,y2:Integer);
var
    outputfile : TEXT;
    row, col   : Integer;
    asciival   : String;

begin
   assign(outputfile,aoifilename);
   rewrite(outputfile);

  { write(outputfile,'col':4);
   for col:=x1 to x2 do write(outputfile,col:4);
   writeln(outputfile);
   writeln(outputfile,'row':4);
```

```
    }
    for row:=y1 to y2 do
      begin
     {   write(outputfile,row:4);}
        for col:=x1 to x2 do
          begin
             asciival:=byte_to_str(image[row]^[col]);
             write(outputfile,asciival:4);
          end;
        writeln(outputfile);
      end;
    close(outputfile);
end;



begin
  x1:=0; y1:=0; x2:=128; y2:=128; {Initial size of area of
interest}
  title1;
  dirname:='';
  fsmask:='*.bin';
  if paramstr(1)=''
    then
      begin

listfiles(dirname,fsmask,archive,binfilename,false,true,true
);
      end
    else binfilename:=paramstr(1);
  parse(binfilename,'.BIN');
  if paramstr(2)=''
    then
      begin
         gotoxy(1,22);
         writeln('Invert image?');
         readln(ch);
          writeln('Save image?');
          readln(ch1);
      end
    else begin s:=paramstr(2);ch:=s[1]; end;
  if paramstr(3)='' then totalrows:=512
                    else begin
val(paramstr(3),totalrows,code); end;
  if upcase(ch)='Y' then invert:=true
                    else invert:=false;
  initgraphics;
  binaryload;
  Area_Of_Interest(x1,y1,x2,y2);N:=x2-x1;NY:=y2-y1;
  restorecrtmode;

  title2;

  cfifilename:=copy(binfilename,1,length(binfilename)-4) +
'.CFI';
  loadcfi(cfifilename,image);
    histo;
```

```
    display3d;

  {*******************calculate SNR************************}
Clrscr;
writeln;
writeln('calculating SNR');
aver:=0;
sizem:=abs((x1-x2)*(y1-y2));
for currentrow:=y1 to y2-1 do
  for collom:=x1 to x2-1 do
    begin
    aver:=image[currentrow]^[collom]+aver;
    end;
aver:=aver/sizem;
rms:=0;
min:=1e5;
max:=0;
for currentrow:=y1 to y2-1 do
  for collom:=x1 to x2-1 do
    begin
    rms:=sqr(image[currentrow]^[collom]-aver)/sizem+rms;
    if  image[currentrow]^[collom]>max then
max:=image[currentrow]^[collom];
    if  image[currentrow]^[collom]<min then
min:=image[currentrow]^[collom];
    end;
rms:=sqrt(rms);
snr1:=2*4.34*ln(255/rms);
snr2:=2*4.34*ln(aver/rms);
writeln;
writeln('SNR=20log(255/RMS)= ',snr1);
writeln('SNR=20log(aver/RMS)= ',snr2);
writeln('max= ',max);
writeln('rms= ',rms);
writeln('min= ',min);
writeln('aver= ',aver);
{*******************calculated SNR************************}

  if upcase(ch1)='Y' then
     begin
     aoifilename:=copy(cfifilename,1,length(cfifilename)-4)
+ '.DAT';
     saveaoi(aoifilename,image,x1,y1,x2,y2);
     end;

end.
```